

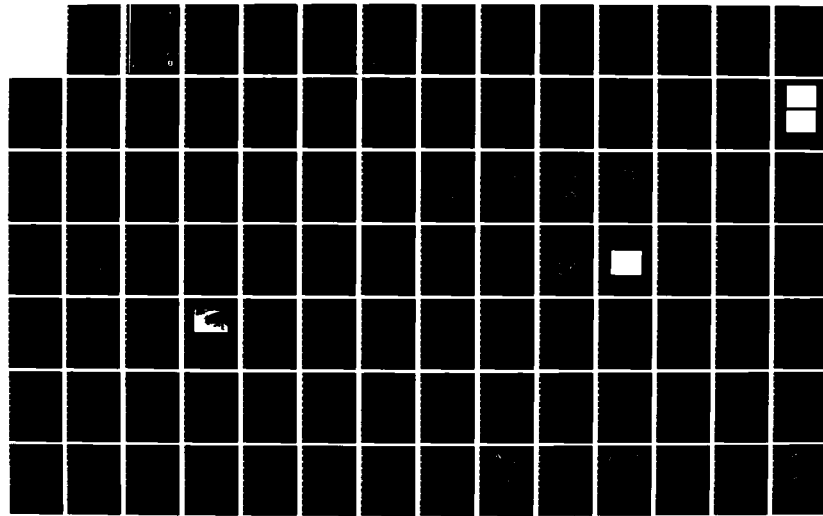
RD-A137 165 THE USE OF INTERACTIVE GRAPHICS PROCESSING IN
SHORT-RANGE TERMINAL WEATHER (U) AIR FORCE GEOPHYSICS
LAB HANSCOM AFB MA D R CHISHOLM ET AL. 31 MAR 83

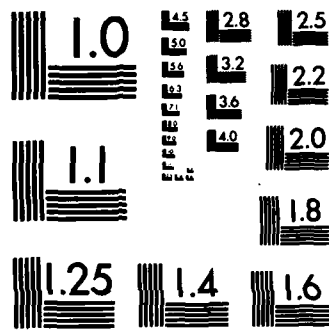
1/2

UNCLASSIFIED AFGL-TR-83-0093

F/G 4/2

NL





MICROCOPY RESOLUTION TEST CHART
NATIONAL BUREAU OF STANDARDS-1963-A

(12)

AFGL-TR-83-0093
ENVIRONMENTAL RESEARCH PAPERS, NO. 833



ADA137165

The Use of Interactive Graphics Processing in Short-Range Terminal Weather Forecasting: An Initial Assessment

DONALD A. CHISHOLM
ARTHUR J. JACKSON
MICHAEL E. NIEDZIELSKI
RANDY SCHECHTER
CHARLES F. IVALDI

31 March 1983

Approved for public release; distribution unlimited.

DTIC FILE COPY
DU

METEOROLOGY DIVISION
AIR FORCE GEOPHYSICS LABORATORY
HANSCOM AFB, MASSACHUSETTS 01731

PROJECT 6670

DTIC
SELECTED
JAN 23 1984
S E

AIR FORCE SYSTEMS COMMAND, USAF



84 01 23 096

This report has been reviewed by the ESD Public Affairs Office (PA) and is releasable to the National Technical Information Service (NTIS).

"This technical report has been reviewed and is approved for publication"

FOR THE COMMANDER



DONALD A. CHISHOLM, Chief
Atmospheric Prediction Branch



ROBERT A. McCLATCHY, Director
Meteorology Division

Qualified requestors may obtain additional copies from the Defense Technical Information Center. All others should apply to the National Technical Information Service.

If your address has changed, or if you wish to be removed from the mailing list, or if the addressee is no longer employed by your organization, please notify AFGL/DAA, Hanscom AFB, MA 01731. This will assist us in maintaining a current mailing list.

Do not return copies of this report unless contractual obligations or notices on a specific document requires that it be returned.

Unclassified

SECURITY CLASSIFICATION OF THIS PAGE (When Data Entered)

DD FORM 1 JAN 73 1473 EDITION OF 1 NOV 65 IS OBSOLETE

Unclassified

SECURITY CLASSIFICATION OF THIS PAGE (When Data Entered)

Unclassified

SECURITY CLASSIFICATION OF THIS PAGE(When Data Entered)

20. (Contd)

storm episodes archived from the 1982-83 season.

The products judged most useful in preparing short-range terminal forecasts included (1) a station model time series display, (2) conventional geographic data displays presented simultaneously as four quadrant panels on one screen, (3) mesoscale surface objective analyses, and (4) a forecast guidance procedure based on 2-D upper-air trajectories and sensible weather algorithms based on imagery from the GOES satellite. The importance of half-hourly visible and IR imagery from the GOES satellite in short-range terminal forecasting was confirmed in this experiment. The participating forecasters relied more heavily on it to prepare their forecasts than any other source. The manipulation of digital imagery in a computer-based interactive graphic system through time-series looping, color enhancements, and overlaying conventional plots and analyses on it, provides a wealth of qualitative and quantitative guidance for forecasting. The numerical forecasts yielded superior rms errors compared to persistence at all forecast intervals except 1 h. At 4 h, the improvement over persistence ranged from about 21 percent for wind forecasts to about 34 percent for total cloud amount, while the 6-h quantitative precipitation forecasts yielded a 39 percent improvement.

Unclassified

SECURITY CLASSIFICATION OF THIS PAGE(When Data Entered)

Preface

The Mesoscale Forecast Experiment could not have been completed successfully without the support and participation of several individuals in AFGL's Meteorology Division (LY) and its contractor (Systems and Applied Sciences Corp.). The principal participating forecasters were Dr. H. A. Brown, Dr. H. S. Muench and Mr. A. J. Jackson of AFGL/LY and Messrs. M. E. Niedzielski, R. Schechter and C. F. Ivaldi of SASC. Mr. J. Pazniokas provided invaluable support as Mesoscale Forecast Experiment test evaluator and data analyst. Mr. R. Fournier effected the orderly integration of new and modified application software with the McIDAS operating system. Ms. Betty Blanchard ably prepared draft and final manuscript versions.

Accession For	
NTIS GRA&I	<input checked="" type="checkbox"/>
DTIC TAB	<input type="checkbox"/>
Unannounced	<input type="checkbox"/>
Justification _____	
By _____	
Distribution/ _____	
Availability Codes	
Dist	Avail and/or Special
A-1	



Contents

1. INTRODUCTION	11
2. INTERACTIVE COMPUTER GRAPHICS SYSTEM	12
2. 1 Automated Weather Distribution System (AWDS)	12
2. 2 Man-Computer Interactive Data Access System (McIDAS)	13
3. MESOSCALE FORECAST EXPERIMENT (MFE)	22
3. 1 Experimental Procedures	22
3. 2 Test Sample	29
4. TEST RESULTS	43
4. 1 Product Assessment	43
4. 2 Forecast Difficulty Assessment	55
4. 3 Forecast Verification Statistics	59
4. 3. 1 Numerical (Deterministic) Forecasts	60
4. 3. 2 Probability Forecasts	65
4. 3. 3 Ancillary Considerations	67
5. CONCLUDING REMARKS AND FUTURE PLANS	72
REFERENCES	75
APPENDIX A: Cold-Front Decision Assistance Procedure	77
APPENDIX B: Coastal Cyclogenesis Decision Assistance Procedure	105
APPENDIX C: Inland Cyclogenesis Decision Assistance Procedure	141
APPENDIX D: Mesoscale Forecasting Experiment Assessment Forms	169

Illustrations

1. AFGL McIDAS Functional Block Diagram	15
2. MDR State Display Centered on Oklahoma (OK)	16
3. MDR City Display Centered on Dallas-Fort Worth (DFW) with Overlaid Weather Symbols	17
4. Temperature Analysis—One-pass Cressman Technique	18
5. Temperature Analysis—Five-pass Barnes Technique	18
6. Station-Model Time-Series Display for 26 Mar 1982	19
7. Line Graph Plot of Surface Pressure for 26 Mar 1982	20
8. Bar Graph Plot of Cloud Heights	21
9. Example of "Menu-Driven" Interactive Procedure Used for Forecast Entry Into Automated Verification Phase of the Mesoscale Forecast Experiment; (a) Interrogation Format and (b) Response Format	25
10. Example of Verification Statistics Compiled for Forecaster After Each Episode	26
11. Twenty-four Hourly Observations for Logan International Airport (BOS) for the Ten Cases of the Mesoscale Forecast Experiment; Hours 6 to 11 Represent Forecast Times	31
12. Twenty-four Hourly Observations for Secondary Station (BDL, JFK or PVD) for the Ten Cases of the Mesoscale Forecast Experiment; Hours 6 to 11 Represent Forecast Times	32
13. General Weather Situation for Mesoscale Forecast Experiment Case No. 1: (a) Surface Pressure Analysis for 1400 GMT, 26 Mar 1982 and (b) 500-mb Height Analysis for 1200 GMT, 26 Mar 1982	33
14. General Weather Situation for Mesoscale Forecast Experiment Case No. 2: (a) Surface Pressure Analysis for 1900 GMT, 26 Apr 1982 and (b) 500-mb Height Analysis for 1200 GMT, 26 Apr 1982	34
15. General Weather Situation for Mesoscale Forecast Experiment Case No. 3: (a) Surface Pressure Analysis for 0500 GMT, 31 Mar 1982 and (b) 500-mb Height Analysis for 0000 GMT, 31 Mar 1982	35
16. General Weather Situation for Mesoscale Forecast Experiment Case No. 4: (a) Surface Pressure Analysis for 1400 GMT, 27 Apr 1982 and (b) 500-mb Height Analysis for 1200 GMT, 27 Apr 1982	36
17. General Weather Situation for Mesoscale Forecast Experiment Case No. 5: (a) Surface Pressure Analysis for 1800 GMT, 11 Mar 1982 and (b) 500-mb Height Analysis for 1200 GMT, 11 Mar 1982	37
18. General Weather Situation for Mesoscale Forecast Experiment Case No. 6: (a) Surface Pressure Analysis for 1800 GMT, 15 Dec 1981 and (b) 500-mb Height Analysis for 1200 GMT, 15 Dec 1981	38

Illustrations

19.	General Weather Situation for Mesoscale Forecast Experiment Case No. 7: (a) Surface Pressure Analysis for 1700 GMT, 1 Dec 1981 and (b) 500-mb Height Analysis for 1200 GMT, 1 Dec 1981	39
20.	General Weather Situation for Mesoscale Forecast Experiment Case No. 8: (a) Surface Pressure Analysis for 1700 GMT, 4 Mar 1982 and (b) 500-mb Height Analysis for 1200 GMT, 4 Mar 1982	40
21.	General Weather Situation for Mesoscale Forecast Experiment Case No. 9: (a) Surface Pressure Analysis for 0600 GMT, 22 Dec 1981 and (b) 500-mb Height Analysis for 0000 GMT, 22 Dec 1981	41
22.	General Weather Situation for Mesoscale Forecast Experiment Case No. 10. (a) Surface Pressure Analysis for 0400 GMT, 6 Apr 1982 and (b) 500-mb Height Analysis for 0000 GMT, 6 Apr 1982	42
23.	Surface Objective Streamline Analysis of Offshore Cold Front Situation on 0000 GMT, 21 July 1982, Using Only Land-based Observations	48
24.	Plotted Surface Wind Observations at Land-based Locations and Ships/Buoys on 0000 GMT, 21 July 1982	49
25.	Surface Objective Streamline Analysis of Offshore Cold Front Situation on 0000 GMT, 21 July 1982, Using Land-based Ship and Buoy Observations	49
26.	Example of Alphanumeric Display of 2-D Trajectory Forecast Guidance Model (PF); Hourly Surface Temperature Forecasts for BOS Based on 0800 GMT (Z) Temperature Analysis and 0000 GMT 700-mb Wind Components	50
27.	Example of Integrated Display of Collocated GOES IR Imagery, Manually Digitized Radar (MDR) Analysis and Plotted Weather Symbols for 2300 GMT, 1 Mar 1983	57
28.	Example of Probability and Numerical (Categorical) Forecasts Generated by Generalized Exponential Markov (GEM) Based on Surface Observation at BOS at 1100 LST, 26 Mar 1982	61
29.	Root Mean Square Error Results of Mesoscale Forecast Experiment Wind Forecasts; Forecaster Consensus (X), Persistence (O) and GEM (Δ)	62
30.	Root Mean Square Error Results of Mesoscale Forecast Experiment Cloud Amount Forecasts; Forecaster Consensus (X), Persistence (O) and GEM (Δ)	63
31.	Root Mean Square Error Results of Mesoscale Forecast Experiment Ceiling Height Forecasts; Forecaster Consensus (X), Persistence (O) and GEM (Δ)	64
32.	Percent Improvement in Cumulative p-score of Mesoscale Forecast Experiment Forecasts of Cloud Amount vs Persistence Forecasts as a Function of Forecast Interval (in hours) for Ten Cases, Two Stations and All Forecasters (X), and for Generalized Exponential Markov (GEM) (Δ)	65

Illustrations

33. Percent Improvement in Cumulative p-score of Mesoscale Forecast Experiment Forecasts of Ceiling Height vs Persistence Forecasts as a Function of Forecast Interval (in hours) for Ten Cases, Two Stations and All Forecasters (X), and for Generalized Exponential Markov (GEM) (Δ)	66
34. Percent Improvement in Cumulative p-score of Mesoscale Forecast Experiment Forecasts of Cloud Amount vs Sample Climatology Forecasts as a Function of Forecast Interval (in hours) for Ten Cases, Two Stations and All Forecasters (X), and for Generalized Exponential Markov (GEM) (Δ)	67
35. Percent Improvement in Cumulative p-score of Mesoscale Forecast Experiment Forecasts of Ceiling Height vs Sample Climatology Forecasts as a Function of Forecast Interval (in hours) for Ten Cases, Two Stations and All Forecasters (X), and for Generalized Exponential Markov (GEM) (Δ)	68
36. Root Mean Square Error Results of Mesoscale Forecast Experiment Wind Forecasts for Primary Forecast Location (P) and Secondary Location (S)	39
37. Root Mean Square Error Results of Mesoscale Forecast Experiment Cloud Amount Forecasts for Primary Forecast Location (P) and Secondary Location (S)	70
38. Root Mean Square Error Results of Mesoscale Forecast Experiment Ceiling Height Forecasts for Primary Forecast Location (P) and Secondary Location (S)	71
39. Percent Improvement vs Persistence of Cumulative Root Mean Square Error Results of Mesoscale Forecast Experiment Wind Forecasts as a Function of Forecast Interval and Number of Forecast Episodes	71
A1. Diagram of Cold Front Decision Assistance Procedure	82
A2. Four Panel Analysis of General Weather Situation (National) Composed of: (a) Pressure (mb Deviation from 1000 mb), (b) Temperature ($^{\circ}$ C), (c) 500-mb Heights (decameters), and (c) 500-mb Absolute Vorticity and 500-mb Wind Flags (m/sec)	91
A3. Four Panel Analysis of General Weather Situation (Regional) Composed of: (a) Pressure (mb Deviation from 1000 mb) and Surface Wind Flags (knots), (b) Temperature ($^{\circ}$ C), (c) 3-h Pressure Change (mb), and (d) Surface Streamlines	93
A4. Surface Divergence	95
A5. Surface Streamlines	96
A6. Surface Temperature ($^{\circ}$ C) With Overlaid Surface Wind Flags (knots)	97
A7. Surface Temperature Advection ($^{\circ}$ C/day)	99
A8. Surface Temperature Change Analysis: (a) 2-h Change ($^{\circ}$ C), (b) 3-h Change ($^{\circ}$ C), (c) 6-h Change ($^{\circ}$ C), and (d) Plot of 6-h Change ($^{\circ}$ C)	101

Illustrations

B1.	Typical East Coast Cyclogenesis Situations: (a) Secondary Cyclogenesis Along Bulge in Warm Front, (b) Secondary Cyclogenesis Near Triple Point Along Coast, (c) Secondary Cyclogenesis Near Triple Point Well Offshore, (d) Cyclogenesis Near Southeast Coast on a Stationary Front, (e) Cyclogenesis Along a Developing Front Within an Inverted Surface Pressure Trough Along Southeast Coast, and (f) Inland Cyclone Moves Toward Coast, Redevelops or Intensifies Along the Coast	113
B2.	Meridional Trough Cyclogenesis	116
B3.	Phased Short-Wave Cyclogenesis	116
B4.	Short-Wave Trough Cyclogenesis	117
B5.	Diagram of Coastal Cyclogenesis Decision Assistance Procedure	118
B6.	Four-Panel Analysis of General Weather Situation (National) Composed of: (a) Pressure (mb) Deviation from 1000 mb, (b) Temperature ($^{\circ}$ C), (c) 500-mb Heights and 500-mb Absolute Vorticity, and (d) Surface Streamlines	130
B7.	Four Panel Analysis of General Weather Situation (Regional) Composed of: (a) Pressure (mb Deviation from 1000 mb), Surface Wind Flags (knots), Weather Symbols, (b) Three-Hour Pressure Change (mb), (c) Temperature ($^{\circ}$ C), and (d) Streamlines	132
B8.	Cross-Section Analysis	134
B9.	300-mb Heights and 300-mb Absolute Vorticity	134
C1.	Diagram of Inland Cyclogenesis Decision Assistance Procedure	148
C2.	Meridional Trough Cyclogenesis	150
C3.	Split Flow Cyclogenesis	150
C4.	Phased-Short-Wave Cyclogenesis	151
C5.	Short-Wave Cyclogenesis	151
C6.	Four-Panel Analysis of General Weather Situation (National) Composed of: (a) Pressure (mb Deviation from 1000 mb), (b) Temperature ($^{\circ}$ C), (c) 500-mb Heights and 500-mb Absolute Vorticity, and (d) Surface Streamlines	159
C7.	Four-Panel Analysis of General Weather Situation (Regional) Composed of: (a) Pressure (mb Deviation from 1000 mb), Surface Wind Flags (knots), Weather Symbols, (b) Temperature ($^{\circ}$ C), (c) Three-Hour Pressure Change (mb), and (d) Surface Streamlines	162
C8.	300-mb Heights and 300-mb Absolute Vorticity	165

Tables

1. Ceiling Height Categories	23
2. 6-h QPF Categories	23
3. Data Characteristics of Mesoscale Forecast Experiment Test Cases	30
4. McIDAS Product Assessment Summary	44
5. Characteristics Assessment of Mesoscale Forecast Experiment Products	52

The Use of Interactive Graphics Processing in Short-Range Terminal Weather Forecasting: An Initial Assessment

I. INTRODUCTION

Computer-driven interactive graphics display systems can now provide extremely useful data reduction and support functions to weather operations and research efforts. As display systems have developed, the amount of data potentially available to meteorologists has increased dramatically in the past decade with the routine availability of imagery from polar-orbiting and geostationary weather satellites, radar, and other remote sensors. Video display systems provide a practical means of converting high volume raw imagery data of low information content into processed visual displays of lower volume and high information content. Conventional weather data, routinely available in weather stations from teletype and facsimile, can be accessed for plotting, analyzing, manipulating, and displaying in a virtually unlimited number of ways by resident software routines once it is stored in the computer system. It is because of the seemingly limitless ways in which the basic data can be manipulated that the potential exists of inundating the user (meteorologist) with more information and data-usage options than can be handled efficiently. This potential becomes greater, operationally, when an aviation or area forecaster is faced with a complicated weather situation that requires the preparation or updating of short-range terminal forecasts for one or more locations in his/her region of interest. On the other hand, such systems offer the opportunity

(Received for publication 28 March 1983)

of major advances in weather station operations, diverse weather support and, perhaps, short-range terminal forecast accuracy.

Recognizing the positive potential of this technology and the need to move from a manual, labor-intensive weather support function to provide more timely response to operational needs, the USAF has embarked on a base weather station modernization program called AWDS (Automated Weather Distribution System). When fully deployed, AWDS will provide support to base weather station operations worldwide and to deployed Air Force and Army tactical units. Within the Air Weather Service it is the primary mission of the base weather station to "provide operational and short-range planning support to the local commands" and to "make terminal airdrome forecasts, provide meteorological watch for points and areas, and provide local weather warnings".¹

A research and development study has been undertaken to examine the potential benefits and/or problems introduced with computer-driven interactive graphics video display systems in the preparation and monitoring (met-watching) of short-range terminal airdrome forecasts. A mesoscale forecasting experiment (described in Section 3) was designed to assess:

- (1) the value of certain mesoscale objective plot, analysis and forecast procedures in the preparation of short-range terminal forecasts,
- (2) the relative difficulty in preparing certain forecasts (elements) using an interactive graphics system,
- (3) the value of certain remotely sensed data in short-range terminal forecasting, and
- (4) the performance of forecasters, in weather episodes with substantial meso-scale variability, in generating both numerical (deterministic) and probabilistic terminal forecasts using an interactive graphics system.

The forecast preparation and met-watching aspects of the experiment were structured to simulate the process and requirements of providing the base weather station support stated above.

2. INTERACTIVE COMPUTER GRAPHICS SYSTEMS

2.1 Automated Weather Distribution System (AWDS)

AWDS will provide a new era of base-level weather support in the Air Force, one in which environmental data and products will be acquired, stored, displayed, analyzed and forecast through modernized computer and dedicated communication

1. Air Weather Service (1982) Air Weather Service Capabilities Master Plan (CMP) 1982-1986, Hq AWS, Scott AFB, Illinois.

systems. In its initial configuration, however, the principal weather data sources will be mainly those presently being used throughout Air Weather Service, namely from the Air Force Global Weather Central (AFGWC) and the Automated Weather Network (AWN). The AWN collects, edits, reformats and transmits weather data between base weather stations worldwide. These data include alphanumeric products such as hourly and special surface weather observations, twice-daily rawinsonde (upper-air) observations, plain language text including advisories, terminal forecasts, and map discussions, which are presently received at base weather stations via the COMEDS teletype circuits. Products available in weather stations from AFGWC include various surface and upper-air analysis and forecast maps that are received via the Air Force's facsimile circuit (AFDIGS). With AWDS these data products will flow directly into an on-site computer facility designed to store, process, and display weather data fields on alphanumeric and color graphic terminals. Resident software in the base weather station's AWDS computer will allow the weatherman-user to request the execution of a wide range of analysis and forecast-guidance procedures.

With AWDS there will be an important difference in the format of data flowing from AFGWC in that objectively-determined analysis and forecast products will be Uniformly Gridded Data Fields (UGDF). That is, the individual, regularly-spaced gridpoint values will be transmitted to base weather stations where they can be contoured and displayed in map form, as required by the weatherman-user. In addition, data flowing from AFGWC will include vector graphic products to describe weather maps, charts, and figures and raster scan products (initially limited to AFGWC's Satellite Global Data Base). The Satellite Global Data Base (SGDB) is comprised mainly of 3 nm resolution visible and IR satellite imagery for each hemisphere. Raw imagery input to the SGDB comes from available polar-orbiting satellites (for example, DMSP and NOAA), which is integrated into the SGDB in real-time after imagery from each quarter-orbit is received at AFGWC. At any one point in time, therefore, the individual pixel values in the global SGDB may come from observations made several hours apart. This characteristic greatly limits the value of the SGDB in mesoscale or short-range forecasting applications.

2.2 Man-computer Interactive Data Access System (McIDAS)

The McIDAS facility at AFGL has access to most of the data that will be available through the Automated Weather Distribution System (AWDS) with the major exceptions being the Uniformly Gridded Data Fields (UGDF) and Satellite Global Data Base (SGDB) from AFGWC. For most short-range forecasting purposes, the forecast grids of the Uniformly Gridded Data Fields (UGDF) have limited value and the analysis grids can be reproduced with McIDAS by analyzing surface and

rawinsonde data. There are other data sources and capabilities available within our McIDAS that are potentially valuable in short-range terminal forecasting applications. One of the purposes of this study is to examine the value of data sources [those planned with the Automated Weather Distribution System (AWDS) and those potentially available through AWDS but not presently planned] to base weather station terminal forecast operations.

Figure 1 is a functional depiction of AFGL's McIDAS, which is similar in its configuration and software to the system originally developed at the University of Wisconsin.² Conventional observational data are obtained by means of the FAA medium speed data link (WB 604). It also provides two other potentially-useful data sources; FOUS bulletins derived from the LFM-II model run at the National Meteorological Center (NMC) twice daily and manually digitized radar (MDR) national summaries that are compiled hourly. Geosynchronous satellite data are available in real-time, normally on a half-hour cycle. Both visible (daytime only) and infrared digital imagery are ingested through the antenna-based Data Acquisition System and, once into the system, are available for accurate geographical and political gridding, enhancement and contouring, sequencing to form time-series loops for cloud tracking or translation purposes and being overlaid with conventional and radar data for integrated displays. Through the Operators Console, the weatherman-user has rapid access to the resident data bases and can request specific data plot, analysis or forecast techniques to be implemented (typically the displayed product is depicted in a minute or less).

It had been found in earlier experimentation with McIDAS for short-range forecasting purposes³ that the lack of radar data can impose limitations on a forecaster's preparation of a short-range terminal forecast. In addition, the objective analysis scheme (a one-pass version of the Cressman successive approximation technique) was often found to unduly suppress mesoscale features. Short-range terminal forecasting puts additional demands on the routine navigation used to properly earth-locate the GOES images and methods used to enhance gray scale contrast of cloud-cloud, cloud-land, and land-water boundaries. Methods to resolve these deficiencies in McIDAS' routine procedures to process satellite imagery were implemented (see Gerlach⁴ for details).

-
2. Smith, E. A. (1975) The McIDAS System, IEEE Trans. Geosci. Elec., GE-13:123-136.
 3. Gerlach, A. M., Ed. (1980) Development of Automated Objective Meteorological Techniques, AFGL-TR-81-0017, Contract F19628-79-C-0033, pp 46-51, AD A097718.
 4. Gerlach, A. M., Ed. (1981) Technique Development for Weather Forecasting, AFGL-TR-82-0020, Contract F19628-81-C-0039, pp 115-116, AD A118744.

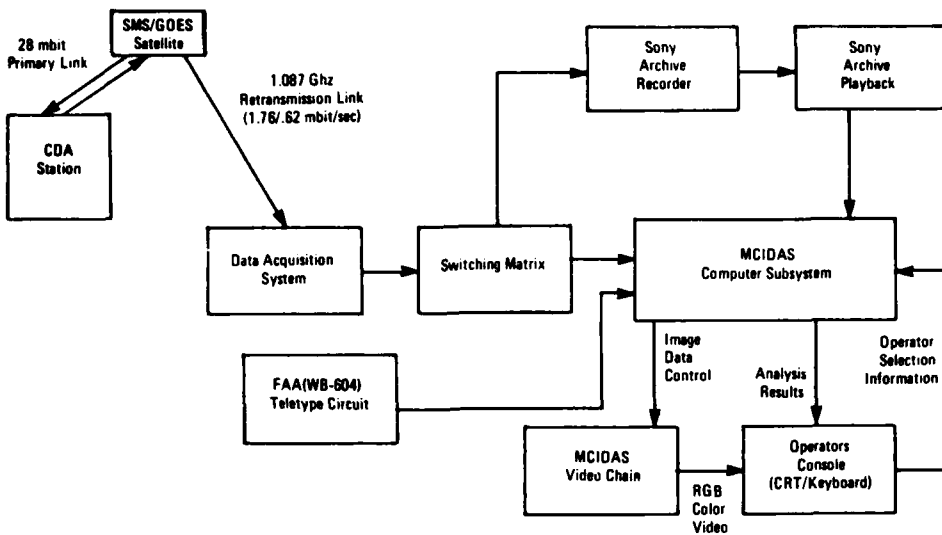


Figure 1. AFGL McIDAS Functional Block Diagram

In addition, new color enhancement procedures were developed for IR imagery based on IR temperature thresholds rather than gray scale values. The first of these, invoked by the weatherman-user with the key-in ENT, enhances 10°C intervals from 30 to -50° C according to a predefined color scheme. This produces a display which in effect is a color contoured field of atmospheric "skin" temperatures. The second command is invoked by the key-in ET, accompanied by user-specified lower and upper temperature values and color intensities, which enhance the specified range and retain any existing enhancement. This option can be particularly useful when the forecaster wants to isolate and evaluate a specific cloud feature, such as cumulus development or precipitation-generating middle clouds.

Prior to conducting this Mesoscale Forecasting Experiment, several new processing and display software routines were developed to increase the availability of mesoscale information. Included were procedures to remap, analyze and display the manually digitized radar (MDR) data, a mesoscale objective analysis technique based on Barnes,⁵ station model and individual parameter time series plot routines,

5. Barnes, S. L. (1964) A technique for maximizing details in numerical weather map analysis, J. Appl. Meteor., 3:396-409.

and a 2-D trajectory forecast model⁶ coupled with satellite-based sensible weather algorithms.⁷

The routines to process manually digitized radar data (see Gerlach⁴ for details) provide the weatherman-user with contoured output levels from the NWS Digital Video Integrator and Processor (DVIP) on map displays covering the continental U.S., one of three regional areas, standard McIDAS state displays (see Figure 2) or standard McIDAS city displays (see Figure 3). Manually digitized radar (MDR) analyses can be time-sequenced (looped), overlaid on concurrent satellite imagery and can have observational data overlaid on it. One or more simple keyboard instructions regarding the time, location and display options will cause internal and automatic sequencing from one program to the next within the system to generate contoured MDR grids. The keyboard instruction, or key-in, that activates MDR processing is MR. It will be referred to later in Section 4.1.

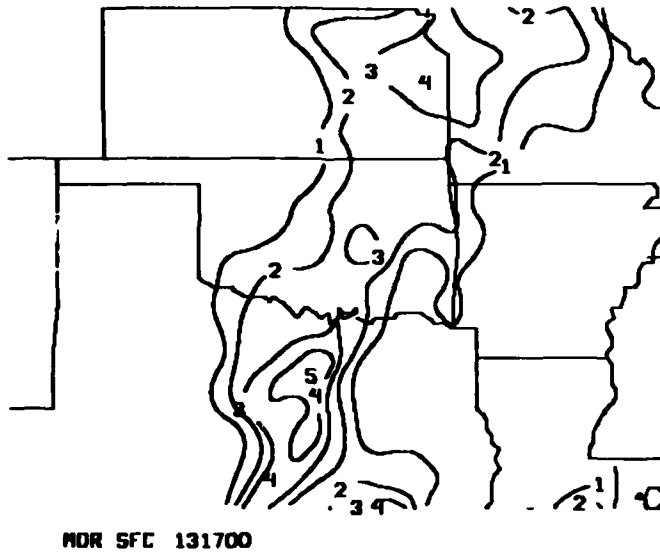


Figure 2. MDR State Display Centered on Oklahoma (OK)

-
6. Wash, C. H., and Whittaker, T. M. (1980) Subsynoptic analysis and forecasting with an interactive computer system. Bull. Am. Meteorol. Soc., 61(No. 12):1584-1591.
 7. Muench, H. S. (1981) Short-range Forecasting of Cloudiness and Precipitation Through Extrapolation of GOES Imagery, AFGL-TR-81-9218, AD A108678.

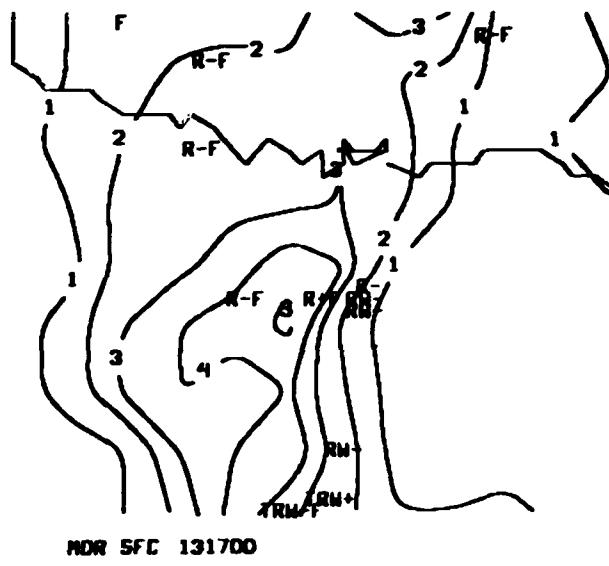


Figure 3. MDR City Display Centered on Dallas-Fort Worth (DFW) with Overlaid Weather Symbols

The Barnes objective analysis technique selected to enhance mesoscale detail in surface analyses includes five passes through the observed data using a decreased scan radius with each successive pass.⁸ Its key-in on McIDAS is KZ. The mesoscale analysis routine differs from the standard one-pass Cressman technique in that it creates the analysis for a 0.5 deg latitude grid rather than a 1 or 2 deg grid. This limits the displayed analysis to an area of 4 deg latitude by 6 deg longitude, controlled by the McIDAS city (3-letter call station) depiction. Figures 4 and 5 are surface temperature analyses generated by the standard analysis routine (Figure 4) and the five-pass Barnes routine (Figure 5) that illustrate the added detail retained by emphasizing mesoscale aspects.

8. Gerlach, A. M., Ed. (1982) Objective Analysis and Prediction Techniques, AFGL-TR-82-0394, Contract F19628-82-C-0023.

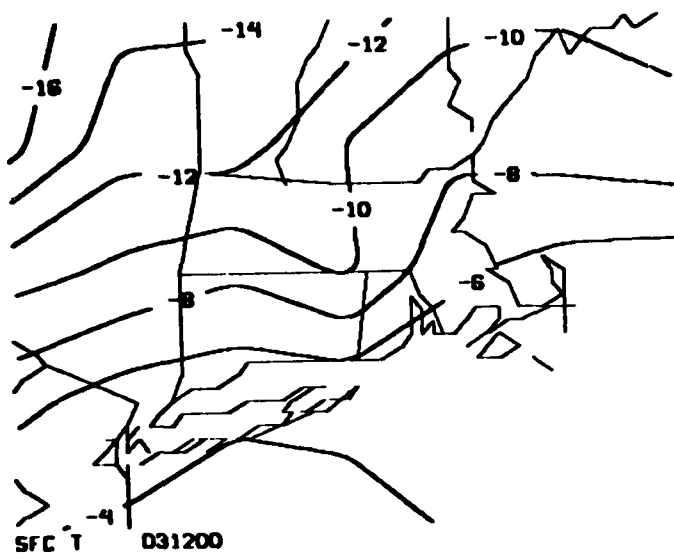


Figure 4. Temperature Analysis—One-pass Cressman Technique

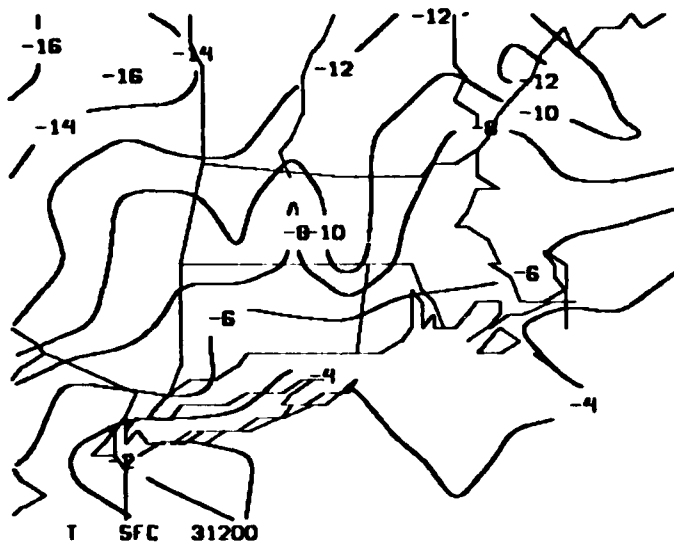


Figure 5. Temperature Analysis—Five-pass Barnes Technique

Two new observation plot routines, designed to enhance the depiction of mesoscale detail in emerging weather situations, were developed for use in the Mesoscale

Forecast Experiment.⁸ The first, invoked with an MS key-in, was a station-model time-series display, as illustrated in Figure 6. Its design allows the weatherman-user to select up to six weather stations and the end point of the time series desired.

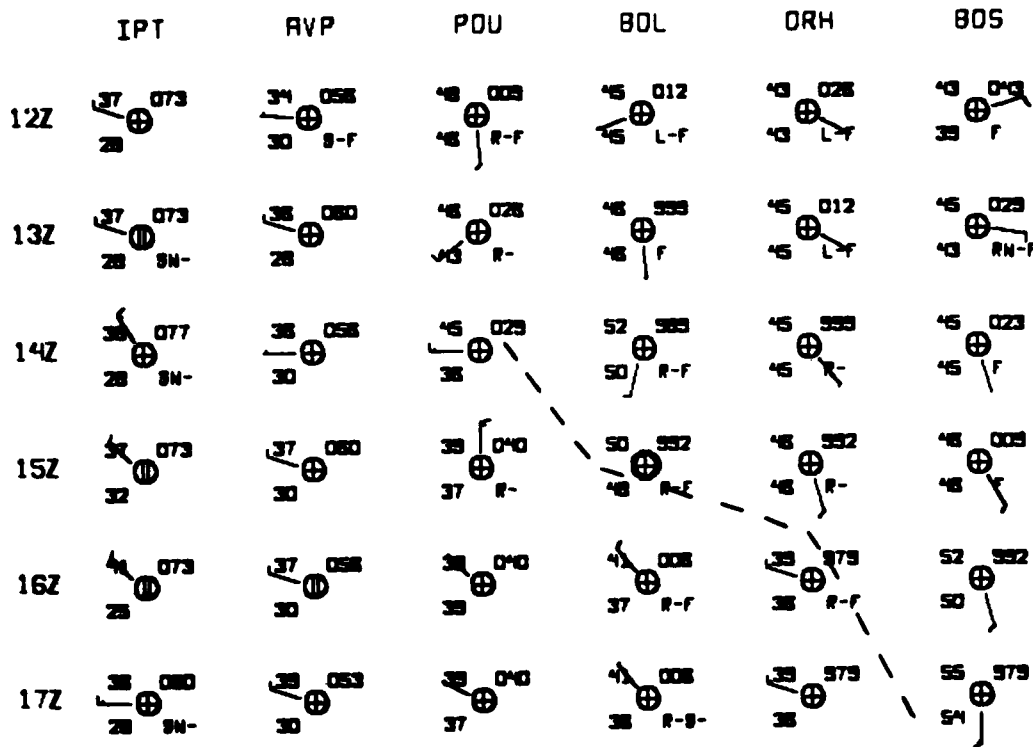


Figure 6. Station-Model Time-Series Display for 26 Mar 1982

The displayed product includes the six one-hourly observations of temperature, dewpoint, surface pressure, present weather, cloud cover, and wind speed and direction in symbolic station model format. This plotting model can aid in locating and tracking (hour-to-hour) synoptic and mesoscale features such as wind shift/frontal boundaries, dry lines and areas of precipitation. One compromise was made in structuring the MS display, namely that the distance between observation stations on the display is not proportional to their actual geographic separation. The user must take care then to factor this into the assessment of weather system translation. The second routine, invoked with a GT key-in, generates a time series line graph display of some specified parameter (temperature, dewpoint, surface pressure, or wind speed) or a bar graph display of others (cloud height and cloud cover). The

line graph format (shown in Figure 7) can accommodate up to 24 h of data and up to six stations on any one display. The bar graph format can accommodate cloud observations for up to six stations at one time (shown in Figure 8) or up to six observations at one station. Multiple cloud layers can be displayed and cloud cover categories are indicated by dots (scattered), dashes (broken) and solid (overcast).

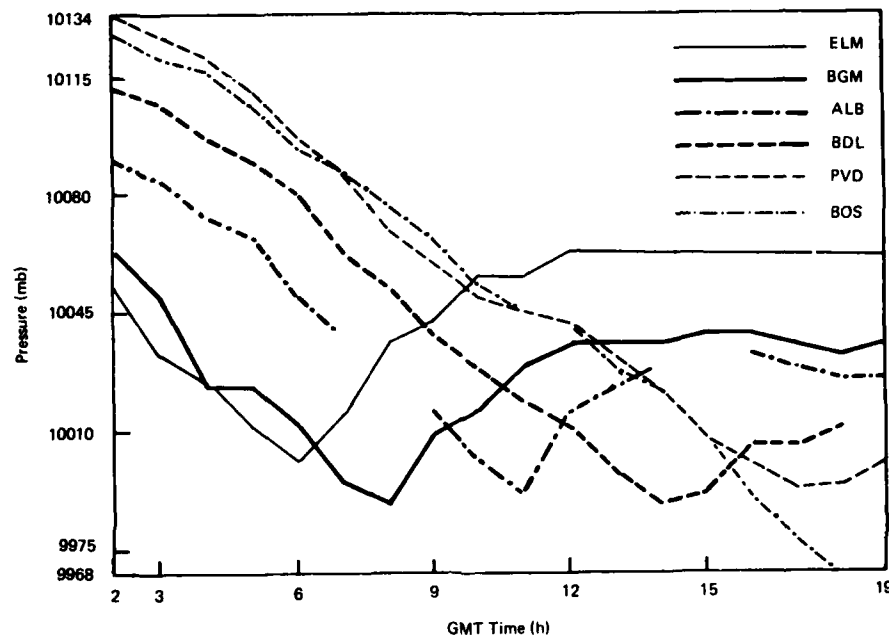


Figure 7. Line Graph Plot of Surface Pressure for 26 Mar 1982

A forecast guidance technique, implemented on McIDAS for the Mesoscale Forecast Experiment, represents a consolidation of methods developed independently in earlier studies.^{6,7} The first, McIDAS key-in PF, calculates a two-dimensional backward trajectory on a single level (for example, 700 mb) or in a single layer (for example a mean density-weighted wind for the 850-500 mb layer) from objectively analyzed rawinsonde winds. The time duration of the trajectory can be specified by the user and, at each hourly trajectory location, a forecast value interpolated from an objectively analyzed grid translated to the forecast location is displayed. Any weather element (for example, ceiling heights) that can be analyzed to a grid can be forecast in this manner. The second, McIDAS key-in CC, estimates the cloud cover category and 1-h precipitation amount from collocated GOES visible

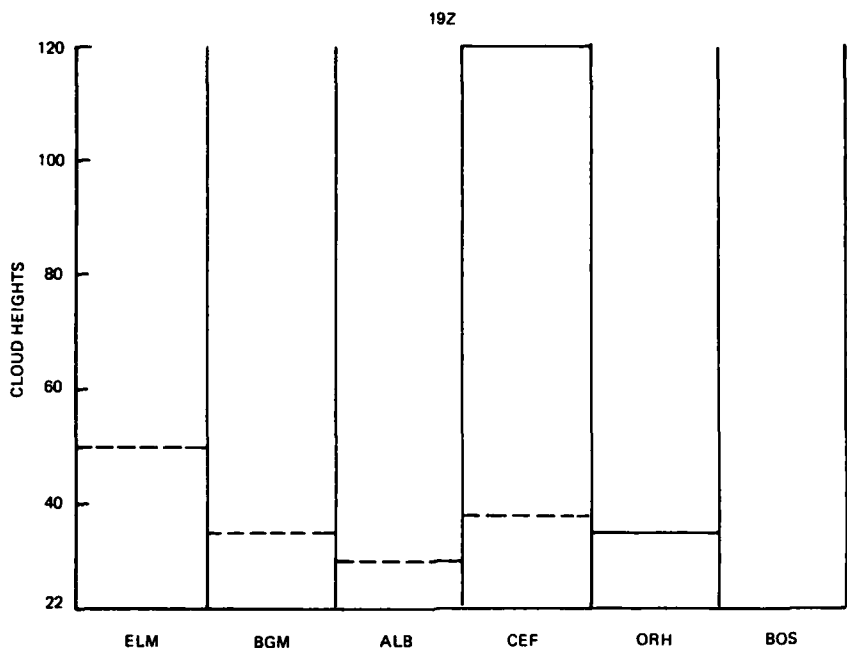


Figure 8. Bar Graph Plot of Cloud Heights

and infrared imagery for an area designated by the electronic cursor. The algorithms, developed on a sample of non-convective storms in the fall and early winter of 1980,⁷ require that the visible brightness values be normalized to correct for solar geometry and anisotropic scattering and that the IR temperatures be adjusted to equivalent black body values. By consolidating these methods, the McIDAS key-in FOR can utilize the calculated trajectory (from PF) to specify six one-hourly upstream locations at which to apply the cloud cover category and 1-h precipitation amount estimating routine (CC). The six consecutive hourly estimates of precipitation amount can then be combined to generate a 6-h quantitative precipitation forecast (QPF).

Based on the earlier experimentation,³ we concluded that an interactive system could be more helpful in operational forecasting if procedures were available within the system to aid the weatherman-user in focusing on the more important aspects of the forecast problem at hand. With that in mind, studies were undertaken to systematize "forecast decision assistance procedures" for certain generic and recurring weather events. The events selected for study were advancing cold fronts, coastal cyclogenesis, and inland cyclogenesis. The results of these studies are included as Appendixes A, B, and C. Of the three, only the Cold Front Decision

Assistance Procedure was available within McIDAS at the time of the Mesoscale Forecast Experiment. Its key-in is FCS. The interactive procedure, available to the weatherman-user, consists of a series of "menu-styled" instructions intended to guide the user through existing analysis and display routines to accurately locate the cold front, follow its development and movement, resolve the distribution and evolution of weather elements in conjunction with the frontal system, and translate that information into a specific forecast for his/her terminal(s). Such a procedure would be particularly useful as a training or orientation aid for new forecasters and personnel new to the use of interactive graphics systems.

3. MESOSCALE FORECAST EXPERIMENT

The procedure established to assess aspects of interactive systems, data sources, and weatherman-user effectiveness was to conduct a forecast test experiments addressing a particular set of short-range terminal forecasting requirements using research meteorologists. Two Mesoscale Forecast Experiment test periods were established; the first to be conducted in the summer of 1982, the second in the summer of 1983. This report is concerned with the results of the 1982 test. To conduct the 1982 test most efficiently, data were archived during winter and early spring storm episodes in 1981-82 in the Northeast U.S. The archived data sets were then restored in McIDAS for the Mesoscale Forecast Experiment, which took place over a 12-week period starting in May 1982. Ten archived episodes were used in the experiment. They are described in Section 3.2. In the Mesoscale Forecast Experiment, the time available for forecast preparation was controlled to real-time limits. The forecasters had a single task and objective during the test; prepare terminal forecasts for two locations using as many of the resources available to them through McIDAS as possible for the purpose of evaluating new and standard products and data sources. One forecast case (winter/early spring storm episode) was conducted each week (typically in two, 4-h periods per forecaster and with three forecasters working together to evaluate the weather situation but independently preparing their forecasts). At the conclusion of each case, each forecaster completed evaluation forms (see Section 3.1) in which the products used and the forecast aspects of the case were assessed. These then, formed the basis for addressing purposes (1), (2) and (3) of the Mesoscale Forecast Experiment as described in the Introduction.

3.1 Experimental Procedures

The specific requirements laid on the forecasters were to forecast (on an hourly cycle) wind speed and direction, total cloud amount, and ceiling height for

periods of 1, 2, 4, and n hours ahead. The period n was the closest interval (greater than 4 h) between forecast time and 06, 12, 18 or 00Z. In addition, 6-h quantitative precipitation forecasts (QPF) were prepared each hour for the "next" full 6-h period ending at 06, 12, 18 or 00Z. Forecasts for two airfield locations were required for each case; the specific locations were predicated on the availability of FOUS bulletins containing model output statistics (MOS), LFM-II guidance and 3-D trajectory forecasts that were made available to the forecasters for guidance purposes. Logan International Airport, Mass. (BOS) being the closest candidate location to AFGL, was a forecast location in each of the cases used in the test. The second location varied among Bradley International Airport, Conn. (BDL), Kennedy International Airport, N.Y. (JFK) and Green Airport, R.I. (PVD) depending on factors related to the episode being tested (see Section 3.2 for specifics).

For wind speed and direction, a numerical or deterministic forecast was prepared. For each of the other elements, both numerical and probability forecasts were prepared. For total cloud amount, the category (clear, scattered, broken or overcast) and the probability of occurrence of each category were required; for ceiling height, a specific height (in 100 ft) and probabilities for the categories listed in Table 1; and for QPF, the 6-h precipitation amount (in inches) and the probabilities for the categories listed in Table 2.

Table 1. Ceiling Height Categories

Category	1	2	3	4	5	6
Height (100 ft)	0-1	2-4	5-9	10-29	30-74	≥ 75

The category breakdown for total cloud amount, ceiling height and 6-hr QPF are compatible with categories of Model Output Statistics (MOS) and related guidance.

Table 2. 6-h QPF Categories

Category	1	2	3	4
QPF (in.)	0-0.24	0.25-0.49	0.50-0.99	≥ 1.00

Computer-based forecast entry and verification procedures previously implemented for preliminary experiments on McIDAS were modified for the MFE.^{3,4} Basically, they were expanded to allow for ceiling height and QPF forecasts. This procedure, referred to as the Mesoscale Forecast Facility (MFF), is a "menu-driven" interactive system designed to ingest individual forecasts into a data file through the use of formatted interrogation/response messages via the McIDAS' keyboard/alpha-numeric CRT terminal interface. Figure 9 depicts a sample message in its interrogation format (part a) and response format (part b). Each of the six principal participants in the experiment had reserved storage in McIDAS in which individual forecasts and verification statistics were accumulated.

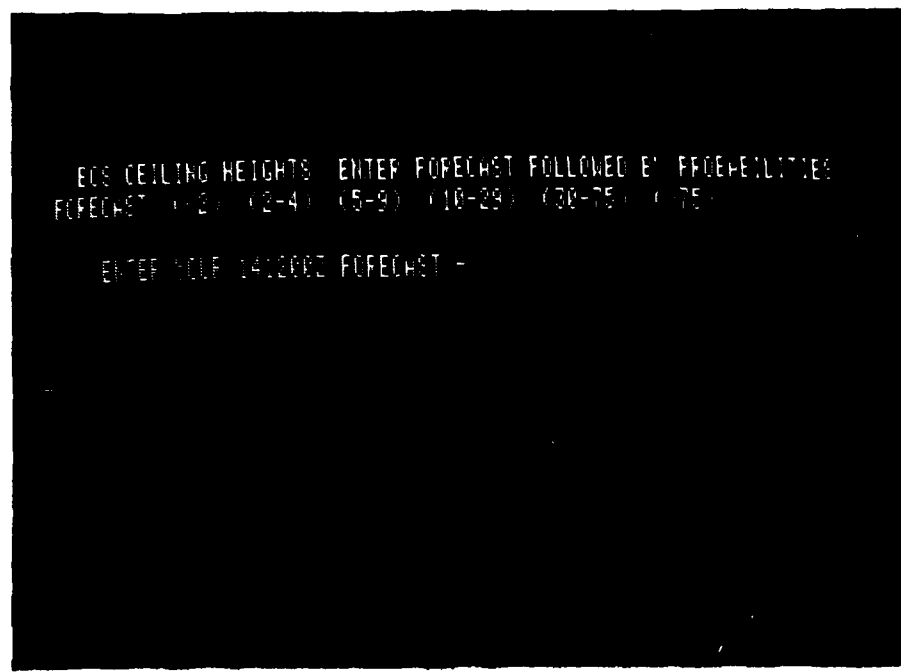
The assessment forms completed after each case are shown in Appendix D. The purpose of the Mesoscale Forecast Variable Assessment was to establish the relative difficulty in preparing forecasts of each element and to try to isolate the reason(s) for the difficulties encountered. An assessment form was completed for each of the forecast elements. The Product Usefulness Assessment was used to measure the relative value in terminal forecasting of the objective display features in McIDAS, especially the new ones created for this experiment. The forecasters were directed to judge the most and least useful products (for the case just completed) and give reasons why they were so rated. In addition, for each product that was used, they completed a form designed to measure characteristics of the coverage, resolution and timeliness of the information available with the particular display.

After each case, the numerical and probability forecasts were verified within the Mesoscale Forecast Facility, and accumulated statistics were summarized and made available to the forecasters for review. Figure 10 is a sample of the accumulated verification statistics compiled for a forecaster. Separate statistics were computed for predictions verified for Logan (BOS) which are denoted PRIMARY, for the other station (denoted SECONDARY) and for the combined verification. The error statistics calculated were: mean absolute error (MAE) and root-mean-square-error (rmse) for numerical forecasts and the p-score (p) and cumulative p-score (cp) for probability forecasts. Mean Absolute Error is computed from:

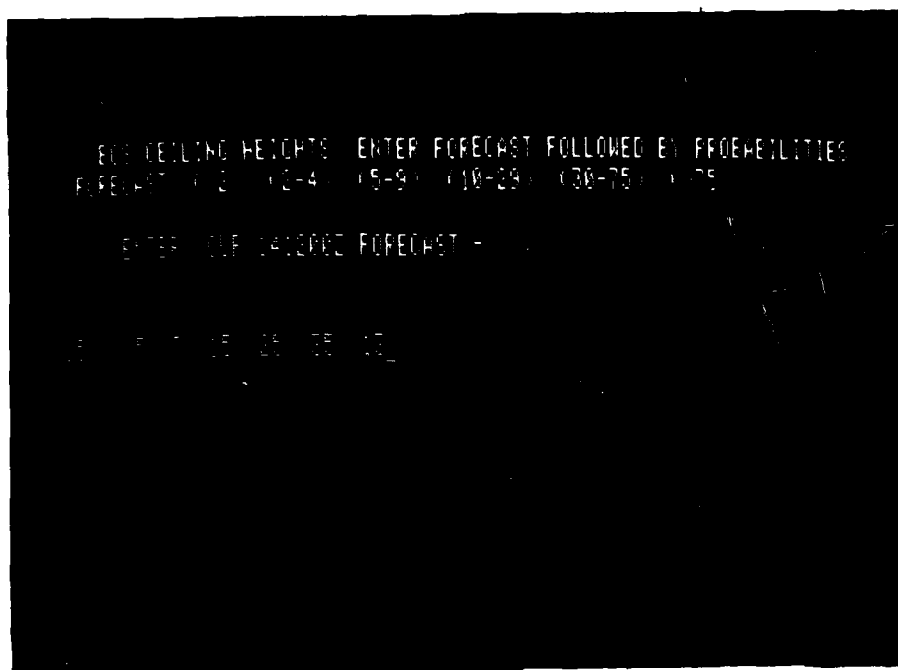
$$MAE = \frac{1}{N} \sum_{i=1}^N |F_i - O_i| \quad (1)$$

where F_i is the forecast value, O_i the observed value and N the number of forecasts. Root-mean-square-error is computed from:

$$rmse = \left[\frac{1}{N} \sum_{i=1}^N (F_i - O_i)^2 \right]^{1/2}. \quad (2)$$



(a)



(b)

Figure 9. Example of "Menu-Driven" Interactive Procedure Used for Forecast Entry Into Automated Verification Phase of the Mesoscale Forecast Experiment; (a) Interrogation Format and (b) Response Format

PREDICTAND	1 HOUR FORECAST	2 HOUR FORECAST	4 HOUR FORECAST	N HOUR FORECAST
WIND	NUMBER OF FORECASTS: 108 PRIMARY 54 SECONDARY 54 MEAN ABS. ERROR: 3.88 RMS ERROR: 4.59 PRIMARY 4.21 SECONDARY 4.92 MEIDKE SCORE: PRIMARY .01 SECONDARY -.25	NUMBER OF FORECASTS: 108 PRIMARY 54 SECONDARY 54 MEAN BS. ERROR: 4.75 RMS ERROR: 5.65 PRIMARY 5.04 SECONDARY 6.21 MEIDKE SCORE: PRIMARY .06 SECONDARY .33	NUMBER OF FORECASTS: 108 PRIMARY 54 SECONDARY 54 MEAN ABS. ERROR: 6.13 RMS ERROR: 7.47 PRIMARY 6.36 SECONDARY 8.44 MEIDKE SCORE: PRIMARY .40 SECONDARY -.05	NUMBER OF FORECASTS: 108 PRIMARY 54 SECONDARY 54 MEAN ABS. ERROR: 7.72 RMS ERROR: 8.54 PRIMARY 8.50 SECONDARY 8.59 MEIDKE SCORE: PRIMARY .29 SECONDARY .19
CLOUD AMOUNT	NUMBER OF FORECASTS: 108 PRIMARY 54 SECONDARY 54 MEAN ABS. ERROR: 1.13 RMS ERROR: .15 PRIMARY .38 SECONDARY .38 P-SCORE: .20 PRIMARY .15 SECONDARY .26 CUMULATIVE P-SCORE: PRIMARY .04 SECONDARY .04 MEIDKE SCORE: PRIMARY .17 SECONDARY .10	NUMBER OF FORECASTS: 108 PRIMARY 54 SECONDARY 54 MEAN BS. ERROR: .07 RMS ERROR: .30 PRIMARY .24 SECONDARY .36 P-SCORE: .13 PRIMARY .09 SECONDARY .16 CUMULATIVE P-SCORE: PRIMARY .02 SECONDARY .01 MEIDKE SCORE: PRIMARY .67 SECONDARY .68	NUMBER OF FORECASTS: 108 PRIMARY 54 SECONDARY 54 MEAN ABS. ERROR: .10 RMS ERROR: .35 PRIMARY .41 SECONDARY .27 P-SCORE: .14 PRIMARY .16 SECONDARY .13 CUMULATIVE P-SCORE: PRIMARY .03 SECONDARY .02 MEIDKE SCORE: PRIMARY .78 SECONDARY .86	NUMBER OF FORECASTS: 108 PRIMARY 54 SECONDARY 54 MEAN ABS. ERROR: .20 RMS ERROR: .64 PRIMARY .86 SECONDARY .27 P-SCORE: .20 PRIMARY .30 SECONDARY .11 CUMULATIVE P-SCORE: PRIMARY .04 SECONDARY .03 MEIDKE SCORE: PRIMARY .74 SECONDARY .89
CEILING HEIGHT	NUMBER OF FORECASTS: 108 PRIMARY 54 SECONDARY 54 MEAN ABS. ERROR: 67.15 RMS ERROR: 217.00 PRIMARY 228.98 SECONDARY 204.55 P-SCORE: .48 PRIMARY .49 SECONDARY .46 CUMULATIVE P-SCORE: PRIMARY .05 SECONDARY .05	NUMBER OF FORECASTS: 108 PRIMARY 54 SECONDARY 54 MEAN BS. ERROR: 35.83 RMS ERROR: 126.40 PRIMARY 112.38 SECONDARY 139.02 P-SCORE: .58 PRIMARY .65 SECONDARY .51 CUMULATIVE P-SCORE: PRIMARY .05 SECONDARY .05	NUMBER OF FORECASTS: 108 PRIMARY 54 SECONDARY 54 MEAN ABS. ERROR: 33.45 RMS ERROR: 104.31 PRIMARY 136.86 SECONDARY 55.09 P-SCORE: .76 PRIMARY .72 SECONDARY .81 CUMULATIVE P-SCORE: .07 PRIMARY .08 SECONDARY .06	NUMBER OF FORECASTS: 108 PRIMARY 54 SECONDARY 54 MEAN ABS. ERROR: 93.54 RMS ERROR: 255.97 PRIMARY 282.30 SECONDARY 226.60 P-SCORE: .88 PRIMARY .79 SECONDARY .97 CUMULATIVE P-SCORE: .12 PRIMARY .09 SECONDARY .11 MEIDKE SCORE: PRIMARY .47 SECONDARY .37

Figure 10. Example of Verification Statistics Compiled for Forecaster After Each Episode
(Example shows statistics after 10th episode)

The Brier or p-score⁹ measures the mean-squared probability error and is computed from:

$$p = \frac{1}{N} \sum_{i=1}^N \left[\sum_{j=1}^n (F_{ij} - O_{ij})^2 \right] , \quad (3)$$

where n is the number of forecast categories for the element, F_{ij} is the forecaster probability for the category and O_{ij} is its observed probability. If the verifying observation falls within the range of a category then the observed probability is 1.0, if it falls outside the range then the observed probability is 0.0. The cumulative p-score is analogous to the ranked probability score proposed by Epstein¹⁰ for evaluating ranked categories. It (cp) is computed from:

$$cp = \frac{1}{N(n-1)} \sum_{i=1}^N \left[\sum_{k=1}^n \left(\sum_{j=1}^n F_{ij} - \sum_{j=1}^n O_{ij} \right)^2 \right] . \quad (4)$$

The method of comparison for the study was persistence, measured directly and in sample (unconditional) climatology form. The Heidke skill score (SS), which measures the percent difference (improvement) of verification scores relative to a set of control forecasts, was calculated using persistence as the control. To calculate skill scores for wind forecasts, the rmse results were used in

$$SS1 = \frac{rmse_p - rmse_f}{rmse_p} \quad (5)$$

where $rmse_p$ is based on a persistence forecast of the wind vector and $rmse_f$ is the forecaster's statistic. For the other elements, the cumulative p-score results were used in

$$SS2 = \frac{cp_p - cp_f}{cp_p} \quad (6)$$

where the p-subscript refers to persistence and f the forecaster. The persistence probability forecast was generated by (a) directly assigning a probability of 1.0 to the category that pertained at forecast (initial) time and a probability of 0.0 to the categories that did not pertain and (b) using sample climatology statistics.

-
- 9. Brier, G. W. (1950) Verification of forecasts in terms of probability, Mon. Wea. Rev., 78:1-3.
 - 10. Epstein, E. A. (1969) A scoring system for probability forecasts of ranked categories, J. Appl. Meteorol., 8:985-987.

Sample climatology results were not compared with quantitative precipitation forecasts (QPF) because of limited sample size. For total cloud amount, the unconditional sample climatology was: clear (0.07), scattered (0.11), broken (0.09), and overcast (0.73). For ceiling height it was by category: 1 (0.02), 2 (0.01), 3 (0.14), 4 (0.18), 5 (0.30), and 6 (0.35) where the category numbers are those defined in Table 1. Each climatology is based on the 120 observations that comprised the conditions that existed at forecast (initial) times for the 10-episode Mesoscale Forecast Experiment sample.

Although not used for direct comparisons in the experiment (that is, compared by means of skill score), the Generalized Exponential Markov (GEM) technique¹¹ was adapted to McIDAS and evaluated on the 10-case sample. GEM predicts the probability distribution of all local surface weather elements hour-by-hour using only the current local surface weather conditions as predictors. The GEM model that was applied is a generalized model originally developed from data at 41 U.S. locations. The output of the GEM technique was not available to the forecasters during this test. It was implemented and evaluated after the test was completed. It will be available during a follow-on test scheduled for Summer 1983. Forecast guidance information derived from NMC's LFM (FOUS Bulletins) was available to the forecasters during the Mesoscale Forecast Experiment in teletype form for the forecast stations. It included the MOS¹² forecasts (FOUS 12), LFM Guidance forecasts (FOUS 60-78)¹³ and 3-D trajectory¹⁴ forecasts (FOUS 50-57). Like GEM, FOUS guidance was not available through McIDAS during this test but has since been integrated into McIDAS to make its wide range of display products available.⁸ The verification of model output statistics was limited to the n-hour forecasts (which verified at 06, 12, 18 or 00Z).

-
11. Miller, R. G. (1981) GEM: A Statistical Weather Forecasting Procedure, NOAA-TR-NWS-28.
 12. Glahn, H. R., and Lowry, D. A. (1972) The use of model output statistics (MOS) in objective weather forecasting, J. Appl. Meteorol., 11:1203-1211.
 13. National Weather Service (1981) FOUS 60-78 Bulletins, NOAA-NWS Tech. Proc. Bull. No. 294.
 14. Reap, R. M. (1972) An operational three-dimensional trajectory model, J. Appl. Meteorol., 11:1193-1202.

3.2 Test Sample

The weather episodes selected for study in the Mesoscale Forecast Experiment were 1981-1982 winter and early spring storm events occurring over the Northeast U.S. To be eligible as a forecast experiment, an episode had to meet two basic requirements. First a 12-24 h period of significant weather in the form of changing cloud cover, ceiling height or winds and/or the occurrence of precipitation in southern New England was required to fully test the utility of an interactive graphics system and forecast aids in preparing short-range mesoscale forecasts. Second, a complete 24-h data set, consisting of conventional hourly surface observations, upper-air data and satellite imagery, along with any other available data or guidance (MDR, MOS, and so forth) was required. This would provide 6-12 h of data for pre-forecast familiarization with the weather situation, 6 h for forecasting and up to 12 h for verification.

The 10 cases chosen for the Mesoscale Forecast Experiment were selected from among 20 cases that had been archived. They comprised three general synoptic situations; midwest cyclones, New England cold fronts, and east coast cyclogenesis, each bringing significant weather changes to New England. Table 3 lists the date, forecast times, forecast stations, a brief synoptic description, and data sources available for each forecast experiment. It should be noted that BOS was the primary forecast station for all ten experiments. The secondary station (PVD, BDL or JFK) was chosen according to the completeness of that station's data sets and the potential of the weather which occurred at that station to provide the best assessment of the products being evaluated. Figures 11 and 12 list the 24 hourly observations of cloud cover, wind speed and direction, ceiling height, 6-h precipitation amount and present weather for the primary forecast station (BOS) and secondary station during each forecast experiment. The general synoptic situation for each case is described below. A surface pressure analysis and 500 mb height analysis near the initial forecast time for each experiment is shown in Figures 13 to 22.

Table 3. Data Characteristics of Mesoscale Forecast Experiment Test Cases

Forecast Experiment Number	Forecast Date / Times	Forecast Stations	Situation	Data Available *				
				Satellite	MDR	SVCA	RAOB	Guidance
1	3/26/82 14-16Z 17-19Z	BOS JFK	cold front moving through New England	Y	N	Y	Y	Y
2	4/26/82 19-21Z 22-00Z	BOS PVD	weak frontal wave moving toward New England	Y	P	Y	Y	Y
3	3/31/82 05-07Z 08-10Z	BOS PVD	approaching pre-frontal cloud band	Y	P	Y	Y	Y
4	4/27/82 14-16A 17-19Z	BOS JFK	cold front moving through New England	Y	P	Y	Y	Y
5	3/11/82 18-20Z 21-23Z	BOS PVD	approaching pre-frontal cloud band	Y	P	Y	Y	N
6	12/15/81 18-20Z 21-23Z	BOS JFK	rapidly deepening cyclone approaching New England	Y	P	Y	Y	N
7	12/1/81 17-19Z 20-22Z	BOS JFK	warm frontal wave approaching New England	Y	P	Y	Y	N
8	3/4/82 17-19Z 20-22Z	BOS PVD	cold front approaching New England	Y	P	Y	Y	N
9	12/22/81 06-08Z 9-11Z	BOS BDL	overrunning precipitation	Y	P	Y	Y	N
10	4/6/82 04-06Z 07-09Z	BOS BDL	explosive coastal cyclogenesis	Y	P	Y	Y	Y

* Y - full set available, N - none available, P - partial set available

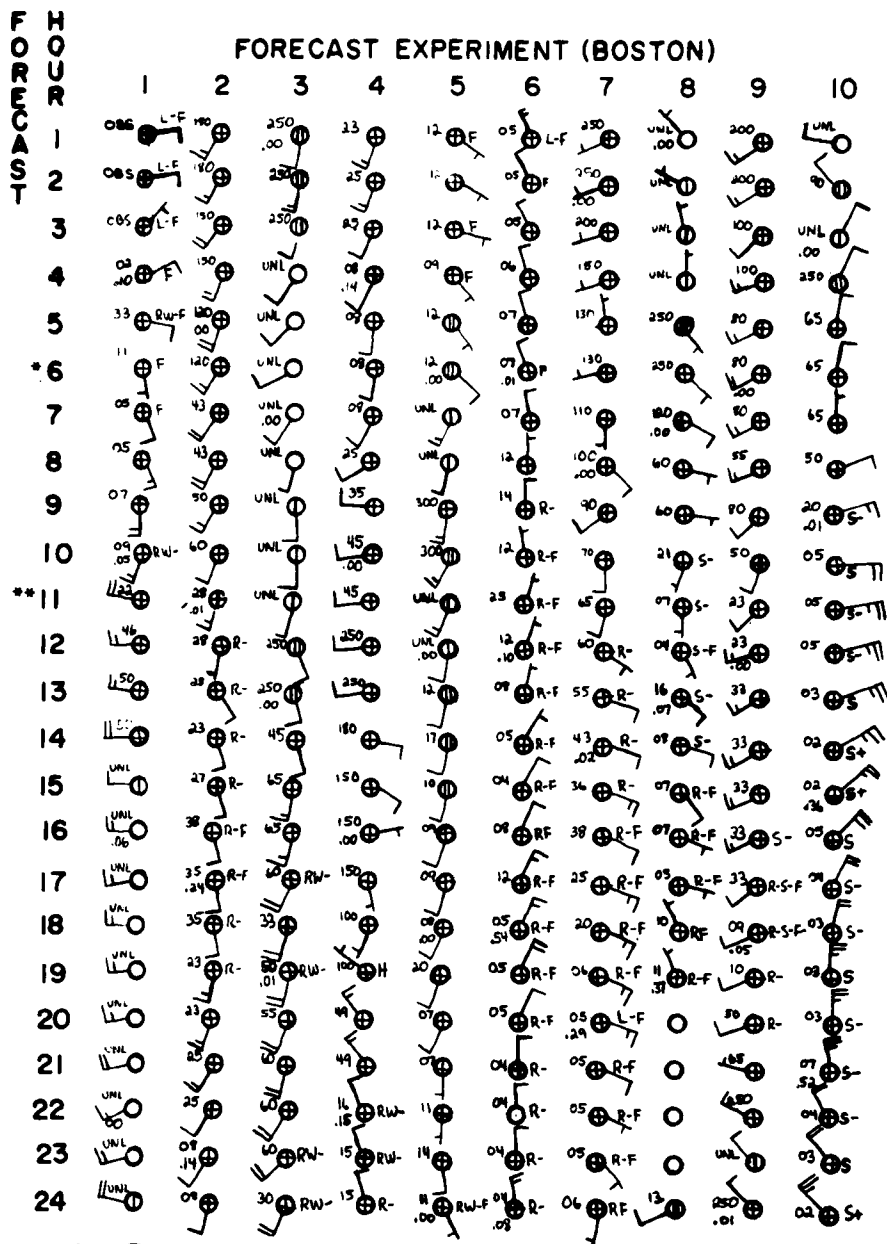
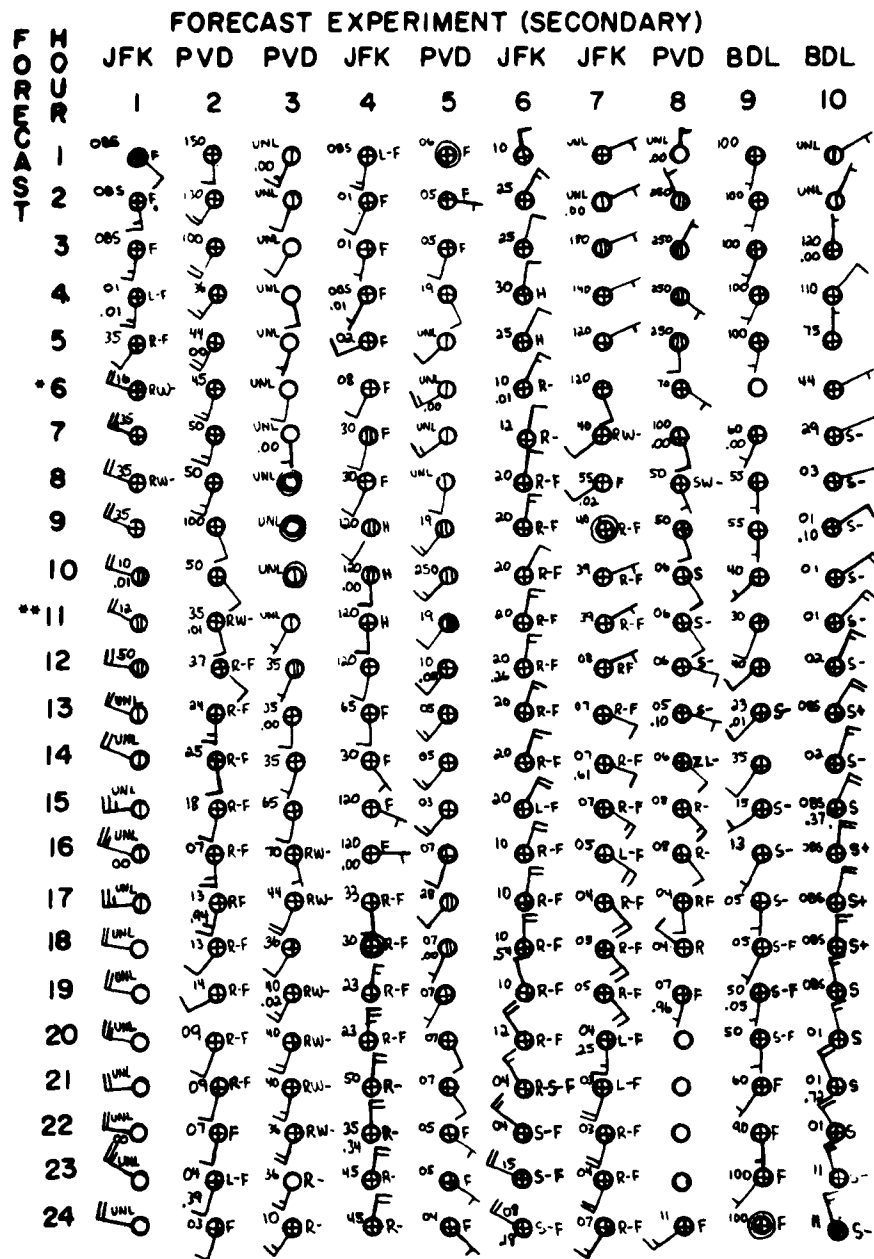


Figure 11. Twenty-four Hourly Observations for Logan International Airport (BOS) for the Ten Cases of the Mesoscale Forecast Experiment; Hours 6 to 11 Represent

Forecast Times. CCH QPF WX CCH = ceiling height (100's of feet, UNL = unlimited, OBS = obscured), QPF: 6-hour precipitation amount (inches), WX: weather symbols, windflags in knots



* 1st Forecast made at 6th hour

** Last forecast made at 11th hour

Figure 12. Twenty-four Hourly Observations for Secondary Station (BDL, JFK or PVD) for the Ten Cases of the Mesoscale Forecast Experiment; Hours 6 to 11

Represent Forecast Times.



CCH = ceiling height (100's of feet),

UNL = unlimited, OBS = obscured), QPF: 6-hour precipitation amount (inches),
 WX: weather symbols, windflags in knots

FORECAST EXPERIMENT 1: At 14 GMT, 26 Mar 1982, a 996-mb cyclone was centered over extreme northeastern New York with a cold front trailing southeastward into central New England, then southwestward into the Atlantic (see Figure 13). The main forecast problem for BOS involved timing the cold front, and changes in cloud cover, ceiling height, and winds associated with the impending frontal passage. Since the front was well east of JFK by 14 GMT the main forecast problem there consisted of timing improvements in cloud cover and ceiling height.

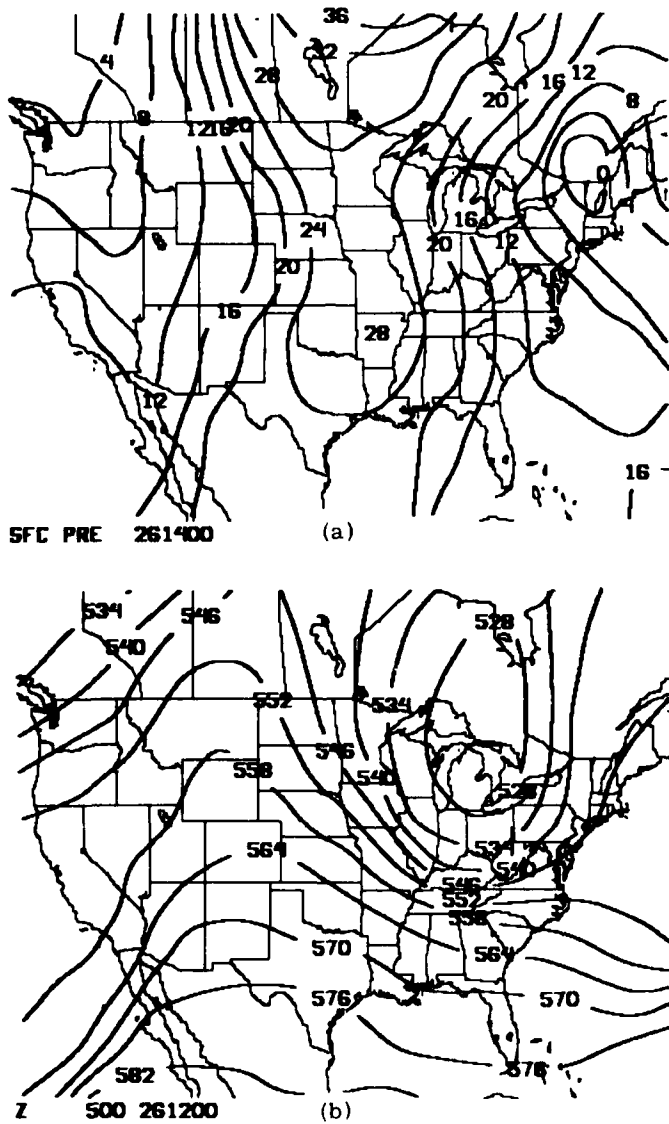
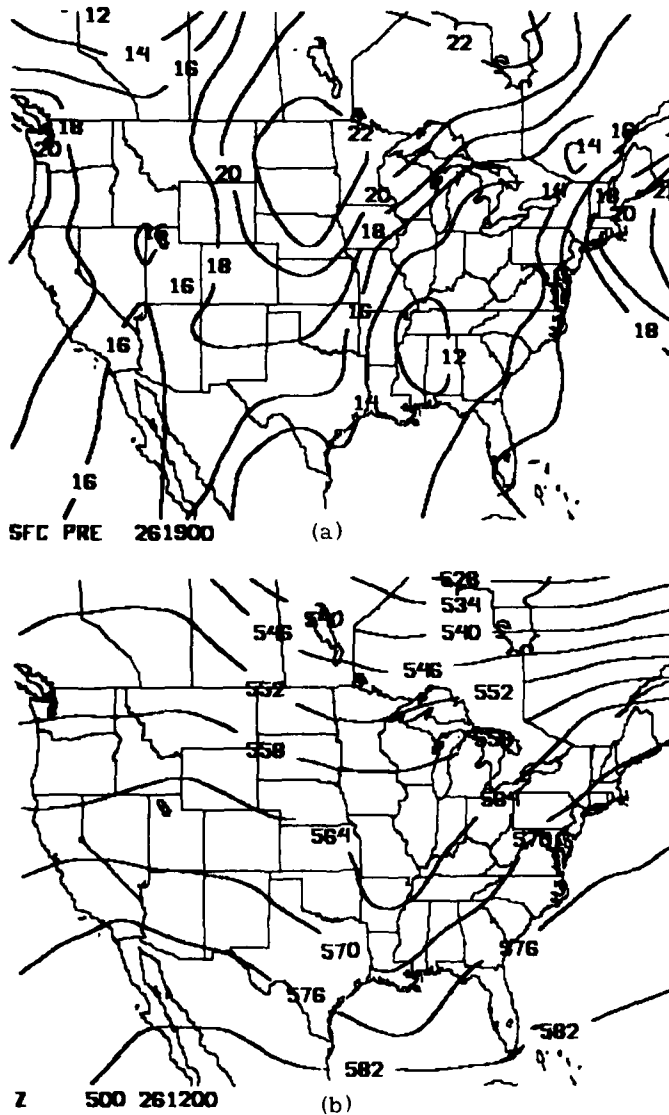


Figure 13. General Weather Situation for Mesoscale Forecast Experiment Case No. 1: (a) Surface Pressure Analysis for 1400 GMT, 26 Mar 1982 and (b) 500-mb Height Analysis for 1200 GMT, 26 Mar 1982

FORECAST EXPERIMENT 2: At 19 GMT 26 April 1982, a weak frontal system and a poorly organized low pressure area were present from the Great Lakes region southward to the Gulf of Mexico (see Figure 14). A large area of light to moderate rainfall associated with the frontal system was occurring from central Massachusetts to the Carolinas. With weak upper-level support, minimal frontal wave development was likely. Since overcast skies were present at forecast time, ceiling height and precipitation amount were the most critical forecast parameters for BOS and PVD.



FORECAST EXPERIMENT 3: The 05 GMT 31 March 1982 surface pressure analysis (Figure 15) indicates a deep cyclone in southwestern Ontario with a trailing cold front marching eastward through the Midwest. Light rain showers and gusty winds were occurring in the prefrontal cloud band. With clear skies over eastern New England, cloud cover, ceiling height, and wind forecasts were of greatest interest.

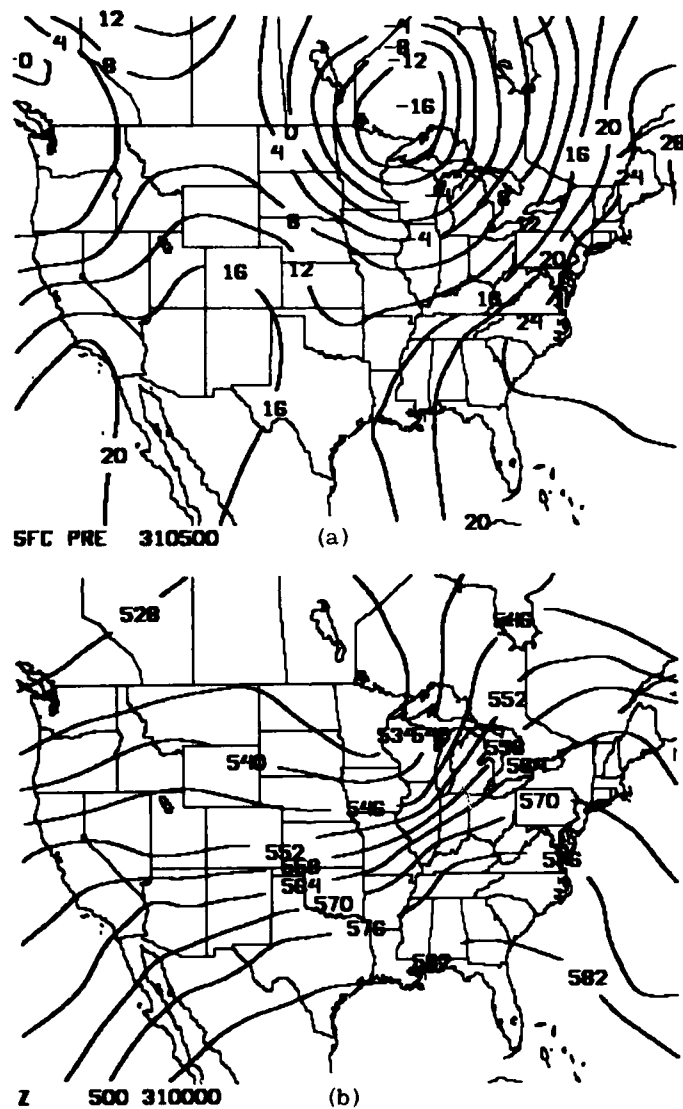


Figure 15. General Weather Situation for Mesoscale Forecast Experiment Case No. 3: (a) Surface Pressure Analysis for 0500 GMT, 31 Mar 1982 and (b) 500-mb Height Analysis for 0000 GMT, 31 Mar 1982

FORECAST EXPERIMENT 4: At 14 GMT 27 April 1982 a pair of cold fronts associated with a weak cyclone in southeastern Canada were located in central New England and eastern New York (see Figure 16). The main forecast problem for BOS consisted of timing the cold fronts and associated wind shifts and ceiling height changes. At 14 GMT the first front was just east of JFK; however, dense fog and low ceilings had been observed for the past 8 h. Thus the main forecast problem for JFK was to determine when the fog would dissipate to increase ceiling heights, and time the passage of the secondary cold front and its associated ceiling height changes and wind shifts.

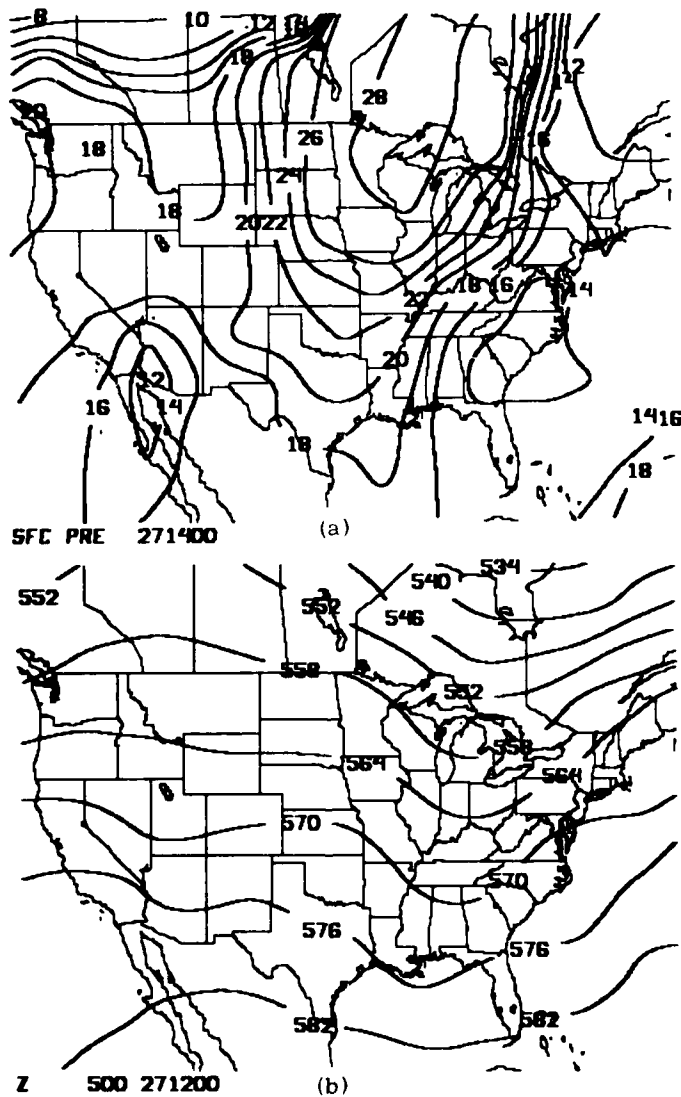


Figure 16. General Weather Situation for Mesoscale Forecast Experiment Case No. 4: (a) Surface Pressure Analysis for 1400 GMT, 27 Apr 1982 and (b) 500-mb Height Analysis for 1200 GMT, 27 Apr 1982

FORECAST EXPERIMENT 5: The 18 GMT 11 March 1982 surface pressure analysis (Figure 17) showed a weak cyclone moving eastward across southern Canada, just north of the Great Lakes. The cold front, surface pressure trough and associated frontal cloud band were spreading across the Midwest. With the cold front and precipitation shield too far west to incur wind, temperature, or precipitation effects upon southern New England, the principal forecast problem for BOS and PVD was cloud amount in the variably cloudy pre-frontal zone.

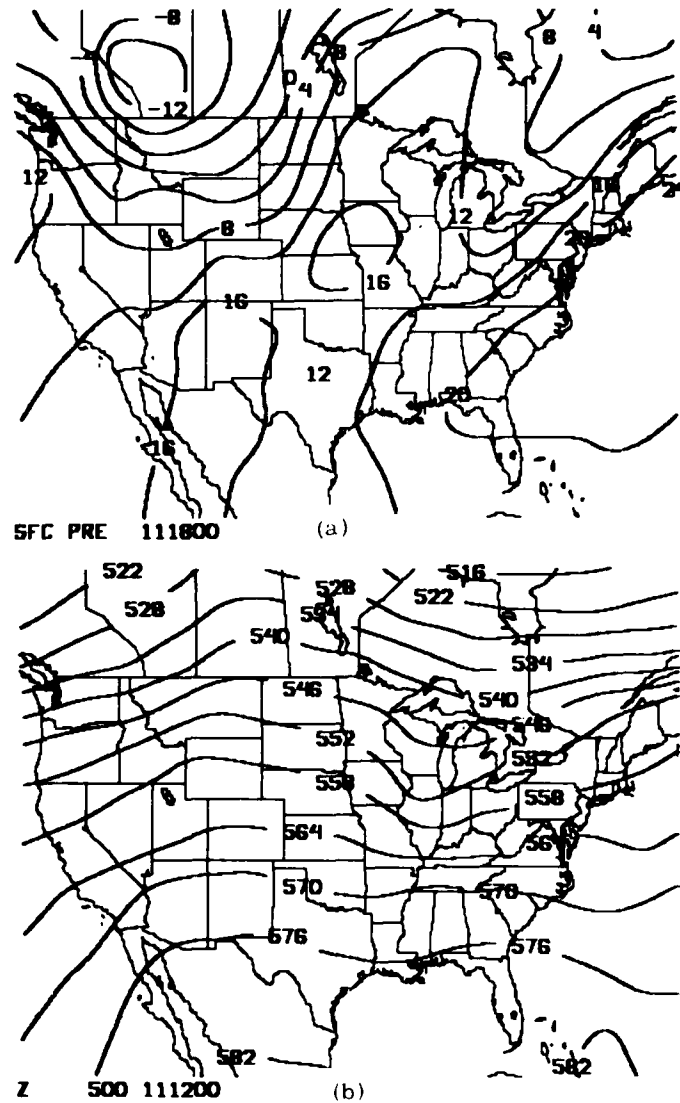


Figure 17. General Weather Situation for Mesoscale Forecast Experiment Case No. 5: (a) Surface Pressure Analysis for 1800 GMT, 11 Mar 1982 and (b) 500-mb Height Analysis for 1200 GMT, 11 Mar 1982

FORECAST EXPERIMENT 6: At 18 GMT 15 December 1981 a developing cyclone was located along the southeastern North Carolina coast (see Figure 18). With a deepening 500-mb trough over the eastern U.S. and strong positive vorticity advection at 500 mb spreading over the Cape Hatteras region, the cyclone had the potential to deepen rapidly as it moved northeastward toward New England. The major problem was to forecast the track and strength of the developing cyclone, and its effect on the wind, ceiling height, and precipitation amount forecast.

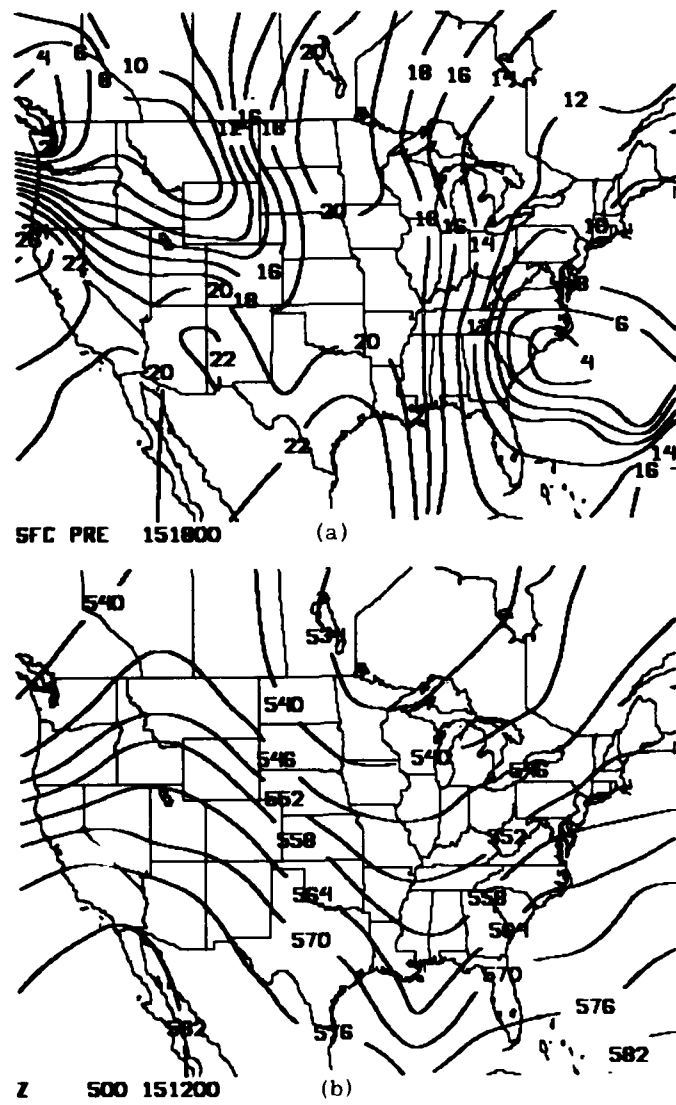


Figure 18. General Weather Situation for Mesoscale Forecast Experiment Case No. 6: (a) Surface Pressure Analysis for 1800 GMT, 15 Dec 1981 and (b) 500-mb Height Analysis for 1200 GMT, 15 Dec 1981

FORECAST EXPERIMENT 7: The surface pressure analysis at 17 GMT 1 December 1981 (Figure 19) showed an intense occluded cyclone in Wisconsin. The occluded front extended from the Ohio valley southward to Georgia. The warm front curved northeastward from Georgia to Cape Hatteras. An area of pressure falls and light to moderate precipitation was developing in the north Carolina-Virginia area, moving northeastward. With weak positive vorticity advection at 500 mb, a very weak frontal wave could develop along the warm front. Thus precipitation amount and lowering ceiling heights, which were the main forecast problem for southern New England, were dependent on the movement of the developing warm frontal wave and its associated precipitation shield.

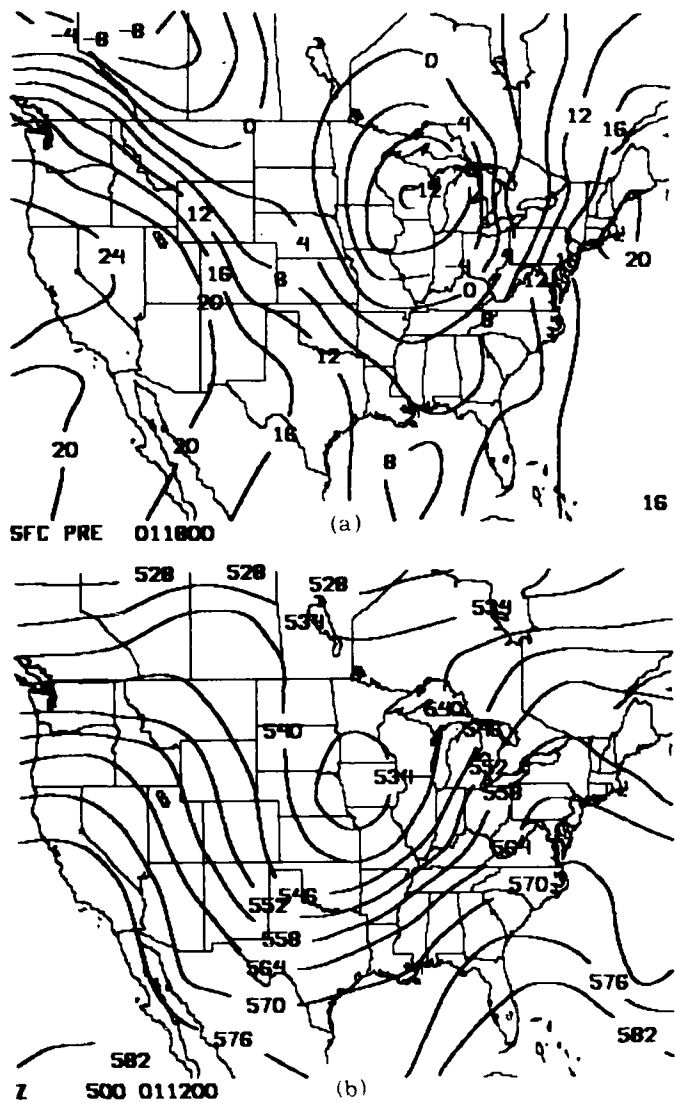


Figure 19. General Weather Situation for Mesoscale Forecast Experiment Case No. 7: (a) Surface Pressure Analysis for 1700 GMT, 1 Dec 1981 and (b) 500-mb Height Analysis for 1200 GMT, 1 Dec 1981

FORECAST EXPERIMENT 8: The 17 GMT 4 March 1982 surface pressure analysis (Figure 20) showed a moderate cyclone centered in Ohio, moving toward the northeast. With moderate vorticity advection at 500 mb overspreading New England, the area of steady light precipitation associated with the Ohio cyclone continued to expand as it moved eastward. Thus the main forecast concern for southern New England was precipitation amount and lowering ceiling heights.

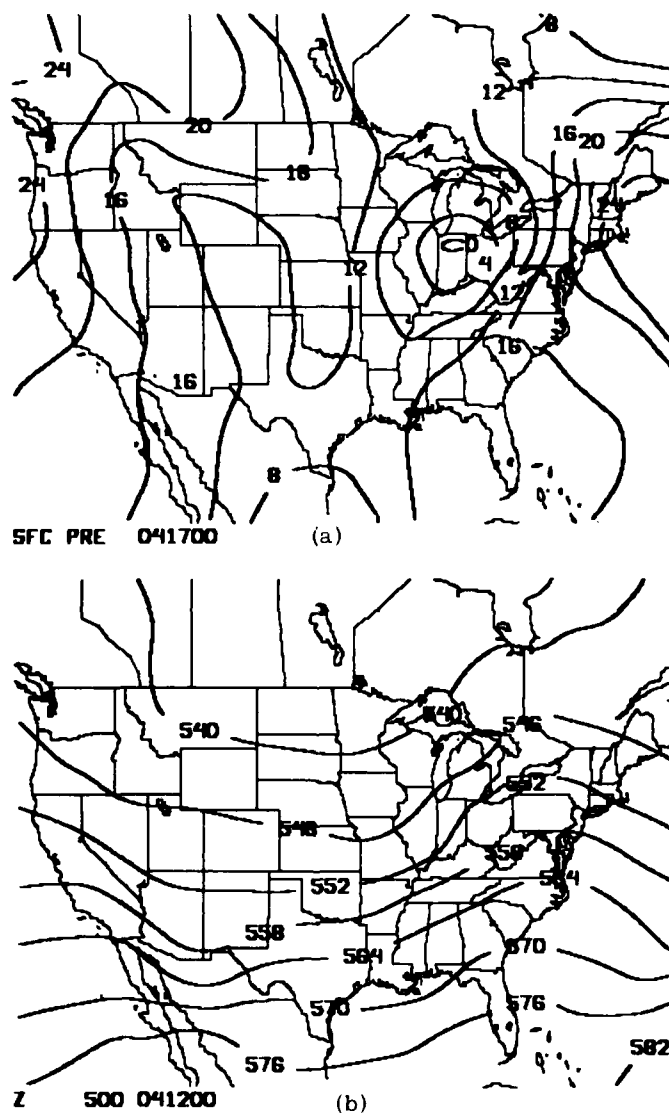


Figure 20. General Weather Situation for Mesoscale Forecast Experiment Case No. 8: (a) Surface Pressure Analysis for 1700 GMT, 4 Mar 1982 and (b) 500-mb Height Analysis for 1200 GMT, 4 Mar 1982

FORECAST EXPERIMENT 9: The surface pressure analysis at 06 GMT 22 December 1981 (Figure 21) showed a strong cold anticyclone moving slowly eastward off the mid-Atlantic coast and a weak cyclone moving into western Oklahoma. The combination of moist southwesterly flow from the two systems and the cold air entrenched over the northeast and mid-Atlantic states created a potential overrunning situation. Therefore precipitation amount and lowering ceiling heights were the main focus of this forecast experiment.

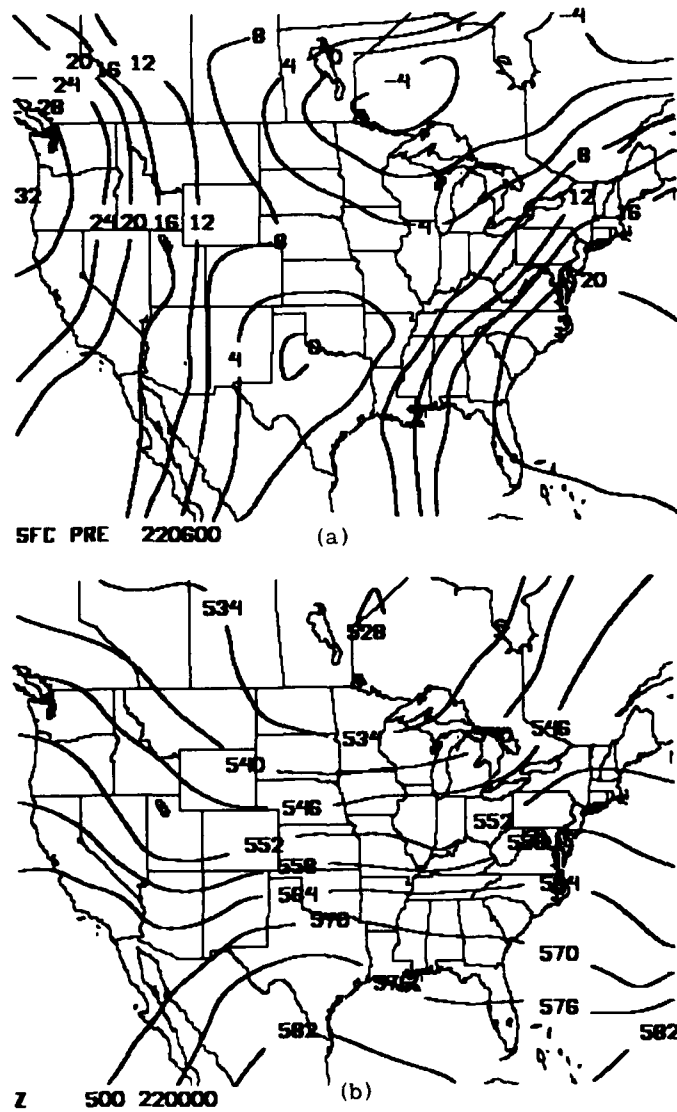


Figure 21. General Weather Situation for Mesoscale Forecast Experiment Case No. 9: (a) Surface Pressure Analysis for 0600 GMT, 22 Dec 1981 and (b) 500-mb Height Analysis for 0000 GMT, 22 Dec 1981

FORECAST EXPERIMENT 10: At 04 GMT 6 April 1982 a developing cyclone was moving into western Pennsylvania (Figure 22). A potent 500-mb short wave trough and strong positive vorticity advection suggested that this cyclone may undergo explosive development off the New Jersey coast with the potential of heavy snow and strong winds over much of New England. Precipitation amount, winds, and ceiling height were of most importance during this forecast experiment.

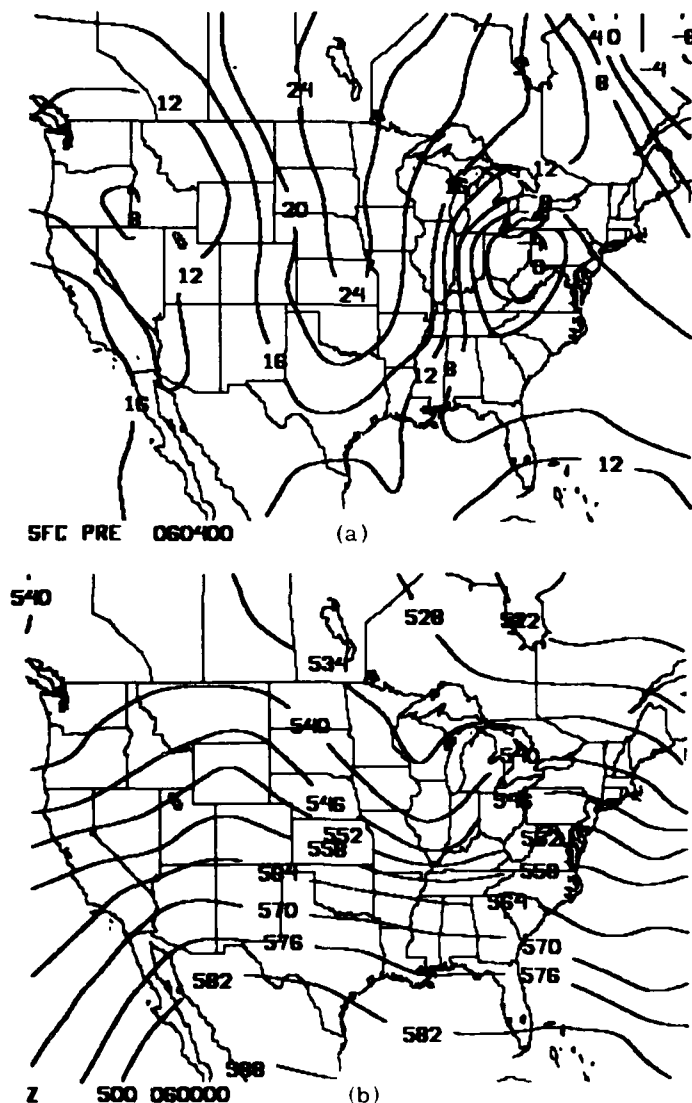


Figure 22. General Weather Situation for Mesoscale Forecast Experiment Case No. 10: (a) Surface Pressure Analysis for 0400 GMT, 6 Apr 1982 and (b) 500-mb Height Analysis for 0000 GMT, 6 Apr 1982

4. TEST RESULTS

4.1 Product Assessment

In the course of the Mesoscale Forecast Experiment tests, the participating forecasters were encouraged to use, to their fullest advantage, any and all of the data sources, display products and analysis/forecast techniques available within McIDAS in the preparation of their forecasts. In that regard they were specifically instructed to use each of the new techniques at least once during each test episode. In so doing, it was felt that a reasonable and fair assessment of these aspects of McIDAS would be accomplished.

Table 4 lists certain aspects of the assessment process for products that were used frequently. The "product key-in" refers to the keyboard instruction that activates the generation of a discrete product on McIDAS. Those without an asterisk are part of the previously existing McIDAS suite of available routines. The primary function of each is listed below:

- IA - geographic (map) plot of weather variable(s) on the color monitor; used with either surface or upper-air data; can include one to four panels per screen; can be plotted over satellite imagery,
- ZI - decoded listing of surface observations on alphanumeric terminal (for example, by stations in a state for a specific time or a time series for a specific station),
- ZK - surface analysis using one-pass Cressman technique on color monitor; ideal for broad-view/quick-look assessment,
- ENT/ET - GOES IR imagery color enhancement based on defined temperature thresholds (in the case of ET, the user defines the threshold),
- KZ - surface analysis using five-pass Barnes technique on color monitor; retains more mesoscale detail,
- PF - 2-D trajectory forecast model based on analyzed rawinsonde observations,
- CC - algorithms to estimate cloud cover and 1-h precipitation amount from GOES visible and IR imagery displayed on alphanumeric terminal,
- KY - upper-air analysis (constant pressure surface) using a two-pass Barnes technique on color monitor,
- MS - station model time series display on color monitor; depicts surface observations for up to six stations for up to 6 h,
- YK - upper-air analysis (constant pressure surface) using a one-pass Cressman technique on color monitor,
- ZP - map plot of one variable on the alphanumeric terminal,
- ZC - contours a previously analyzed and stored grid array and displays it on the color monitor,

- MR - contoured geographic analysis of manually-digitized radar on color monitor; displayed independently or in conjunction with concurrent satellite imagery and/or surface observations,
 TP - log p-skew T display of rawinsonde observations on color monitor,
 GT - individual variables line or bar graph time series display on color monitor,
 FCS - menu-driven forecast decision-assistance procedures using the alphanumeric terminal,
 FI - decoded display of FOUS bulletins (MOS, LFM guidance and 3-D trajectories) on alphanumeric terminal.

Table 4. McIDAS Product Assessment Summary

Product Key In	Generation Time on McIDAS (sec)	Number of Uses	Usefulness		Rating	
			Most	Least	Average	Number
IA	30	215	10	--	1.4	13
ZI	3	177	--	--	--	--
ZK	40	166	--	--	--	--
ENT/ET	8	160	5	--	2.2	32
KZ*	70	61	7	4	2.7	36
PF*	5	58	6	2	2.6	10
CC*	20/2	34	2	4	3.1	20
KY	25	33	--	--	--	--
MS*	35	31	17	1	1.9	35
YK	22	19	--	--	--	--
ZP	5	16	--	--	--	--
ZC	65	14	--	--	--	--
MR*	45	11	1	9	3.3	36
TP*	60	11	2	17	5.4	16
GT*	20	10	2	5	4.6	14
FCS*	--	--	--	4	--	--
FI	3	--	2	--	2.9	18

* See Section 2.2 for detailed discussion of product function.

The second column indicates the approximate amount of time (in seconds) that elapses from the time the key-in of the command is displayed until McIDAS finishes generating the product. Since McIDAS' graphics device is considerably slower than state-of-the-art devices and its central processing unit is a 24-bit machine without hardware multiple-divide capability, substantially shorter generation times should be achievable. Each of these times reflects the creation of products on the local scale typically used in this experiment (that is, as generated by McIDAS state and city displays of the type shown in Figures 2 and 3). The generation of national or regional (for example, eastern U.S.) maps generally increases the times indicated by a factor of 3 or 4. Obviously, none of these routines are very time consuming; most of them are executed in well under 60 sec. The new routines, tailored to increase the depiction of mesoscale information, do not increase elapsed time substantially. The 5-pass procedure KZ, which recovers a large portion of the mesoscale detail suppressed in the 1-pass technique ZK takes only 30 sec longer. The more extensive upper-air analysis (KY) takes only 3 sec longer than the 1-pass procedure (YK). Neither of the tailored plot routines (MS and GT) are time consuming (35 and 20 sec, respectively). Even the multi-step procedure of remapping, analyzing, and displaying manually digitized radar data (MR key-in) takes less than a minute, while the application of the forecast guidance technique based on 2-D trajectories (PF) and satellite algorithms (FOR) has a combined elapsed time of 25 sec. Key-ins that use the black and white alphanumeric terminal (ZI, PF, ZP, and FI) are executed in 5 sec or less.

The column "No. of Uses" refers to the extent to which the individual key-ins were invoked during the 10-episode test period. The popularity of the top three features (IA, ZI and ZK) is clearly evident and reflects the interactive nature of the process typically used by a forecaster in monitoring and resolving the aspects of a forecast problem. In the preliminary and intermediate stages of the process there is a fair amount of reviewing and sorting of various aspects of the storm's general evolution that can be treated effectively through a mental (subjective) integration of observation listings (ZI) and map plotting (IA). Typically the forecasters chose to generate (with the IA command) a 4-panel display of a particular variable (for example, present weather or wind flags) for four consecutive hours to resolve system translation estimates. In the later stages of the forecast process, where concern for precision and timing increased, the forecasters turned to the tailored products (such as KZ, MS, PF, and FOR) to focus on specific aspects of the storm's evolution.

The limited use of other tailored products (MR, TP, GT, FCS) was attributed to different factors. Despite the concerted effort to develop processing routines to map and display manually digitized radar (MDR) data for these tests (the MR key-in), there were some shortfalls that resulted in data losses and misprocessing that

drastically reduced the availability of MDR data in several of the episodes. This was compounded in other cases by non-receipt of MDR data on the WB604 circuit for certain hours or geographical areas. In the two or three episodes with reliable and continuous MDR data, the MR key-in was used frequently and was found to provide good corroborating evidence for ceiling height and quantitative precipitation forecasts. The routine to display log p-skew T soundings of area radiosondes (TP) was used about once per episode and deemed to be of limited value to this forecast exercise because of a lack of timeliness and horizontal representativeness. The value of the time-series parameter plot (GT), illustrated in Figure 7, was deemed to be limited because it could only be applied to continuous variables such as pressure, temperature, and wind speed, which were (with the exception of wind speed) not germane to the forecast problem being treated in the experiment. Finally, the cold front decision assistance procedure (FCS) was generally judged to be too time consuming and not needed by the participating forecasters, all of whom had previously become expert in using McIDAS' interactive capabilities. However, the long-range intent in developing such procedures is to train forecasters new to a particular area or new to using an interactive system.

The use of GOES imagery (visible and IR) in these tests was extensive, especially for storms developing and moving up the east coast where a large portion of the developing and advecting weather was out over the water where conventional data coverage was sparse, at best. The only aspect of satellite imagery the forecasters were specifically asked to assess was a new procedure for enhancing the IR temperature images based on temperature thresholds rather than pixel gray shade values. The "conventional" GOES imagery display options, which include animation (time series looping), channel switching (alternating visible and IR images to evaluate cloud layering), color enhancement of brightness and IR gray scales, and overlaying conventional analyses and data plots, were used extensively and were judged to be very helpful to effective short range terminal forecasting. IR imagery enhanced by temperature (ENT and ET) was not deemed to add significantly to the forecast process beyond the information available in the "conventional" satellite products.

The information presented in Table 4 under the heading "Usefulness" summarizes the consensus assessment of the forecasters on the relative usefulness in terminal forecasting of the products and data sources available to them. The numbers shown reflect the total number of times a participating forecaster judged a product most (or least) useful. (The first page of the Product Usefulness Assessment in Appendix D shows the form completed.) There were up to six forecasters participating in each of the 10 test episodes, thus there was the potential of 60 responses in each category (most and least). In fact, a total of 54 assessments were completed because six of the episodes involved just five forecasters.

The routine MS was found to be the most useful of the set evaluated. Two factors emerged in the experiment regarding the value of this product. The first is the ability (and ease) of specifying the stations to be included in the cross-section and tailoring it to the episode under consideration. The second is the wealth of basic information it provides that is important to the terminal forecast problem in a format that permitted extensive subjective interpretation to track one or more elements and define its spatial extent. It was found to be more useful for the 1-3 h forecast interval of the type required in base weather stations in support of aircraft arrivals and local area requirements.

The second most useful product was the IA routine. It is the only previously existing McIDAS routine that was used extensively in the later stages of the forecast process. The others (ZI, ZK, and so on) were used mainly to get brief, general overviews of the storm's progress and were used infrequently in the later stages. Because of this prevailing usage, we chose not to include them in the assessment. The value of the map plotting routine (IA) is comparable but complementary to the MS routine. In its typical use in the experiment, a four-panel display was generated on the color graphics terminal. Either the latest observations of four variables were plotted on separate panels (quadrants of screen) for the Northeast area or maps of the last 4 h of one variable were displayed. Like MS, either option of IA provides a wealth of information for subjective interpretation. It complements MS in that it provides more information on the spatial extent and evolution of the weather system and also provides greater guidance on the forecast problem beyond 3 h.

The mesoscale surface objective analysis routine (KZ) was found to be most useful for the wind forecasts. It provided more detailed streamline, pressure, and pressure change analyses than does the standard routine (ZK). This aided in resolving the movement and timing of wind shift (and frontal passage) lines and pressure gradient changes that would influence the wind speed forecast. It was found to have only limited additional value for the other elements of the test. The density of observation stations in the coastal New England area is generally compatible with the resolution and detail inherent in the KZ analysis, while the density in other areas may not be.

A major problem with any objective analysis procedure is data-void regions. (Probably the most important such region is the Atlantic Ocean off the east coast of the U.S.). In its existing structure, McIDAS did not decode and use ship and buoy reports in its plot and analysis routines. During the course of this test it was concluded that the system should be modified to include them because of the difficulty in tracking and evaluating surface weather phenomena over the water. Although not available for the episodes involved in this Mesoscale Forecast Experiment, new routines have been incorporated for the next series of tests that will permit the use of available ship and buoy reports in the analyses. Figures 23 to 25 illustrate the

impact they can have on an objective streamline analysis in the cold frontal weather situation that existed off the southeast New England coast on the evening of 20 July 1982. Figure 23 is the streamline analysis for 21 July/00 GMT derived solely from land-based airways observations. With the exception of its overland position in extreme eastern Maine, it does not capture features to aid in locating the position and orientation of the offshore cold front. Figure 24 depicts (through the IA key-in) wind flag observations at land-based locations and from ships and buoys that were reported at 00 GMT; note there were nine ship and buoy reports within the analysis area. Figure 25 is the same analysis as Figure 23 but with the available ship and buoy reports included in the analysis. Not only is the location of the offshore front clearly indicated but evidence of a wave along the front to the south of Nantucket Island is present. Generally, ship and buoy reports are only available on a 6-h cycle. When they are available, however, they may be essential to effective short-range forecasting.

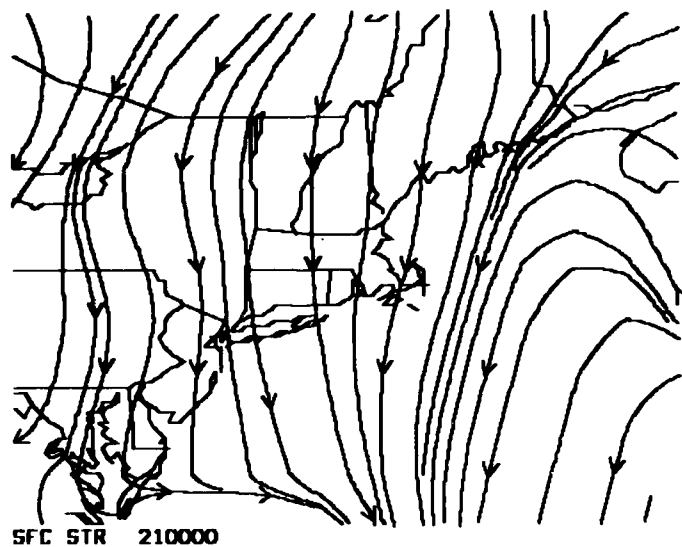


Figure 23. Surface Objective Streamline Analysis of Offshore Cold Front Situation on 0000 GMT, 21 July 1982, Using Only Land-based Observations

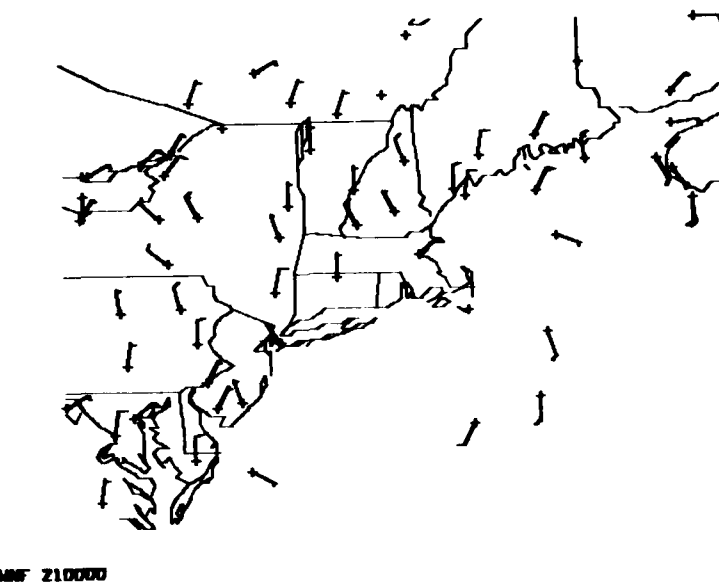


Figure 24. Plotted Surface Wind Observations at Land-based Locations and Ships/Buoys on 0000 GMT, 21 July 1982

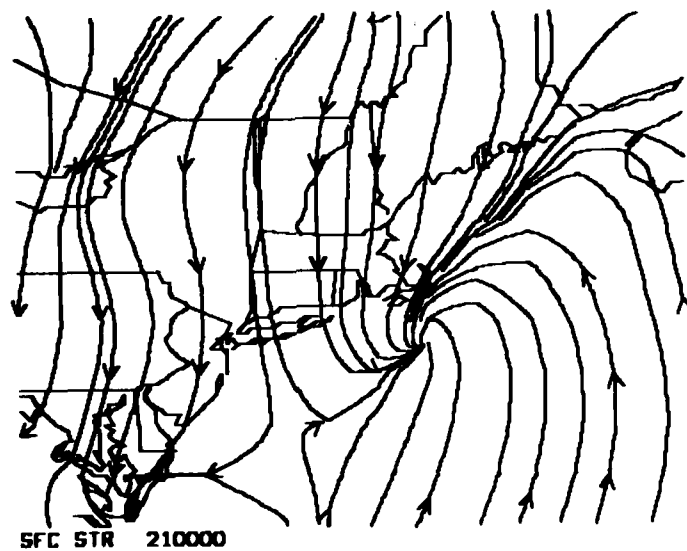


Figure 25. Surface Objective Streamline Analysis of Offshore Cold Front Situation on 0000 GMT, 21 July 1982, Using Land-based, Ship and Buoy Observations

The 2-D trajectory forecast guidance model (PF) was found to be helpful in many instances, both with (through CC) and without the use of satellite imagery. Most forecasters used the 2-pass Barnes analysis (KY) to generate a 700-mb wind analysis (u and v components) based on the most recent rawinsonde observations. The hour-by-hour forecasts of the user-specified variable (for example, 1-h precipitation amount), based on the trajectory and appropriate analyzed grids, would be displayed on the alphanumeric terminal as illustrated in Figure 26. These products were found to provide quantitative guidance on overall timing, hour-to-hour changes and development aspects of the system. Obviously, the further the forecast time was removed from 00/12 GMT (the time of the rawinsonde observation) the less reliable this guidance became.

FF 40 44 12 EOS					
FORECAST CF T	AT BOS	4237	7103	POW	DOL
FT 1000 Z	5 73			5 54	19 32
FT 0000 Z	5 18			5 57	19 35
FT 0000 Z	5 05			5 61	19 38
FT 0000 Z	5 02			5 62	19 39
FT 0000 Z	5 00			5 63	19 40
FT 0000 Z	4 98			5 64	19 41
FT 0000 Z	4 96			5 65	19 42
FT 0000 Z	4 94			5 66	19 43
FT 0000 Z	4 92			5 67	19 44
FT 0000 Z	4 90			5 68	19 45
FT 0000 Z	4 88			5 69	19 46
FT 0000 Z	4 86			5 70	19 47
FT 0000 Z	4 84			5 71	19 48
FT 0000 Z	4 82			5 72	19 49
FT 0000 Z	4 80			5 73	19 50
FT 0000 Z	4 78			5 74	19 51
FT 0000 Z	4 76			5 75	19 52
FT 0000 Z	4 74			5 76	19 53
FT 0000 Z	4 72			5 77	19 54
FT 0000 Z	4 70			5 78	19 55
FT 0000 Z	4 68			5 79	19 56
FT 0000 Z	4 66			5 80	19 57
FT 0000 Z	4 64			5 81	19 58
FT 0000 Z	4 62			5 82	19 59
FT 0000 Z	4 60			5 83	19 60
FT 0000 Z	4 58			5 84	19 61
FT 0000 Z	4 56			5 85	19 62
FT 0000 Z	4 54			5 86	19 63
FT 0000 Z	4 52			5 87	19 64
FT 0000 Z	4 50			5 88	19 65
FT 0000 Z	4 48			5 89	19 66
FT 0000 Z	4 46			5 90	19 67
FT 0000 Z	4 44			5 91	19 68
FT 0000 Z	4 42			5 92	19 69
FT 0000 Z	4 40			5 93	19 70
FT 0000 Z	4 38			5 94	19 71
FT 0000 Z	4 36			5 95	19 72
FT 0000 Z	4 34			5 96	19 73
FT 0000 Z	4 32			5 97	19 74
FT 0000 Z	4 30			5 98	19 75
FT 0000 Z	4 28			5 99	19 76
FT 0000 Z	4 26			6 00	19 77
FT 0000 Z	4 24			6 01	19 78
FT 0000 Z	4 22			6 02	19 79
FT 0000 Z	4 20			6 03	19 80
FT 0000 Z	4 18			6 04	19 81
FT 0000 Z	4 16			6 05	19 82
FT 0000 Z	4 14			6 06	19 83
FT 0000 Z	4 12			6 07	19 84
FT 0000 Z	4 10			6 08	19 85
FT 0000 Z	4 08			6 09	19 86
FT 0000 Z	4 06			6 10	19 87
FT 0000 Z	4 04			6 11	19 88
FT 0000 Z	4 02			6 12	19 89
FT 0000 Z	4 00			6 13	19 90
FT 0000 Z	3 98			6 14	19 91
FT 0000 Z	3 96			6 15	19 92
FT 0000 Z	3 94			6 16	19 93
FT 0000 Z	3 92			6 17	19 94
FT 0000 Z	3 90			6 18	19 95
FT 0000 Z	3 88			6 19	19 96
FT 0000 Z	3 86			6 20	19 97
FT 0000 Z	3 84			6 21	19 98
FT 0000 Z	3 82			6 22	19 99
FT 0000 Z	3 80			6 23	20 00
FT 0000 Z	3 78			6 24	20 01
FT 0000 Z	3 76			6 25	20 02
FT 0000 Z	3 74			6 26	20 03
FT 0000 Z	3 72			6 27	20 04
FT 0000 Z	3 70			6 28	20 05
FT 0000 Z	3 68			6 29	20 06
FT 0000 Z	3 66			6 30	20 07
FT 0000 Z	3 64			6 31	20 08
FT 0000 Z	3 62			6 32	20 09
FT 0000 Z	3 60			6 33	20 10
FT 0000 Z	3 58			6 34	20 11
FT 0000 Z	3 56			6 35	20 12
FT 0000 Z	3 54			6 36	20 13
FT 0000 Z	3 52			6 37	20 14
FT 0000 Z	3 50			6 38	20 15
FT 0000 Z	3 48			6 39	20 16
FT 0000 Z	3 46			6 40	20 17
FT 0000 Z	3 44			6 41	20 18
FT 0000 Z	3 42			6 42	20 19
FT 0000 Z	3 40			6 43	20 20
FT 0000 Z	3 38			6 44	20 21
FT 0000 Z	3 36			6 45	20 22
FT 0000 Z	3 34			6 46	20 23
FT 0000 Z	3 32			6 47	20 24
FT 0000 Z	3 30			6 48	20 25
FT 0000 Z	3 28			6 49	20 26
FT 0000 Z	3 26			6 50	20 27
FT 0000 Z	3 24			6 51	20 28
FT 0000 Z	3 22			6 52	20 29
FT 0000 Z	3 20			6 53	20 30
FT 0000 Z	3 18			6 54	20 31
FT 0000 Z	3 16			6 55	20 32
FT 0000 Z	3 14			6 56	20 33
FT 0000 Z	3 12			6 57	20 34
FT 0000 Z	3 10			6 58	20 35
FT 0000 Z	3 08			6 59	20 36
FT 0000 Z	3 06			6 60	20 37
FT 0000 Z	3 04			6 61	20 38
FT 0000 Z	3 02			6 62	20 39
FT 0000 Z	3 00			6 63	20 40
FT 0000 Z	2 98			6 64	20 41
FT 0000 Z	2 96			6 65	20 42
FT 0000 Z	2 94			6 66	20 43
FT 0000 Z	2 92			6 67	20 44
FT 0000 Z	2 90			6 68	20 45
FT 0000 Z	2 88			6 69	20 46
FT 0000 Z	2 86			6 70	20 47
FT 0000 Z	2 84			6 71	20 48
FT 0000 Z	2 82			6 72	20 49
FT 0000 Z	2 80			6 73	20 50
FT 0000 Z	2 78			6 74	20 51
FT 0000 Z	2 76			6 75	20 52
FT 0000 Z	2 74			6 76	20 53
FT 0000 Z	2 72			6 77	20 54
FT 0000 Z	2 70			6 78	20 55
FT 0000 Z	2 68			6 79	20 56
FT 0000 Z	2 66			6 80	20 57
FT 0000 Z	2 64			6 81	20 58
FT 0000 Z	2 62			6 82	20 59
FT 0000 Z	2 60			6 83	20 60
FT 0000 Z	2 58			6 84	20 61
FT 0000 Z	2 56			6 85	20 62
FT 0000 Z	2 54			6 86	20 63
FT 0000 Z	2 52			6 87	20 64
FT 0000 Z	2 50			6 88	20 65
FT 0000 Z	2 48			6 89	20 66
FT 0000 Z	2 46			6 90	20 67
FT 0000 Z	2 44			6 91	20 68
FT 0000 Z	2 42			6 92	20 69
FT 0000 Z	2 40			6 93	20 70
FT 0000 Z	2 38			6 94	20 71
FT 0000 Z	2 36			6 95	20 72
FT 0000 Z	2 34			6 96	20 73
FT 0000 Z	2 32			6 97	20 74
FT 0000 Z	2 30			6 98	20 75
FT 0000 Z	2 28			6 99	20 76
FT 0000 Z	2 26			7 00	20 77
FT 0000 Z	2 24			7 01	20 78
FT 0000 Z	2 22			7 02	20 79
FT 0000 Z	2 20			7 03	20 80
FT 0000 Z	2 18			7 04	20 81
FT 0000 Z	2 16			7 05	20 82
FT 0000 Z	2 14			7 06	20 83
FT 0000 Z	2 12			7 07	20 84
FT 0000 Z	2 10			7 08	20 85
FT 0000 Z	2 08			7 09	20 86
FT 0000 Z	2 06			7 10	20 87
FT 0000 Z	2 04			7 11	20 88
FT 0000 Z	2 02			7 12	20 89
FT 0000 Z	2 00			7 13	20 90
FT 0000 Z	1 98			7 14	20 91
FT 0000 Z	1 96			7 15	20 92
FT 0000 Z	1 94			7 16	20 93
FT 0000 Z	1 92			7 17	20 94
FT 0000 Z	1 90			7 18	20 95
FT 0000 Z	1 88			7 19	20 96
FT 0000 Z	1 86			7 20	20 97
FT 0000 Z	1 84			7 21	20 98
FT 0000 Z	1 82			7 22	20 99
FT 0000 Z	1 80			7 23	21 00
FT 0000 Z	1 78			7 24	21 01
FT 0000 Z	1 76			7 25	21 02
FT 0000 Z	1 74			7 26	21 03
FT 0000 Z	1 72			7 27	21 04
FT 0000 Z	1 70			7 28	21 05
FT 0000 Z	1 68			7 29	21 06
FT 0000 Z	1 66			7 30	21 07
FT 0000 Z	1 64			7 31	21 08
FT 0000 Z	1 62			7 32	21 09
FT 0000 Z	1 60			7 33	21 10
FT 0000 Z	1 58			7 34	21 11
FT 0000 Z	1 56			7 35	21 12
FT 0000 Z	1 54			7 36	21 13
FT 0000 Z	1 52			7 37	21 14
FT 0000 Z	1 50			7 38	21 15
FT 0000 Z	1 48			7 39	21 16
FT 0000 Z	1 46			7 40	21 17
FT 0000 Z	1 44			7 41	21 18
FT 0000 Z	1 42			7 42	21 19
FT 0000 Z	1 40			7 43	21 20
FT 0000 Z	1 38			7 44	21 21
FT 0000 Z	1 36			7 45	21 22
FT 0000 Z	1 34			7 46	21 23
FT 0000 Z	1 32			7 47	21 24
FT 0000 Z	1 30			7 48	21 25
FT 0000 Z	1 28			7 49	21 26
FT 0000 Z	1 26			7 50	21 27
FT 0000 Z	1 24			7 51	21 28
FT 0000 Z	1 22			7 52	21 29
FT 0000 Z	1 20			7 53	21 30
FT 0000 Z	1 18			7 54	21 31
FT 0000 Z	1 16			7 55	21 32
FT 0000 Z	1 14			7 56	21 33
FT 0000 Z	1 12			7 57	21 34
FT 0000 Z	1 10			7 58	21 35
FT 0000 Z	1 08			7 59	21 36
FT 0000 Z	1 06			7 60	21 37
FT 0000 Z	1 04			7 61	21 38
FT 0000 Z	1 02			7 62	21 39
FT 0000 Z	1 00			7 63	21 40
FT 0000 Z	0 98	</td			

Not surprisingly, there was an inverse reaction to particular products regarding assessment as least useful as compared to the most useful assessment. For example only one respondent judged the MS routine least useful while 17 judged TP to be for reasons stated earlier. The strong negative assessment of the MR routine, which generates analyzed maps of manually digitized radar data, reflects the processing problems and lack of consistent availability cited earlier. As a data source and product format for short-range terminal forecasting uses, it (MR) was not provided a sufficient evaluation in this phase of the experiment.

The last portion of Table 4, titled "Rating", summarized the relative ranking of each of the mesoscale products based on all forecasters and all test episodes. The second and third pages of the Product Usefulness Assessment form directed the forecasters to rank order from most to least useful each product used in each test episode. Up to six products were ranked in each case and the average value listed in Table 4 reflects its mean rating. The second column merely denotes the number of ratings that went into the average. Those with an average rating less than 3.0 correspond well with the products judged most useful and those with a rating greater than 3.0 with the least useful. For each product evaluated, the forecasters provided assessments of specific characteristics of the product. The results are summarized in Table 5 [parts (a) - (i)]. The numbers, which represent the total responses in each category for the full test, do not provide especially conclusive evidence that could result in product improvement. In those cases where the product was judged to provide too little information (ratings of 2 or less), it reflects a limitation in the basic data source (manually digitized radar, rawinsonde, surface observations). The deficiencies noted in FOUS guidance (FI key-in) have been overcome by additional analysis and display products that will be available in later tests. For most products, there clearly was not a strong consensus of the product's characteristics, a reflection of user preference that varies depending on the weather situation being evaluated.

Considering the general acceptance and usage of MS, the relatively low assessment of its resolution could well be overcome with a higher resolution color monitor that would permit a better representation of geographic separation and/or more stations and time periods. In part the limited value of rawinsonde data (through TP) reflected the distance from them to the forecast stations used in this experiment.

Table 5. Characteristics Assessment of Mesoscale Forecast Experiment Products

(a) Product: ENT/ET							
	Not Enough	1	2	3	4	5	Too Much
Volume of Information		2	13	10	3		
Newness of Information		1	17	8	2		
Area Resolution		2	15	9	2		1
Area Coverage		2	11	7	3		2
Time Resolution	1	8	15	3	1		
Time Coverage		3	16	6	2		
Ease of Acquiring			16	10	1		
Time to Acquire		14	12	1			
(b) Product: MDR/MR							
	Not Enough	1	2	3	4	5	Too Much
Volume of Information		6	6	10	7	1	
Newness of Information		1	6	20	3		
Area Resolution		4	8	13	4		
Area Coverage		2	5	6	0	1	
Time Resolution		5	11	11	2	1	
Time Coverage		4	4	12	5	2	
Ease of Acquiring			6	16	6	2	
Time to Acquire	2	5	14	4			
(c) Product: TP							
	Not Enough	1	2	3	4	5	Too Much
Volume of Information			3	9	3	1	
Newness of Information		7	6	3			
Area Resolution		4	8	2			
Area Coverage		3	4				
Time Resolution		1	9	2			
Time Coverage		1	3	5	1		
Ease of Acquiring				6	8	2	
Time to Acquire				5	7	2	1

Table 5. Characteristics Assessment of Mesoscale Forecast Experiment Products (Contd)

(d) Product: MS						
	Not Enough	1	2	3	4	5
Volume of Information		10	18	5		
Newness of Information		5	23	4	1	
Area Resolution	3	21	6	1	1	
Area Coverage	1	11	9	5	2	
Time Resolution		19	9	5		
Time Coverage		8	14	4	4	
Ease of Acquiring	1	4	11	7	9	
Time to Acquire	1	2	11	10	6	

(e) Product: GT						
	Not Enough	1	2	3	4	5
Volume of Information	1	8	2			
Newness of Information			9	1		
Area Resolution	1	9	1			
Area Coverage	1	4	1			
Time Resolution		8	2	1		
Time Coverage			9	1	1	
Ease of Acquiring			9	1	1	
Time to Acquire			8	1		

(f) Product: KZ						
	Not Enough	1	2	3	4	5
Volume of Information		6	15	10	1	
Newness of Information		5	24	4	1	
Area Resolution	20	9	3	1		
Area Coverage	9	9	3	1		
Time Resolution	19	13	0	1		
Time Coverage	1	20	7	4		
Ease of Acquiring		1	17	14	2	
Time to Acquire	2	7	7	12	1	2

Table 5. Characteristics Assessment of Mesoscale Forecast Experiment Products (Contd)

(g) Product: IA							
	Not Enough	1	2	3	4	5	Too Much
Volume of Information		3	5	1	1		
Newness of Information		1	6	2	1		
Area Resolution	1	6	2	0	2		
Area Coverage	1	3	3	0	1		
Time Resolution	2	6	2	0	1		
Time Coverage		2	5	2	2		
Ease of Acquiring			7	1	2		
Time to Acquire		1	5	2	1		

(h) Product: PF/CC							
	Not Enough	1	2	3	4	5	Too Much
Volume of Information		5	7	3	1		
Newness of Information		5	3	6	1		
Area Resolution	1	0	7	4	1		1
Area Coverage		1	5	4			
Time Resolution		1	7	4	4		
Time Coverage		1	7	3	4		
Ease of Acquiring		6	1	6	2		
Time to Acquire		3	4	5	1		

(i) Product: FI							
	Not Enough	1	2	3	4	5	Too Much
Volume of Information	1	1	8	1	2		1
Newness of Information	1	6	6	1			
Area Resolution	3	5	5	1			
Area Coverage		5	2	4			
Time Resolution	3	6	3	0	1		
Time Coverage	3	4	2	2			2
Ease of Acquiring	2	6	3	3			
Time to Acquire	1	6	2	3			

4.2 Forecast Difficulty Assessment

The second aspect of the forecaster assessment of the Mesoscale Forecast Experiment dealt with the terminal forecasts themselves. The forecasts that were prepared included wind speed and direction, total cloud cover, ceiling height, and 6-h precipitation amount for intervals of 1, 2, 4, and n h (10 or less based on criteria cited in Section 3.1). These elements and intervals were selected to represent the primary forecast responsibility in base weather station support to aircraft takeoff/landings and local area missions. After each case, each forecaster completed a Mesoscale Forecast Variable Assessment form (shown in Appendix D), one for each of the four variables.

Thirty-six of the fifty-four respondents judged ceiling height forecasting most difficult, eight judged wind speed and direction most difficult while total cloud amount and 6-h QPF were each judged to be most difficult by five respondents. Conversely, 29 of 54 respondents (including one "no response") judged total cloud amount the easiest of the four to forecast, 15 judged the 6-h quantitative precipitation forecast easiest, 9 judged wind, and no one judged ceiling height easiest of the four variables to forecast. In each case they were also asked to indicate the forecast interval beyond which they had little confidence in their forecasts. For the most difficult variable set of responses, that interval averaged 1.5 h, ranging from 0 to 4 h. For the second most difficult set, it averaged 2.9 h and ranged from 0 to 6 h. For the third most difficult set, it averaged 4.2 h and ranged from 0 to 10 h. For the easiest set, it averaged 8.6 h and ranged from 3 to 12 h.

The difficulty in accurately forecasting cloud ceiling heights at airfields has been recognized for a number of years. The inherent variability of storm system low clouds (in space and time), their sensitivity to local factors (such as terrain and water bodies), the limits in our ability to observe and report on their characteristics and the limits in our understanding of the complex physics by which they evolve, all serve to diminish the extent to which cloud ceiling can be forecast. Short range terminal forecasting of the type evaluated here is especially dependent on the observational component and deficiencies in that component created the most difficulty for the forecasters. While half-hourly GOES satellite imagery substantially increases observational data on storm system evolution, at best it provides only inferential data on ceiling conditions. Several of the episodes occurred at night when only IR imagery was available, thereby limiting the extent to which forecasters could try to deduce lower cloud conditions through an integrated evaluation of visible and infrared imagery. On more than one occasion low stratus ceilings advected into the forecast locations from the ocean areas to the east and south under a middle and/or high cloud shield that precluded the detection of the stratus by GOES. Two other night-time observation shortfalls complicated the already

difficult forecast problem. First, certain surface observation locations operate on a limited daily schedule in which operations are curtailed at night (most commonly, midnight to 06 LST). Second, some observers fail to detect and/or report changes in cloud conditions in a timely manner (the "sunrise special" observation was not uncommon) thereby adding more "noise" to the naturally variable time and space character of low clouds in these kinds of weather systems.

Despite the inherent difficulty in forecasting ceiling heights, the display products tailored to mesoscale details (including the use of the bar graph displays of cloud observations through the GT key-in) were relied on heavily in trying to arrive at the ceiling forecast. Among other things, they reinforced the extent to which the cloud fields were irregularly distributed, which resulted in "flatter" probability forecasts. Certain forecasters used the 2-D trajectory and satellite-based guidance procedures (PF and CC) for shorter term changes to the longer-range trends provided through the FOUS/MOS 6- and 12-h ceiling probability forecasts. Shortcomings were attributed to evolving wind fields diminishing the representativeness of the trajectories and terrain-related cloud differences that could not be translated effectively. Satellite imagery was depended on to track the translation of, and internal changes in, the overall cloud system and to estimate (in conjunction with displays such as MS) the timing of major changes in ceiling conditions. When it was available, manually digitized radar data provided supporting inferences on areas of lower ceiling height (especially in areas void of surface observations). The ability to remap the manually digitized radar analysis, geographically overlay it on concurrent GOES imagery, and then plot observations (for example, present weather symbols) on both, demonstrated some of the real potential inherent in computer-driven interactive color display systems. Figure 27 is an example of such an integrated display for 2330 GMT, 1 March 1983. The integrated real-time description (nowcast) it presents to an aviation or local area forecaster, especially when sequenced through several hours in an animated time-series loop, can provide the subjective basis for improved understanding of the evolving weather system and for improved short-range forecasts. The forecaster's ability to understand the complexity of the system (and to more properly forecast it) can be seriously limited by the lack of manually digitized radar and, in particular, GOES-type satellite imagery.

Like ceiling height, terminal area winds can be variable, particularly during an evolving winter storm, and they can be especially sensitive to local factors (such as terrain and water bodies). The major problem with the observational component of wind is the fact that certain locations operate on a limited schedule that aggravates the already sparse distribution of surface wind observations routinely available. While supplemental cloud-related observations can be obtained from satellites for data-void regions (for example, over water), remote sensing sources are not presently available for surface or near-surface winds.

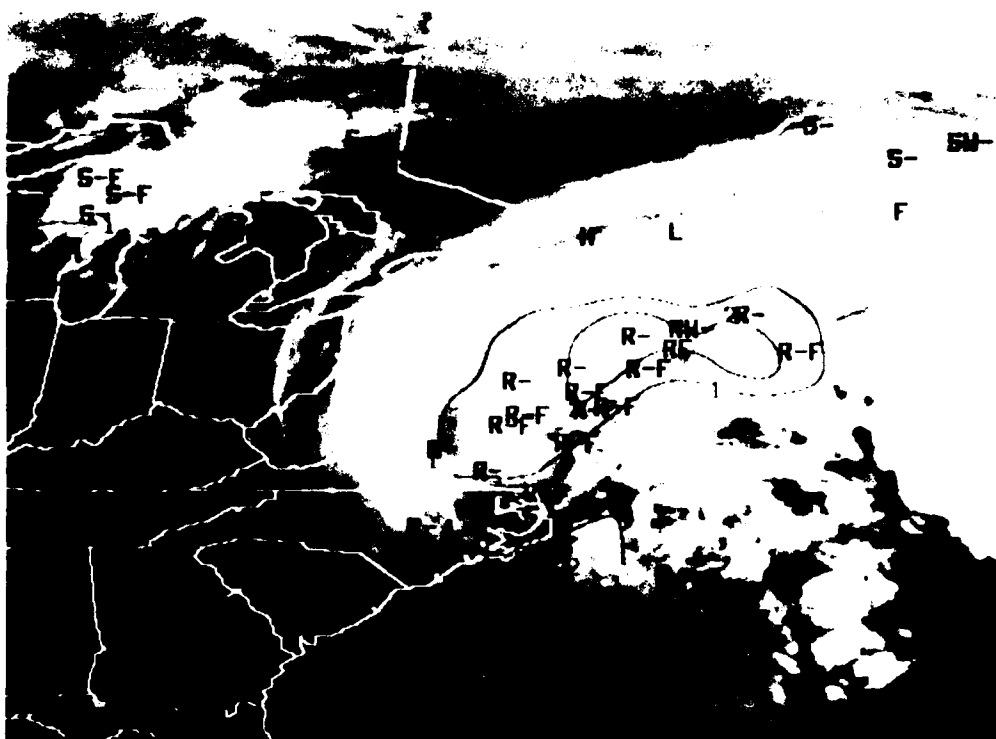


Figure 27. Example of Integrated Display of Collocated GOES IR Imagery, Manually Digitized Radar (MDR) Analysis and Plotted Weather Symbols for 2330 GMT, 1 Mar 1983

The mesoscale plot and analysis routines (MS, KZ, and so forth) were found to be useful in resolving the location and movement of mesoscale/synoptic scale perturbations such as inland convergence zones, sea breeze fronts, frontal boundaries, and isallobaric centers, which aided in resolving the terminal wind forecasts. Typically, a two-stage process was used, in which a detailed surface streamline or pressure analysis (KZ) was generated followed by a station-model time series (MS) along a line from the forecast station (for example, BOS) through a particular feature depicted in the surface analysis to a station perhaps 50-100 km beyond the feature. These depictions provided the simultaneous time-space representations of wind-related features that could be obtained given the limits of available observations. The surface and boundary layer wind speed and direction forecasts presented in FOUS bulletins (FOUS 12 and FOUS 61) were found to provide reasonable guidance, especially for the 4- and n-h forecast intervals. This guidance, presented at 6-h intervals, was generally well-tuned to diurnal variations in wind

speed, which was helpful for general trends in the terminal forecasts. The other sources of data and guidance available within the Mesoscale Forecast Experiment were of little value for wind forecasting. These included the GOES satellite imagery, manually digitized radar, and 2-D trajectory forecast model.

Products not expected to be immediately available within the initial configuration of AWDS were found to be especially useful in 6-h quantitative precipitation forecasting. These included satellite imagery, manually digitized radar analyses, and the trajectory and satellite-based forecast guidance (PF/CC). The integrated displays of present weather codes and manually digitized radar (MDR) analyses superimposed on the GOES imagery provided a visual confirmation of the portions of the cloud systems that are the precipitation-producers. Then satellite data, with or without manually digitized radar analysis, can be used effectively to track the progression of rain areas to time its arrival at the forecast locations. When the storm system was out over the Atlantic, satellite data provided the only sure source of information. In the absence of hourly rainfall amounts, the intensity changes in the visible and IR imagery were used to approximate the 6-h QPF totals. The color enhancement of IR imagery based on temperature thresholds (ENT/ET) aided in evaluating the growth or decay of rain-producing cloud masses. Sequencing (looping) of the color-enhanced imagery for a 2-3 h period was a commonly used procedure of resolving onset and duration estimates at the forecast locations. During daylight, the forecasters were able to use both visible and IR loops (individually or in an interlaced display). Nighttime periods were obviously limited to IR only but for precipitation forecasting purposes it, by itself, provides valuable guidance. The trajectory-algorithm guidance (PF/CC) is only applicable under daytime conditions and then must be constrained to the central 75-80 percent of the daylight regime due to the sensitivity of the algorithms to solar angle variations.

Without satellite and/or radar data, a forecaster must rely on hourly precipitation intensity observations (light, moderate, or heavy) as the basis for departing from FOUS or other centrally-generated guidance. There are times, unfortunately, when the hourly intensity values can be quite inconsistent with 3- or 6-h amounts. The station model time-series display (MS) was found to be most useful in trying to reconcile precipitation characteristics, particularly when used in conjunction with four-panel displays (IA) to define the geographic precipitation distribution. The LFM-based precipitation guidance (FOUS 61-LFM Guidance and FOUS 12-MOS) provided excellent guidance on the precipitation potential of the storm system; guidance which the forecasters could adjust to information on actual storm tracking and intensity. The 6-h QPF FOUS guidance was used more than the guidance for the other forecast variables.

Clearly, total cloud amount (or cloud cover) was found to be the easiest variable to forecast during these winter-early spring east coast storm situations. The

relative ease was aided by the availability of half-hourly updates of visible and IR imagery. In most situations it provided all the information needed to prepare the cloud cover forecast. When the middle and high cloud leading edge of a storm system's cloud shield advanced into the forecast region during nighttime periods, inconsistencies between satellite IR depictions of cloud cover and concurrent surface observations of sky conditions would occasionally exist. Invariably this was attributable to untimely surface observations which nonetheless provided some uncertainty in the forecast process in which some forecasters tried to factor "observer-deficiencies" into their cloud category probability forecasts. Timing and duration of cloud cover characteristics were generally resolved through repeated time series looping of visible and/or IR digital imagery.

The most widely used non-satellite product for tracking total cloud amount conditions was the station model time series (MS), particularly for tracking the leading (trailing) edge of overcast and ceiling conditions. The forecasts for the 4- and n-h periods were often finalized after giving consideration to the FOUS (MOS) guidance.

4.3 Forecast Verification Statistics

It was noted in Section 3.1 that numerical and probability forecasts were generated for two locations based on data available on an hourly cycle (six times per episode) for 10 winter-spring east coast storm episodes, independently by up to six forecasters per episode. A computerized verification procedure was implemented to accumulate and update the performance statistics on each forecaster after each case was completed and provide it to each of them in the form illustrated by Figure 10. There were, in fact, a total of 54 forecaster-days during the total Mesoscale Forecast Experiment, which translates into a total of 648 terminal forecasts generated of each variable (54×6 forecasts/case $\times 2$ stations/case), for each forecast interval. Because verifying observations would, on occasions, not be available to the verification program due to data transmission or error problems, the actual number of verified forecasts was 628. This is a data sample from which qualitative, and not statistically robust, conclusions can be reached.

Several bases for qualitative comparison were also considered. Some of these "forecasts" (persistence, model output statistics) were available to the forecasters while they were preparing their forecasts. Others (Generalized Exponential Markov) were not, due to logistics at AFGL. As noted earlier, model output statistics guidance should properly only be evaluated at the 6-h intervals its forecasts are tailored to (00, 06, 12 and 18Z). GEM and persistence can properly be evaluated concurrently with every terminal forecast subjectively generated in the Mesoscale Forecast Experiment. As a result, the presentation of verification statistics included

here will include reference to the performance of Generalized Exponential Markov (GEM) and persistence but not of Model Output Statistics (MOS). Reference to MOS' performance in these episodes will be descriptive and selectively made where deemed appropriate.

The Generalized Exponential Markov (GEM) technique is a fundamental statistical weather forecasting procedure developed through the pioneering research of R.G. Miller.¹¹ Miller defines GEM as "a statistical technique for predicting the probability distribution of local surface weather elements hour by hour. It uses only the current local surface weather conditions as predictors. From these probability distributions, categorical predictions are made for each surface weather element." For use in the Mesoscale Forecast Experiment, the GEM technique was adapted to McIDAS to generate wind, cloud cover and ceiling height forecasts for both forecast locations which were verified at 1-, 2-, 4-, and 6-h intervals coincident with Mesoscale Forecast Experiment forecaster verifications. We adapted the minicomputer version of GEM to McIDAS which unfortunately could not be easily adapted to the variable nature of our n-h forecast. For that reason, only the 1-, 2-, and 4-h GEM results will be presented. Figure 28 is an example of a GEM forecast for BOS during one forecast episode. Three things must be recognized regarding the application of GEM in the experiment. First, GEM is founded on a Markov assumption (that is, the future state is completely determined by the present state and is independent of the way in which the present state has developed). Second, it uses multivariate linear regression equations that were developed from continuous observational samples that spanned a 10-yr period (1954-1965) and, as such, are climatologically and statistically sound. Third, in the Mesoscale Forecast Experiment, it was applied to cases that represented "heavy weather" and do not therefore reflect the characteristics of the full sample from which the GEM statistical operators were developed. It was felt, however, that GEM's universal and easy applicability made it proper and appropriate to include its performance in the qualitative assessment of the Mesoscale Forecast Experiment.

4.3.1 NUMERICAL (DETERMINISTIC) FORECASTS

Figures 29-31 summarize the rmse statistics of the numerical or deterministic predictions of wind speed and direction (vector error), cloud amount (category error), and ceiling height (100 ft error) respectively. The absolute value ceiling height errors have been influenced by the treatment of the "no ceiling" forecasts and observations. They were converted to a value of 999 (100 ft) in the verification routine which means that when "non-matches" occurred, the resulting individual errors are quite large resulting in inflated rmse statistics. The same procedure was applied to all forecasts, thus relative performance comparisons are still valid.

GGG EEEEE M M
 G E MM MM
 G GGG EEE M M M
 G G E M M
 GGG EEEEE M M

TDL AND NIEDZIELSKI
 FOR AFGL
 FOR STATION BOS
 VALID FOR 6 HOURS AFTER MAR 26, 11 LOCAL

FORECAST INTERVAL = 1 HOUR(S)

CLOUD AMOUNT -	CLEAR -1	SCATTERED 0	BROKEN 6	OVERCAST 95
----------------	-------------	----------------	-------------	----------------

CEILING HEIGHT -	< 2 0	2-4 13	5-9 63	10-29 18	30-75 7	>75 1
------------------	----------	-----------	-----------	-------------	------------	----------

FORECAST INTERVAL = 2 HOUR(S)

CLOUD AMOUNT -	CLEAR -2	SCATTERED 1	BROKEN 9	OVERCAST 93
----------------	-------------	----------------	-------------	----------------

CEILING HEIGHT -	< 2 0	2-4 11	5-9 53	10-29 24	30-75 11	>75 1
------------------	----------	-----------	-----------	-------------	-------------	----------

FORECAST INTERVAL = 4 HOUR(S)

CLOUD AMOUNT -	CLEAR -4	SCATTERED 4	BROKEN 12	OVERCAST 89
----------------	-------------	----------------	--------------	----------------

CEILING HEIGHT -	< 2 0	2-4 10	5-9 33	10-29 33	30-75 18	>75 7
------------------	----------	-----------	-----------	-------------	-------------	----------

FORECAST INTERVAL = 6 HOUR(S)

CLOUD AMOUNT -	CLEAR -3	SCATTERED 5	BROKEN 13	OVERCAST 86
----------------	-------------	----------------	--------------	----------------

CEILING HEIGHT -	< 2 0	2-4 9	5-9 23	10-29 35	30-75 20	>75 12
------------------	----------	----------	-----------	-------------	-------------	-----------

HOUR	TT	DPD	VV	WEATHER	DDFF	PPP	C1	H1	C2	H2	TS	CIG
11	52	3	1000		1715	9876	OVC	5	CLR	UNL	OVC	5
12	52	3	1000		1715	9876	OVC	5	CLR	UNL	OVC	5
13	52	3	1000		1715	9876	OVC	5	CLR	UNL	OVC	5
15	52	3	1000	RW-	1715	9876	OVC	7	CLR	UNL	OVC	7
17	52	3	1000	RW-	1715	9876	OVC	7	CLR	UNL	OVC	7

Figure 28. Example of Probability and Numerical (Categorical) Forecasts Generated by Generalized Exponential Markov (GEM) Based on Surface Observation at BOS at 1100 LST, 26 Mar 1982

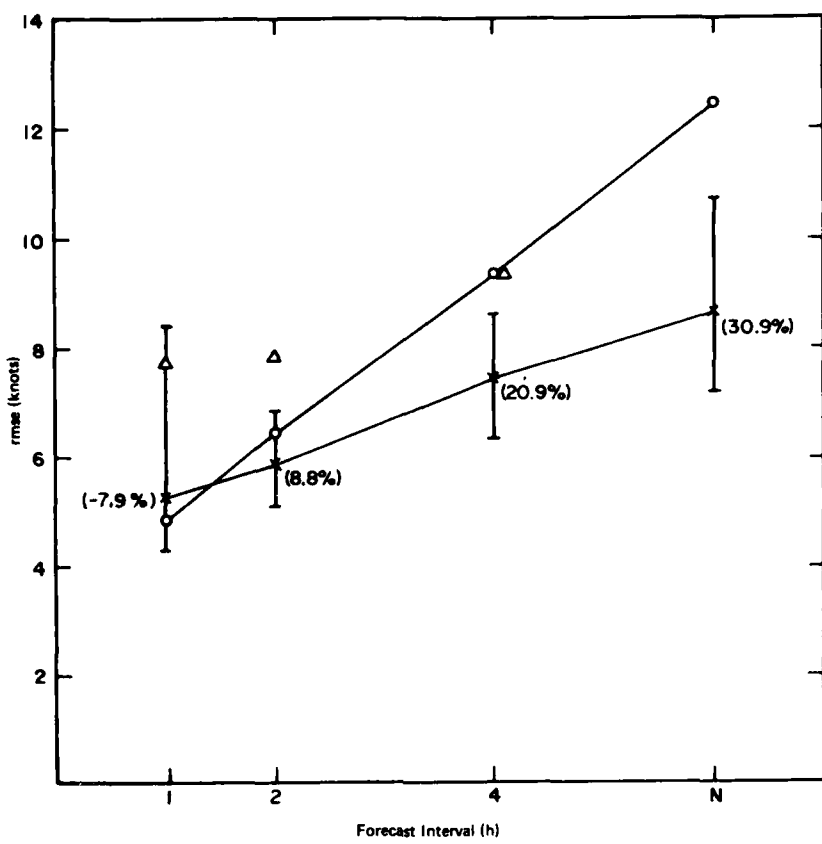


Figure 29. Root Mean Square Error Results of Mesoscale Forecast Experiment Wind Forecasts. Vector Error (in knots) as a Function of Forecast Interval (in hours) for Ten Cases, Two Stations and All Forecasters (X), Persistence (O), and for Generalized Exponential Markov (GEM) (Δ)

In each figure the results are accumulated over all episodes for both forecast locations, for all forecasters as a group (X), persistence (O) and GEM (Δ). The range in individual forecaster performance over the test period is also indicated by the vertical bar through each group verification statistic which spans the best to worst rmse performance. The numbers shown in parentheses at each forecast interval reflect the percent difference between the forecaster performance as a group and persistence. Recall that the n-hour forecasts ranged in length from 5 to 10 h, being determined in an individual forecast by the requirement to be valid at 00, 06, 12, or 18Z. No attempt has been made to further separate the n-hour forecasts.

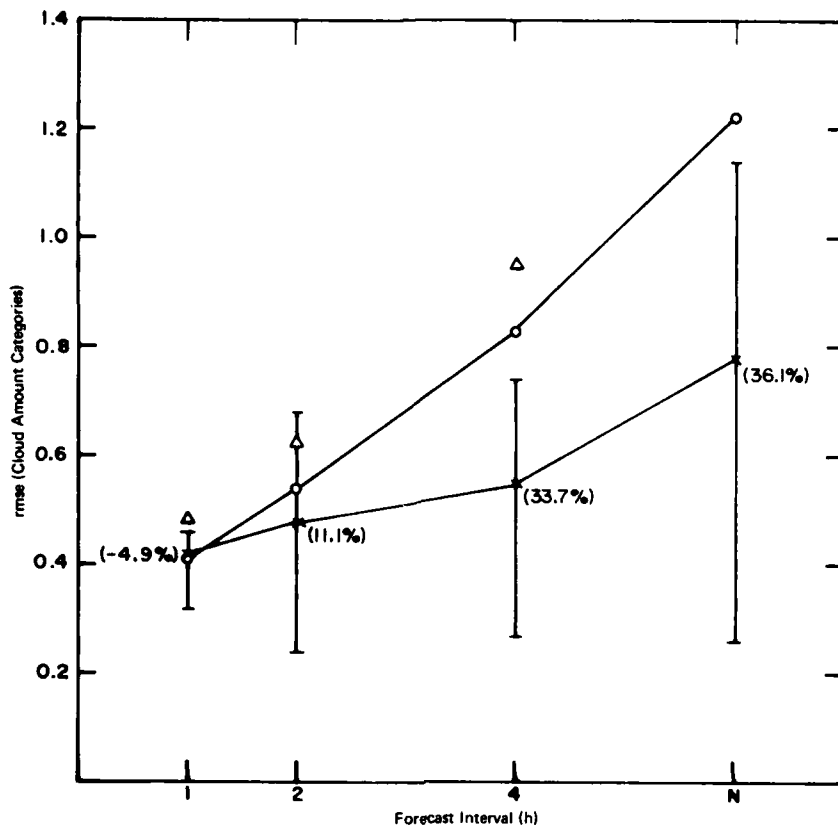


Figure 30. Root Mean Square Error Results of Mesoscale Forecast Experiment Cloud Amount Forecasts. Error (in cloud amount categories) as a Function of Forecast Interval (in hours) for Ten Cases, Two Stations and All Forecasters (X), Persistence (O), and for Generalized Exponential Markov (GEM) (Δ)

Several convincing, though qualitative, conclusions can be drawn from these results. First, with the exception of the 1-h forecasts, the Mesoscale Forecast Experiment forecasters outperformed persistence by an impressive margin for each of the forecast variables. The growth rate in the persistence error is close to monotonic for each variable, reflecting the dynamic or changeable nature of the weather associated with the test episodes and implies changes associated with disturbances of longer periodicities. For the forecasters as a group, their errors also grew with forecast interval but not nearly as rapidly as persistence, which of course, is reflected in the percent improvement statistics, which increased with forecast interval. Despite the fact that all the forecasters had access to the same

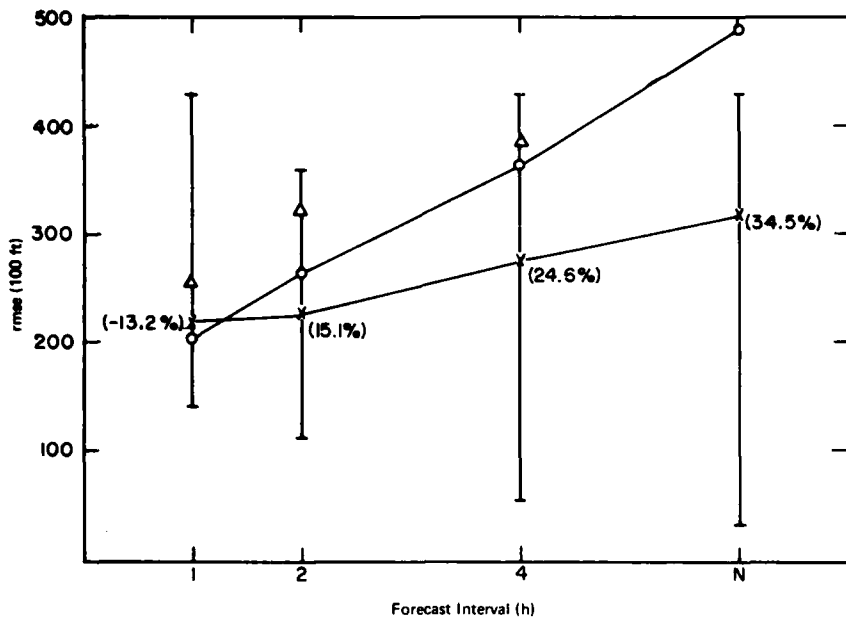


Figure 31. Root Mean Square Error Results of Mesoscale Forecast Experiment Ceiling Height Forecasts. Error (in 100 ft) as a Function of Forecast Interval (in hours) for Ten Cases, Two Stations and All Forecasters (X), Persistence (O), and for Generalized Exponential Markov (GEM) (Δ)

resources, there was clearly a fairly substantial range in forecast skill as reflected by the range in rmse statistics, particularly for ceiling height, acknowledged to be the most difficult variable to forecast. GEM's performance in generating numerical forecasts was generally worse than persistence (and most forecasters) for these episodes. With few exceptions, initial conditions at forecast time were much more degraded than the climatological norms on which GEM's statistical operator were developed. In addition, the cases selected for the Mesoscale Forecast Experiment involved prolonged periods of inclement weather. Because of its Markov characteristics, GEM would tend to forecast conditions back toward normal thereby increasing its error relative to persistence. The 6-h quantitative precipitation forecast errors by the forecasters as a group were better than persistence by about 39 percent ranging from 27 to 54 percent. Persistence resulted in an rmse error of 0.37 in. while the forecasters averaged 0.23 inches. GEM is not structured to provide 6-h quantitative precipitation forecasts.

4.3.2 PROBABILITY FORECASTS

Probability forecasts were generated for cloud amount categories (clear, scattered, broken, overcast), ceiling height categories (see Table 1) and for 6-h QPF categories (see Table 2). These categories correspond to limits established for Model Output Statistics and related NWS probability guidance. The results are summarized in two forms: (1) against the probability of persistence and (2) against the Mesoscale Forecast Experiment sample climatology. The category that existed at forecast time was assigned a probability of 1.0 (100 percent) and the other categories a value of 0.0 in the first case. Figures 32 and 33 summarize the percent improvement in cumulative p-score (cp) statistics accumulated for the forecasters as a group (X), individually, and for GEM (Δ) versus probability forecasts based on persistence, for cloud amount and ceiling height respectively.

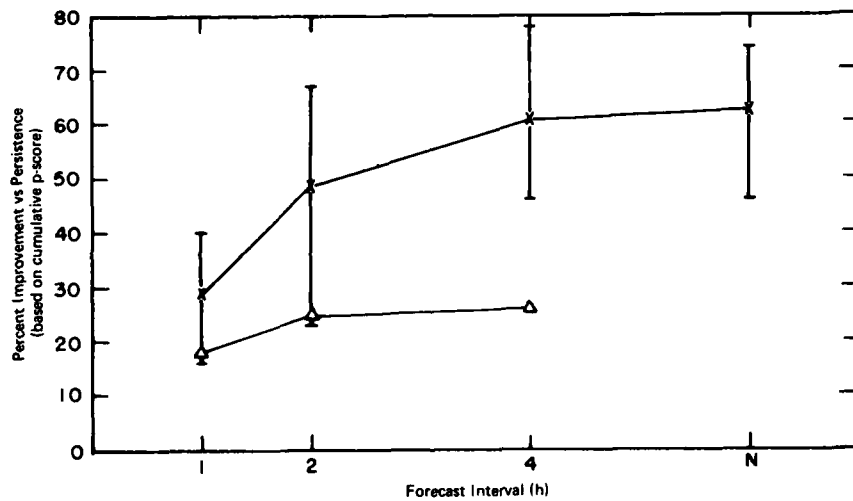


Figure 32. Percent Improvement in Cumulative p-score of Mesoscale Forecast Experiment Forecasts of Cloud Amount Versus Persistence Forecasts as a Function of Forecast Interval (in hours) for Ten Cases, Two Stations and All Forecasters (X) and for Generalized Exponential Markov (GEM) (Δ)

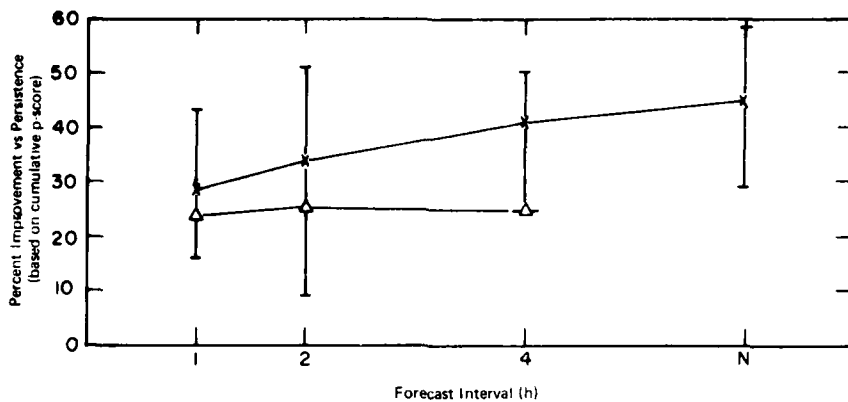


Figure 33. Percent Improvement in Cumulative p-score of Mesoscale Forecast Experiment Forecasts of Cloud Amount Versus Persistence Forecasts as a Function of Forecast Interval (in hours) for Ten Cases, Two Stations and All Forecasters (X) and for Generalized Exponential Markov (GEM) (Δ)

The probability forecasting results were consistent with the rmse statistics. They showed a fairly wide range in individual forecaster skill, and substantially better results than persistence from the forecasters, both as a group and individually. GEM does not perform as well as the forecasters as a group, does yield better scores than the weaker forecasters, and (when evaluated in probability form) does perform better than persistence (probability). The results of the 6-h QPF probability forecast verification was a 42 percent improvement versus persistence in cumulative p-score. Figures 34 and 35 summarize the forecasters (grouped) and GEM versus sample climatology as a control forecast. As one would expect, the cumulative p-score verification of the climatology model does not vary substantially as the forecast interval increases. The forecasters and GEM's cumulative p-scores do vary (degrade) with increasing forecast interval. As a result the percent improvement versus climatology decreases with time as can be seen in Figures 34 and 35.

Because the number of individual Model Output Statistics (MOS) forecasts that could properly be verified at each station was effectively limited to one per episode, quantitative comparisons are not appropriate. The general consensus among the participating forecasters was that MOS (and the other FOUS bulletins) provide terminal forecasting guidance that should be given careful consideration in the forecast preparation process, particularly for forecasts of 3 h or longer. For this reason the processing capability of AFGL's McIDAS facility has been extended since the 1982 tests to generate a wide range of display/analysis products depicting text,

geographic mapping, and tailored depictions of Model Output Statistics, (LFM) Guidance and 3-D trajectory bulletin information.⁸ Particular emphasis will be placed on evaluating these products in the 1983 Mesoscale Forecast Experiment that will be conducted with winter/spring episodes collected and archived during the 1982/83 season.

4.3.3 ANCILLARY CONSIDERATIONS

Two other aspects of the Mesoscale Forecast Experiment were investigated and evaluated by means of the rmse results. First, was there a difference in forecaster performance at the primary location (BOS) considered in each episode as compared with the secondary location (JFK, BDL or PVD) that would suggest evidence of local factors contributing to the forecast process? Second, was there a systematic change in forecast performance that could be attributed to the forecasters learning how to use the interactive system and the new products available to them as the experiment proceeded through its 10 episodes?

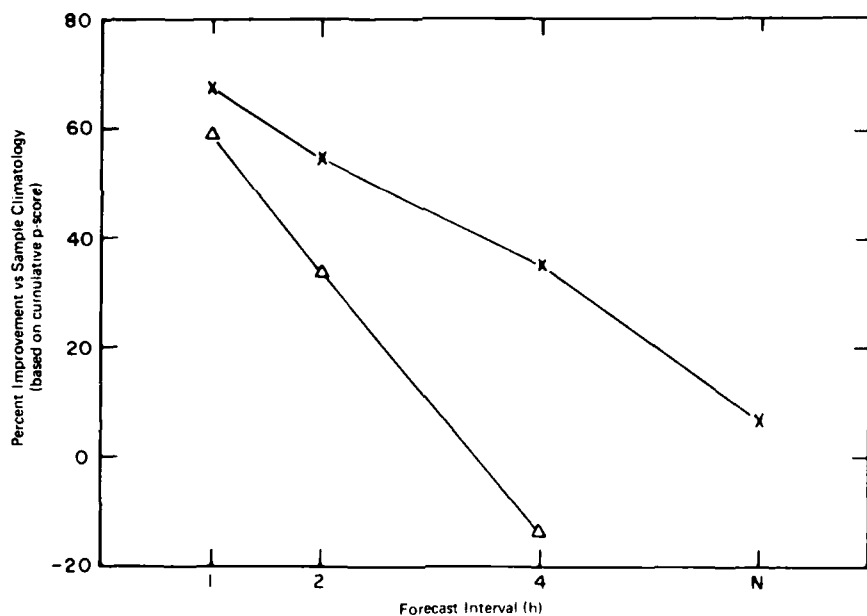


Figure 34. Percent Improvement in Cumulative p-score of Mesoscale Forecast Experiment Forecasts of Cloud Amount Versus Sample Climatology Forecasts as a Function of Forecast Interval (in hours) for Ten Cases, Two Stations and All Forecasters (X) and for Generalized Exponential Markov (GEM) (Δ)

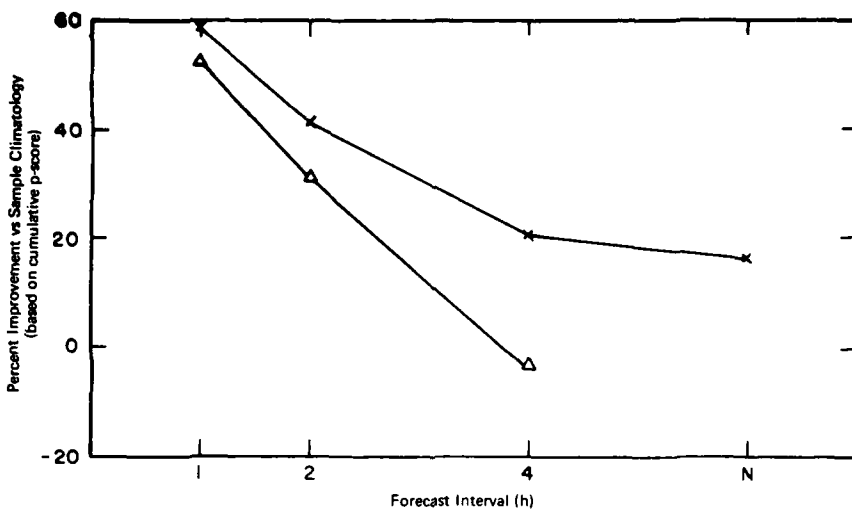


Figure 35. Percent Improvement in Cumulative p-score of Mesoscale Forecast Experiment Forecasts of Ceiling Height Versus Sample Climatology Forecasts as a Function of Forecast Interval (in hours) for Ten Cases, Two Stations and All Forecasters (X) and for Generalized Exponential Markov (GEM) (Δ)

Figures 36 to 38 depict the rmse statistics for wind vector (Figure 36), cloud amount (Figure 37), and ceiling height (Figure 38) for the primary forecast locations (P) and the secondary locations (S) for the forecasters as a group (X), persistence (Θ), and for GEM (Δ). These results are merely a separation by forecast location of the results presented in Figures 29-31 respectively. Again, the numbers in parentheses represent the percent difference between the forecasters and persistence rmse's. With the exception of the wind forecasts, there is no evidence of local factors contributing to differences in forecaster performance. There is, however, evidence to suggest that a better familiarity with local wind characteristics at Logan (BOS) than at the other locations did contribute to improved forecaster performance. Note that the other locations (JFK, BDL, and PVD) are sited such that there is a substantially data-void area immediately to their southwest, the direction from which these systems typically moved. The better forecast performance at BOS occurred despite the fact that Logan's winds were highly non-persistent during these episodes as evidenced by vector errors in excess of 10 knots at 4 hours and beyond and errors which averaged about 2 knots higher at Logan than at the secondary locations at all forecast intervals. Also, the mean scalar wind is higher at BOS due to different exposure (in part, height of wind sensor off ground). GEM's performance does not appear to be any better (or worse) at the separate forecast locations, at least based on these small samples.

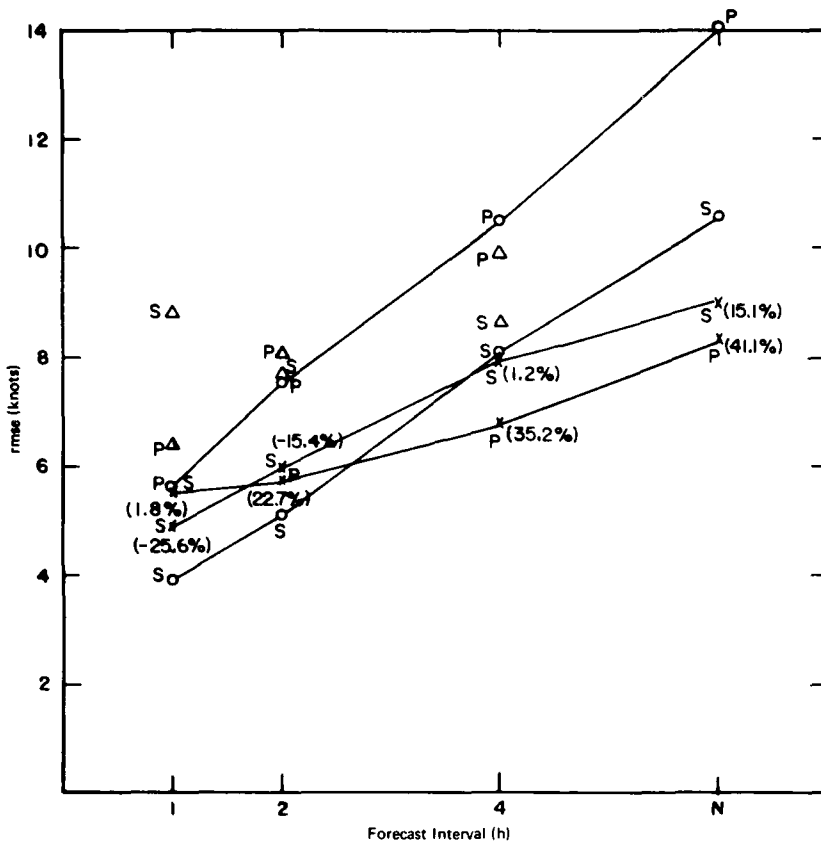


Figure 36. Root Mean Square Error Results of Mesoscale Forecast Experiment Wind Forecasts for Primary Forecast Location (P) and Secondary Location (S). Vector Error (in knots) as a Function of Forecast Interval (in hours) for Ten Cases and All Forecasters (X), Persistence (O) and for Generalized Exponential Markov (GEM) (Δ)

Figure 39 depicts the cumulative change in the forecasters wind vector rmse results versus persistence for each forecast interval. There was an initial period of adjustment downward until the results after 6 episodes had been accumulated. This just reflects variations in performance in the individual episodes which can cause wide fluctuations in the cumulative statistics until the verification sample size increases. From case 6 through 10 there is slight evidence of improving performance relative to persistence for each forecast interval. The 1-h results improve from -13 to -3 percent, 2-h from 5 to 11 percent, 4-h from 8 to 18 percent, and n-h from 14 to 31 percent. This

admittedly weak quantitative evidence is reinforced, however, by the judgment of the participating forecasters who generally felt that their ability to forecast terminal weather conditions was improved during the experiment mainly because of their confidence in and familiarity with the new products available to them.

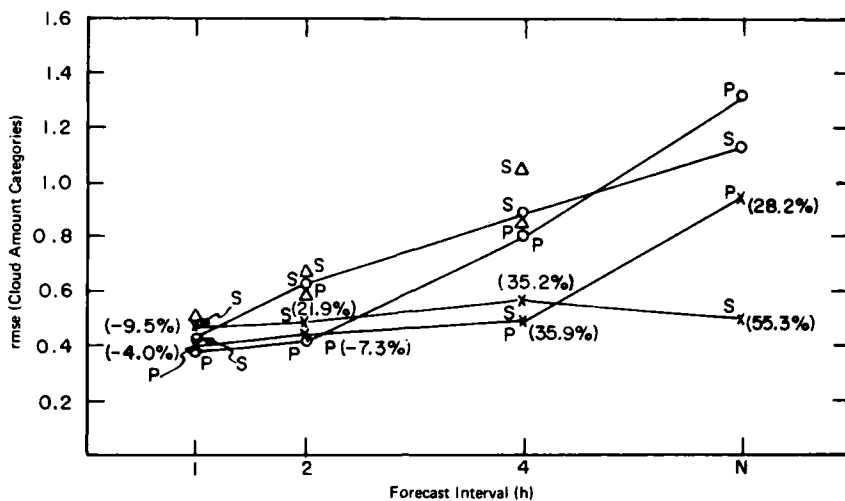


Figure 37. Root Mean Square Error Results of Mesoscale Forecast Experiment Cloud Amount Forecasts for Primary Forecast Location (P) and Secondary Location (S). Error (in Cloud Amount Categories) as a Function of Forecast Interval (in hours) for Ten Cases and All Forecasters (X), Persistence (○) and for Generalized Exponential Markov (GEM) (Δ)

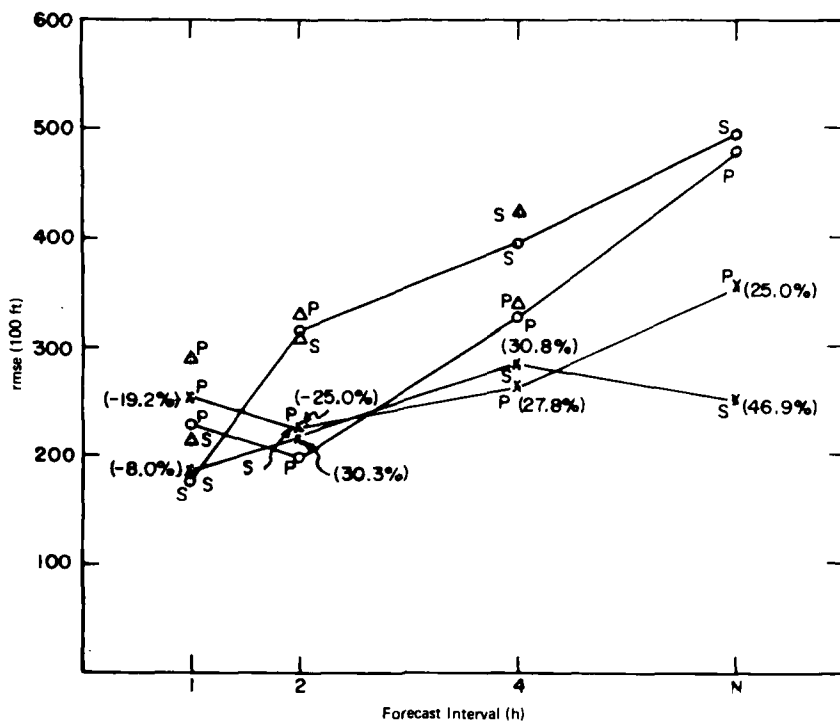


Figure 38. Root Mean Square Error Results of Mesoscale Forecast Experiment Ceiling Height Forecasts for Primary Forecast Location (P) and Secondary Location (S). Error (in 100 ft) as a Function of Forecast Interval (in hours) for Ten Cases and All Forecasters (X), Persistence (O) and for Generalized Exponential Markov (GEM) (Δ)

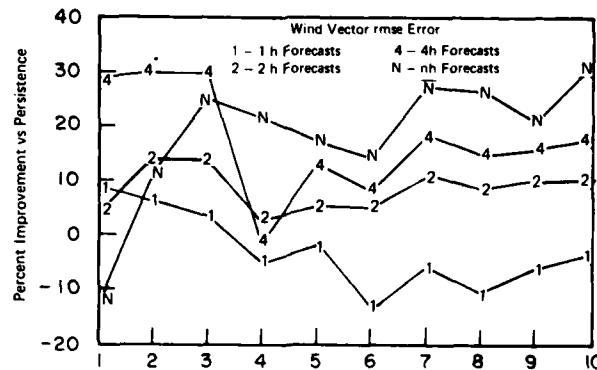


Figure 39. Percent Improvement vs Persistence of Cumulative Root Mean Square Error Results of Mesoscale Forecast Experiment Wind Forecasts as a Function of Forecast Interval and Number of Forecast Episodes

5. CONCLUDING REMARKS AND FUTURE PLANS

A Mesoscale Forecast Experiment was conducted using the AFGL McIDAS facility and data from ten winter/spring east coast storm episodes. The Mesoscale Forecast Experiment was structured to emulate aspects of the aviation terminal weather support function in base weather stations, using a computer-driven interactive graphics display system of the type envisioned with the Automated Weather Distribution System (AWDS) and having access to weather data sources initially planned with AWDS and those that could be made available in future, expanded AWDS configurations. The Mesoscale Forecast Experiment was designed to assess numerous display and analysis products tailored to provide mesoscale detail, of remotely-sensed data sources, and of the ability of forecasters to prepare certain short-range terminal forecasts.

After each participating forecaster concluded his involvement with each forecast episode, he completed two assessment forms. The first addressed the value of certain display products and data sources in preparing terminal forecasts of wind speed and direction, total cloud amount, ceiling height and 6-h QPF. The second required an assessment of the relative difficulty in forecasting each of the four elements accompanied by a discussion of the products/data sources important to the forecast preparation process. Over the course of the 10-episode test, there were 54 sets of assessment forms completed. In addition, a statistical verification of forecaster performance was conducted for the numerical and probability forecasts that were generated.

The products judged to be most useful in the preparation of short-range terminal forecasts included (1) a station model time series display, (2) conventional geographic data displays presented simultaneously as four quadrant panels on one screen, (3) mesoscale surface objective analyses, and (4) a forecast guidance procedure based on 2-D upper-air trajectories and sensible weather algorithms based on GOES imagery. Two factors contributed to the usefulness of these products compared to the others evaluated. First, it was the ease and flexibility of their implementation through McIDAS coupled with the high degree of basic, but tailored, information they provided to the forecasters for subjective interpretation in the forecast preparation process. Second, they retained or highlighted a greater degree of mesoscale aspects of the developing extratropical storm systems being used in the Mesoscale Forecast Experiment.

The importance of half-hourly GOES visible and IR imagery in short-range terminal forecasting was confirmed in this experiment. The participating forecasters relied more heavily on it to prepare their cloud cover, 6-h QPF, and ceiling height (to a lesser degree) forecasts than any other source. The manipulation of digital imagery in a computer-based interactive graphics system through

time-series looping, color enhancement and overlaying conventional data plots and analyses on it provides a wealth of qualitative and quantitative guidance for forecasting purposes. When the storm system is over water (east coast winter storms often are) GOES imagery often provides the only data source on storm behavior and movement. The limited availability of manually-digitized radar (MDR) in this experiment precluded an adequate evaluation of its displays and products by the participating forecasters. The 1982/83 winter storm episodes to be used in the 1983 Mesoscale Forecast Experiment will provide a better opportunity for that evaluation.

Ceiling height was found to be the most difficult component to forecast due to its inherent variability during storm situations, its sensitivity to terrain considerations and the limits of our ability to fully observe and report it from ground-based or satellite perspectives. Terminal wind conditions were deemed to be the second most difficult variable to properly resolve in forecasts for durations up to 10 h. Not surprisingly, the 6-h QPF forecast process benefits more from GOES imagery and MDR displays than the other forecast variables with the result that it was judged the second easiest variable to forecast. Total cloud amount (cloud cover), was judged to be the easiest to forecast and, in most cases, the forecasters relied almost totally on the half-hourly GOES imagery to resolve their forecasts of it.

The conclusions drawn from the statistical verification of the forecasters' numerical and probability forecasts must be viewed as qualitative indicators (albeit convincing in most cases) of relative skill because of the sample size (approximately 630 forecasts of each variable for each forecast interval). The numerical or deterministic forecasts yielded superior rmse's compared to persistence at all forecast intervals except 1 h. At 4 h, the improvement over persistence ranged from about 21 percent for wind forecasts to about 34 percent for total cloud amount while the 6-h quantitative precipitation forecasts yielded a 39 percent improvement. The forecasters probability forecasts were consistently better than persistence probability and showed skill versus sample climatology, even at the n-h interval. A generalized statistical prediction technique called GEM was evaluated for the cases studied and found to result in slightly worse rmse's and much better cumulative p-score results than persistence. This was an anticipated outcome because the Mesoscale Forecast Experiment test sample was purposely confined to "heavy weather" episodes in order to provide a more substantial evaluation of products and data sources.

The 1982 Mesoscale Forecast Experiment was the first of two planned tests; the second will be conducted in the summer of 1983 using winter and early spring storm episodes archived during the 1982-1983 season. Improvements will have been made to individual products based on the 1982 Mesoscale Forecast Experiment assessment, MDR data will be more fully available for evaluation. FOUS bulletins

will be integrated into the interactive processing options available to the forecasters, and the GEM forecasts will be available through McIDAS as guidance and as a control technique. A certain number of experiments will be conducted in which data available to the forecasters will be limited to that which will be available through AWDS when it is initially deployed. Forecast difficulty and product usefulness assessment forms will be used to gather feedback from the participating forecasters but with some modifications (improvements) of the 1982 Mesoscale Forecast Experiment forms.

References

1. Air Weather Service (1982) Air Weather Service Capabilities Master Plan (CMP)1982-1986, Hq AWS, Scott AFB, Illinois.
2. Smith, E. A. (1975) The McIDAS System, IEEE Trans. Geosci. Elec., GE-13:123-136.
3. Gerlach, A. M., Ed. (1980) Development of Automated Objective Meteorological Techniques, AFGL-TR-81-0017, Contract F19628-79-C-0033, pp 46-51, AD A097718.
4. Gerlach, A. M., Ed. (1981) Technique Development for Weather Forecasting, AFGL-TR-82-0020, Contract F19628-81-C-0039, pp 115-116, AD A118744.
5. Barnes, S. L. (1964) A technique for maximizing details in numerical weather map analysis, J. Appl. Meteorol., 3:396-409.
6. Wash, C. H., and Whittaker, T. M. (1980) Subsynoptic analysis and forecasting with an interactive computer system, Bull. Am. Meteorol. Soc., 61(No. 12):1584-1591.
7. Muench, H. S. (1981) Short-range Forecasting of Cloudiness and Precipitation Through Extrapolation of GOES Imagery, AFGL-TR-81-0218, AD A108678.
8. Gerlach, A. M., Ed. (1982) Objective Analysis and Prediction Techniques, AFGL-TR-82-0394, Contract F19628-82-C-0023, AD A131465.
9. Brier, G. W. (1950) Verification of forecasts in terms of probability, Mon. Wea. Rev., 78:1-3.
10. Epstein, E. A. (1969) A scoring system for probability forecasts of ranked categories, J. Appl. Meteorol., 8:985-987.
11. Miller, R. G. (1981) GEM: A Statistical Weather Forecasting Procedure, NOAA-TR-NWS-28.
12. Glahn, H. R., and Lowry, D. A. (1972) The use of model output statistics (MOS) in objective weather forecasting, J. Appl. Meteorol., 11:1203-1211.
13. National Weather Service (1981) FOUS 60-78 Bulletins, NOAA-NWS Tech. Proc. Bull. No. 294.
14. Reap, R. M. (1972) An operational three-dimensional trajectory model, J. Appl. Meteorol., 11:1193-1202.

Appendix A

Cold-Front Decision Assistance Procedure

A1. THE COLD-FRONT PROBLEM

Accurate short-range forecasting of frontal movement and its associated weather can be a challenging problem. Cold fronts often produce rapidly changing weather conditions. Thunderstorms, strong winds, and colder temperatures accompany many warm season cold fronts while snow squalls, sharply falling temperatures, and dangerous wind-chill conditions can accompany cold season cold fronts. Classically, a cold frontal passage is closely marked by a wind shift, temperature drop, pressure rise, infiltration of drier air, and an end to precipitation. Most cold frontal passages are readily apparent to the trained observer/analyst because they exhibit several of these characteristics while other weaker cold fronts may be barely noticeable except for a slight wind shift or dew-point drops.

The emergence of interactive minicomputer display systems such as McIDAS* offer the potential for improved short-range forecasting of frontal position and the rapidly changing weather associated with cold fronts. Displays of conventional meteorological data such as temperature, wind flags, streamlines and other meteorological parameters can aid the forecaster in accurately determining frontal position. Displays of computed parameters such as temperature advection, change

* McIDAS: Man-computer Interactive Data Access System



of temperature or pressure over a given time period and "time-series loops"^{*} of various parameters can give an indication of temperature changes, frontal speed, and the potential of frontal cyclogenesis. The ability to tailor the processing and analysis to a specific forecast problem in an interactive computer-driven display in near real-time opens a whole new methodology to the forecaster. This decision assistance procedure is the first in a series to document interactive procedures developed for operational forecasters using systems like McIDAS.

A2. COLD FRONT DIAGNOSTIC AIDS

Short-range forecasting of a cold front has four basic concerns: (1) speed of the front; (2) weather associated with the front; (3) temperature drop behind the front; and (4) winds ahead of and behind the front. A weather forecaster using a McIDAS system has a potentially valuable tool not available to forecasters today. First, he or she can display analyses of conventional surface data within 5 to 10 min of observation time and secondly, he or she has many computer analyses to aid him or her that are not available to forecasters relying on conventional teletype and facsimile products. These capabilities have been valuable in developing forecaster aids for use in short-range prediction problems. Depending on the particular situation, all or some of the following analyses should prove to be helpful. Each recommended analysis will be discussed, stating its physical interpretation and its potential uses in a short-range cold frontal forecast situation.

A2.1 Temperature Advection Analysis

Temperature advection is simply wind flow across isotherms. Therefore, cold advection can be defined as flow across the isotherms from a colder region into a warmer region while warm advection is just the opposite. The more nearly perpendicular the winds are to the isotherms, the stronger the winds, and the greater the temperature gradient, the stronger the temperature advection will be.

A surface temperature advection analysis is useful in several ways. First, it gives a good indication of frontal location in an area where an organized band of cold or warm temperature advection is occurring. The 0° C/day isopleth of a cold front marks the boundary between the warm advection ahead of the front and the cold advection behind the front. The temperature advection analysis also gives an indication of the potential for temperature change. A band of cold temperature

* Time Series Loop: A series of individual analyses displayed sequentially to demonstrate the movement of a particular field over time.

advection with a maximum of -60°C/day could result in as much as a 12° C temperature drop in just 2 h.^{A1}

A time series loop of temperature advection analyses at 1-h or 2-h intervals is also valuable for following the movement of an advection band associated with a front. A 6- to 12-h time-series loop previous to forecast time gives a good indication of frontal movement and changes in intensity. Care must be taken in evaluating temperature advection fields during the daylight hours. A cold front may appear to be strengthening due to increased cold advection values. In fact the cause may be differential heating which is greater in the warm sector thus increasing the temperature gradient across the front and resulting in increased advection values.

McIDAS-analyzed temperature advection analyses can also be helpful in locating secondary cold fronts that may not be readily apparent in conventional analyses.

A2.2 Streamline Analysis

A streamline is defined as a line which is everywhere tangent to the instantaneous wind vector. Near the earth's surface where frictional forces come into play, atmospheric flow always has a component across the isobars (that is, cross-isobaric flow), from high to low pressure, to compensate for friction. Thus the characteristic orientation of streamlines around a low pressure system is to spiral inward, while streamlines spiral outward around a high pressure system. Streamline analyses usually show the distinct wind shift and confluence zone associated with a surface cold front.

A streamline analysis is useful in locating high and low pressure centers, and distinct wind shift lines typical of fronts. Following the progression of the wind shift line can aid the forecaster in timing the frontal passage (FROPA) and the wind shift that will accompany it. More importantly, the streamline analysis can aid in detecting areas of developing confluence along a front that may indicate frontal cyclogenesis. Such cyclogenesis could have a major impact on the short range forecast by slowing down the frontal movement and increasing precipitation rates. In this situation, a streamline analysis, along with a 3-h isallobaric analysis, should lead to more timely and accurate short-range forecasts of cold front movement as compared to a forecaster limited to conventional weather data.

A1. Gulezian, D. P. (1980) Severe weather checklist used at national weather service forecast office, Portland, Maine. Bull. Am. Meteorol. Soc., 61(12):1592-1599.

A2.3 Wind Divergence Analysis

Horizontal divergence is defined as the net flow of air through a boundary. Divergence is an outward net flow through a boundary, while convergence is an inward net flow through the boundary.

Surface divergence computed from analyzed surface wind components can give an indication of the strength of the cold frontal convergence band. Generally, the stronger the surface convergence band, the greater the upward vertical velocities and the greater the potential for increased cloudiness and precipitation. The potential for pre-frontal squall line formation and evolution can be examined using surface divergence fields.

Observation has shown that for short-range cloud forecasting, the divergence analysis overlaid upon simultaneous satellite data can be helpful to monitor areas of cloud development or decay. Also, strong convergence in an area of developing streamline confluence and rapid pressure falls suggests the development of frontal cyclogenesis, which in turn, could slow down the front and increase precipitation rates.

A2.4 Isallobaric Analysis

A pressure change (isallobaric) analysis is useful in many situations. In forecasting weather associated with a cold front, it can be used to determine the potential for frontal cyclogenesis. Occasionally during a cold front situation, a small wave develops on or just ahead of the front. The development of such a wave can slow down the front, increase precipitation rates, and cause an error of several hours in the timing of a forecast.

In a situation where wave formation is possible, the forecaster should follow the motion and development of 3-h pressure falls over at least the past 6 h. Integrating the isallobaric analysis with information from the wind field, pressure, divergence, and streamline analyses, will aid in the decision as to whether a wave will develop or not. Generally, an organized area with 3-h pressure falls of at least 3 mb is necessary for such development. Occasionally, very rapid 3-h pressure falls (5 or 6 mb/3h) may develop ahead of a front or squall line, indicating the increasing potential of cyclogenesis or severe weather.

A2.5 Temperature Change Analysis

Depending upon the frontal situation being evaluated, a plot or analysis of 1- to 6-h temperature change can give a good indication of the temperature change that can be expected after FROPA. This analysis can aid the forecaster in determining whether the temperature change will occur immediately after FROPA or several hours later, as in a secondary front situation. The temperature change analysis

is most useful in forecasting temperatures associated with strong, rapidly moving, well defined fronts. It is less useful in forecasting weak fronts where cloud and precipitation patterns can affect the pattern of temperature changes.

Temperature change analyses often do not indicate the maximum temperature changes occurring with a cold front. Since the most rapid temperature changes generally occur in a narrow band, the objective analysis routine often smooths out the maximum temperature changes. A plot of temperature change at selected stations often provides a better indication of the full magnitude of temperature change to expect.

A3. A COLD FRONT DECISION ASSISTANCE PROCEDURE

Drawing on the analysis procedures discussed in the previous section, an interactive decision assistance procedure for forecasters dealing with short-range cold front forecast situations was formulated. It is broadly structured as shown in Figure A1 and the details of it are discussed below. A procedure of this type is ideally suited for incorporation in a minicomputer-driven, interactive graphics terminal system like McIDAS or systems being developed for Air Weather Service (SDHS - Satellite Data Handling System and AWDS - Automated Weather Distribution System). It has been programmed into AFGL's McIDAS and will undergo further evaluation in real-time and displaced real-time cold front situations.

A3.1 Assess General Weather Situation

Before proceeding into any forecast problem, a forecaster should first become familiar with the overall weather situation by examining some basic meteorological parameters on both a national and regional scale. A general understanding of the present weather situation can normally be attained by studying four national analyses which can be displayed simultaneously on McIDAS as a "four-panel analysis": surface pressure, surface temperature, 500-mb heights and 500-mb vorticity (with overlaid 500-mb wind flags). The surface pressure analysis identifies the locations of highs and lows and can give a general location of fronts and weather. The surface temperature analysis can help in locating fronts and temperature gradients. The 500-mb height and vorticity analyses indicate movement and development of synoptic scale surface features. The regional analysis should concentrate on a four-panel analysis depicting surface pressure (with overlaid wind flags and weather symbols), temperature, 3-h pressure change and streamlines. The regional analyses give a more detailed picture of existing weather conditions within the forecast area.

* A four-panel analysis displays four analyses simultaneously, one in each quadrant of the video screen. It is useful in that it allows a different parameter to be displayed in each quadrant (with overlays if desired) or the same parameter can be displayed at four different observation times.

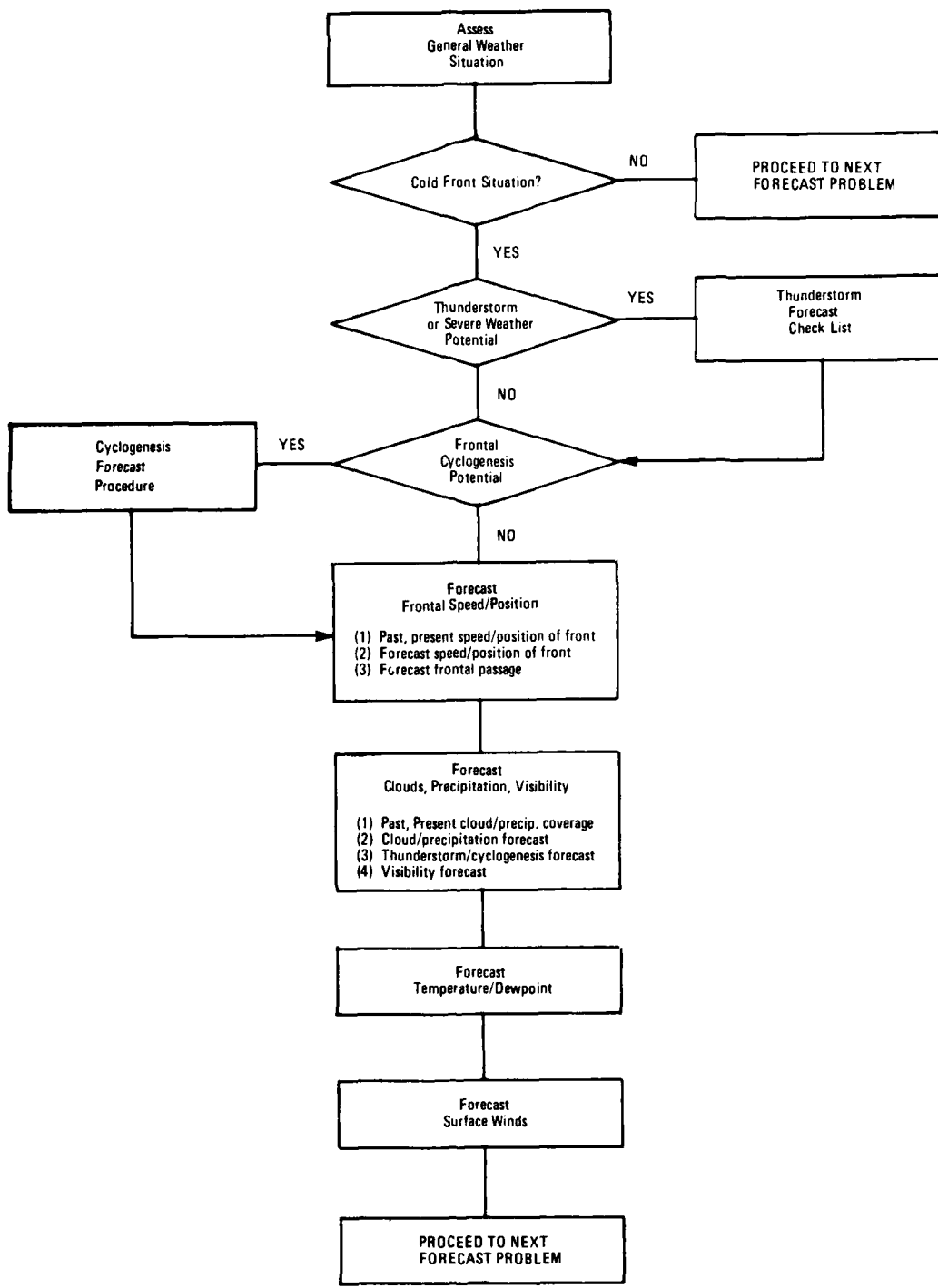


Figure A1. Diagram of Cold Front Decision Assistance Procedure

The analyses suggested above are the bare minimum necessary to assess the general weather situation. In many situations a more thorough investigation of upper air data is necessary and suggested. Wind flow, moisture and temperature patterns at 850, 700, and 300 mb are often necessary for a thorough understanding of the general weather situation.

Consult: National Analyses: surface pressure, surface temperature, 500-mb heights, 500-mb vorticity (with overlaid wind flags).

Regional Analyses: surface pressure (with overlaid wind flags and weather symbols), surface temperature, 3-h pressure change, surface streamlines.

A3.2 Cold Front Situation?

Based on the assessment of the general weather situation, does it appear that a cold front will affect the forecast region within the next 12 h? If cold frontal activity is likely to occur, continue with the Cold Front Decision Assistance Procedure.

A3.3 Thunderstorm Potential

Cold fronts, especially during the spring and summer seasons, are frequently accompanied by thunderstorms of varying degrees of severity. A frontal zone under the influence of warm, humid airflow at the surface associated with strong positive vorticity advection (PVA) in upper levels is especially susceptible to thunderstorm development. This section is intended to determine if the cold front approaching the forecast area has the potential of producing thunderstorms, and if so, to what intensity. The first step in this determination is to ask three pertinent questions:

- (1) Are thunderstorms presently occurring at or ahead of the cold front within 500 km of the forecast area?
- (2) Does radar or satellite data suggest the development of thunderstorms or a pre-frontal squall line in the cumulus or initial growth stage within 500 km of the forecast area?
- (3) Are the sounding stability indices or general weather conditions (warm moist air mass, strong PVA, or strong surface heating) favorable for thunderstorm development?

If the answer to any of the three questions is yes, consult the Thunderstorm Forecast Checklist to determine:

⁷A Thunderstorm Forecast Checklist has not been developed or evaluated as part this study. (See Reference A1 for example).

(a) If thunderstorms are already occurring, could they become strong or severe?

(b) If thunderstorms are not occurring, but atmospheric conditions appear favorable for development, does the Thunderstorm Checklist suggest thunderstorm development and if so, to what intensity?

If the answer to all three questions is no, continue with the Cold Front Decision Assistance Procedure.

Consult: radar, satellite and sounding data, and hourly observations in forecast region.

A3.4 Frontal Cyclogenesis Potential

Occasionally a low pressure system may develop on a cold front; this can increase precipitation rates and wind speed, and decrease frontal speed. In a frontal zone with strong PVA, a digging 500 mb trough or an area of moderate warm advection the forecaster must consider the possibility of frontal cyclogenesis. If any of the questions below are answered yes, or if any other meteorological data suggests frontal or pre-frontal cyclogenesis, consult the Cyclogenesis Forecast Decision Assistance Procedure.

(1) Is there or will there be, moderate to strong PVA or a 500 mb trough overtaking the frontal zone during the next 12 h?

(2) Does the regional surface pressure analysis show an area of "baggy" isobars along or just ahead of the front, possibly indicating the initial stages of wave development?

(3) Is there an organized area of 2-3 mb/3 h or greater pressure falls along the front?

(4) Does the divergence analysis show an intensifying area of convergence?

(5) Does the streamline analysis suggest the development of a cycrogenic circulation on the front?

(6) Is the cold front occluding in an area of any of the above conditions?

If all answers are no, continue with the Cold Front Assistance Procedure.

Consult: 500 mb heights, 500 mb vorticity, 3-h pressure change, surface divergence, and surface streamline.

A3.5 Frontal Speed/Position Forecast

A3.5.1 PAST AND PRESENT SPEED/POSITION OF FRONT

To determine the past and present speed of the front, the forecaster should draw the position of the front at 3-h intervals for the past 12 h on a regional map of the forecast area. A four-panel analysis of temperature with overlaid wind flags may

be sufficient to accurately locate the positions of a well-defined front. Dewpoint, pressure, streamline, temperature advection, and divergence analyses may be helpful in locating more diffuse fronts.

A3.5.2 FORECASTED SPEED/POSITION OF FRONT

As a first guess for the forecasted frontal position for the next 12 h, advect the frontal position by 3-h extrapolations using the past and present positions, making adjustments if the frontal speed is increasing or decreasing.^{A2} Next, adjust the "first guess" positions according to the following rules governing frontal movement.

- (1) Surface cold fronts (on the average) move with 70-100 percent of the normal component of the surface geostrophic wind (calculated from surface isobars) in the cold air.^{A2}
- (2) If a cold front has been moving at a constant speed over the last 12 h, chances are good it will continue to do so for at least the next 3 or 4 h.
- (3) If cyclogenesis is occurring or if the Cyclogenesis Forecast Checklist determines that cyclogenesis is likely to occur in the next 12 h, forecast decreased frontal speed according to when (in the next 12-h forecast period) cyclogenesis will occur and how rapidly the new cyclone is expected to intensify.
- (4) If a rapidly deepening cyclone is developing on the front or ahead of the front (as in a secondary coastal storm), the front could slow down considerably.
- (5) If the upper level flow will become more perpendicular to the surface front during the forecast period, forecast increased frontal speed.
- (6) If upper level flow will become more parallel to the surface front (digging upper level trough) during the forecast period, forecast decreased frontal speed.
- (7) If pressure rises behind the front are increasing significantly, forecast increased frontal speed.
- (8) If the cold front is moving into a region dominated by a well established high pressure system with a strong circulation (especially in the summer, for example the Bermuda High) forecast decreased frontal speed. Cold fronts under such conditions may stall for long periods, weaken considerably or even dissipate.
- (9) If none of the above conditions exist at forecast time and are not expected to exist during the forecast period forecast relatively steady frontal movement similar to the past 12 h.

A2. Petterson, S. (1956) Weather Analysis and Forecasting, Second Edition, Volume I., McGraw-Hill Book Company, Inc., New York.

A3.5.3 FRONTAL PASSAGE FORECAST

Accurate timing of the frontal passage can be a critical element of a short-range forecast. Brief but heavy showers, strong wind shear and wind gusts, low ceilings, low visibilities and falling temperatures can all occur during FROPA. After determining a frontal position every 3 h for the next 12 h, determine time of FROPA by interpolating between forecasted 3-h cold front positions. Consult: temperature with overlaid wind flags, dewpoint, pressure, streamline, temperature advection, and divergence.

A3.6 Cloud, Precipitation, and Visibility Forecast

General Statements:

- (1) Cold fronts with upper level winds nearly parallel to the surface front have a wide band of pre-frontal and post-frontal clouds and/or precipitation. Clearing generally does not occur until passage of the 700-mb trough. A3
- (2) Cold fronts with upper level winds more perpendicular to the surface front have a narrow band of pre-frontal clouds and precipitation with rapid clearing after frontal passage. A3
- (3) Synoptic scale cloud and precipitation belts directly associated with cold fronts tend to move at the normal component of the 700-mb wind across the belt. A4
- (4) Mesoscale cloud bands (convective showers, thunderstorms) tend to move with the 700-mb wind. A5

A3.6.1 PAST AND PRESENT COVERAGE OF CLOUDS AND PRECIPITATION

For a short-range forecast, areas of clouds and precipitation should be outlined on a regional map distinguishing between areas of light and heavy precipitation and melted and frozen precipitation at least every 3 h for the past 12 h. During severe weather episodes, this should be done as often as new data becomes available. Consult: surface weather plot, cloud cover analysis, satellite data, and radar data.

-
- A3. Air Weather Service (1970) Some Techniques for Short-Range Terminal Forecasting, AWSTR 233.
 - A4. Moncrieff, M. W., and Green, J. S. A. (1972) The propagation and transfer properties of steady convective overturning in shear, Quart. J. Roy. Meteor. Soc., 98:336-352.
 - A5. Bellon, A., Lovejoy, S., and Austin, G. L. (1980) Combining satellite and radar data for the short-range forecasting of precipitation. Mon. Wea. Rev. 108:1554-1566.

A3.6.2 CLOUD AND PRECIPITATION FORECAST

As a first guess advect cloud and precipitation areas by 1- to 3-h extrapolations making adjustments if speed or areal coverage is increasing or decreasing. Convective-type cloud and precipitation areas should be advected hourly while the better organized synoptic scale cloud and precipitation areas can be advected in 3-h intervals. This type of extrapolation is most accurate for the 0-4 h forecasts.^{A1} Beyond 4 h, cloud and precipitation patterns can change considerably due to the effects of mesoscale or synoptic scale forcing. A weather region influenced by

- (1) positive vorticity advection (PVA),
- (2) a digging and/or approaching upper level trough,
- (3) warm advection,
- (4) strong surface convergence,
- (5) frontal or pre-frontal wave development,
- (6) unstable lapse rate and strong local heating,
- (7) orographic uplift, or
- (8) moist flow off a "warm" body of water

can have rapid development and intensification of cloud and precipitation areas. In a region where any of the above conditions is forecasted to occur during the forecast period, the forecast should include the possibility of increasing cloud and precipitation coverage and enhanced precipitation rates if moisture is available. Areas of moderate precipitation can rapidly develop in a frontal zone with strong PVA. In a region where any of the above cloud or precipitation enhancement conditions are expected to occur, satellite and radar data should be analyzed closely for intensifying or newly developing cloud and precipitation areas. In mountainous terrain, upper level troughs often produce cloud and/or precipitation from air that was cloud-free upstream.

Occasionally, bands of precipitation that form in the cold air behind the front will propagate across the frontal zone, eventually becoming prefrontal bands or squall lines. Visible and IR satellite data should be studied carefully in these situations although often these bands can only be tracked by radar.

Cloud or precipitation areas may weaken or dissipate when

- (1) approaching a region occupied by very dry air,
- (2) approaching a region occupied by a strong high pressure system,
- (3) undergoing negative vorticity advection, or
- (4) approaching an upper air ridge.

If rapid clearing is occurring behind the front, the forecasted end to precipitation and clearing skies should coincide with the forecasted time of frontal passage.

A3.6.3 THUNDERSTORM AND CYCLOGENESIS FORECAST

If the Thunderstorm Checklist indicates that thunderstorms are possible the forecast should reflect the likelihood of severe weather and the associated heavy rain, low visibility, and strong wind.

If the Cyclogenesis Forecast Checklist indicates that a frontal wave will develop, precipitation rates may increase and the front may slow down to extend cloudiness and precipitation many hours. Often, a very small, poorly organized coastal wave can generate moderate precipitation amounts if moisture is available. The larger the wave and the more rapid the development, the slower the cold front will move and the greater the precipitation amounts will be. Such a situation can be drastically misforecasted.

A3.6.4 VISIBILITY FORECAST

Forecasted changes in visibility should coincide with forecasted changes in cloud cover and precipitation. A lowering cloud ceiling and the beginning of precipitation results in lower visibility. The use of a "Trend Chart" is suggested to compare the succession of events at one or more upstream stations to aid in cloud cover, cloud height, precipitation, and visibility forecasts. The Trend Chart can be especially useful in timing events such as the time between the arrival of an overcast sky and the onset of precipitation and lower visibilities. It can also aid in the cloud height and visibility forecasts by giving upstream conditions.

Frontal and pre-frontal visibility forecasts are not always dependent on tracking cloud and precipitation areas. Radiational cooling or warm moist flow over a snow surface ahead of the front can produce fog. Also, the visibility can be reduced by haze in the pre-frontal zone on a warm humid summer day.

Consult: Trend Chart, surface weather plot, cloud cover analysis, visibility plot, satellite data, and radar data.

A3.7 Temperature Forecast

For temperature forecasts, temperature fields can generally be advected according to frontal movements with modifications for diurnal heating or cooling, clouds, precipitation, and wind. Also, account for local effects such as sea breezes or lake breezes that may occur before or after FROPA.

The most difficult aspect of the temperature forecast in a cold front situation is determining the temperature change that can be expected after FROPA.

Temperature change analyses of 2, 3, and 6 h can give a good indication of temperature changes that can be expected. These analyses are most useful for fast moving, strong cold fronts. When using a temperature change analysis be aware of the effects of the diurnal temperature cycle. The temperature analysis can show

the location and movement of the cold front and the intensity of the temperature gradient.

A four-panel analysis or a time-series loop of temperature advection analyses shows the progression of temperature advection bands and changes in intensity. These analyses indicate the potential for temperature change that can be expected ahead of and behind the front.

Temperature advection analyses are also useful in locating secondary cold fronts. Occasionally the primary cold front associated with a strong winter cyclone will sweep through an area with slight temperature changes, light winds, and light precipitation, only to be followed by a more significant secondary cold front or surface trough anywhere from one hour to many hours later, marking the leading edge of rapidly falling temperatures, snow squalls and strong winds.

Consult: (2-, 3-, 6-h) temperature change, surface temperature, and temperature advection.

A3.8 Wind Forecast

Streamlines give a good indication of how wind direction is changing in the pre-frontal zone. Winds often tend to become stronger and more nearly parallel to the front as the front progresses eastward. Streamlines also give a general idea of the wind shift which occurs after FROPA. A wind flag plot should also be examined for a more detailed understanding of the turning of the wind and wind speeds ahead of and behind the front. For most cold front situations the wind shift occurs with passage of the cold front.

A plot of wind gusts can be a valuable diagnostic tool both ahead of and behind the front. Be aware of secondary cold fronts and the associated wind shifts and gusts, especially after an intense winter storm.

In forecast situations where the pressure gradient is forecast to increase significantly, forecast increased wind speeds. If cyclogenesis is occurring to the south or southwest of the forecast region, winds may shift from southerly to more easterly and become stronger. Watch for possible wind shifts and gusts caused by bands of pre-frontal showers or thunderstorms. Also, account for possible sea or lake breezes in the warm sector especially during weak flow conditions.

Consult: streamlines, wind flags, and wind gusts.

A4. CASE STUDY: A MIDWEST COLD FRONT ON 18 DECEMBER 1980

This section discusses a typical application of the Cold Front Decision Assistance Procedure and the contribution of the MCDAS Cold Front Diagnostic Aids in a short-range real-time cold frontal forecast situation. The case to be discussed is a

strong cold front that marched through the Midwest on 8 December 1980. The forecasts were prepared for Toledo, Ohio. Forecast parameters were weather, temperature, and wind direction and forecast lengths were 1, 3, and 6 h.

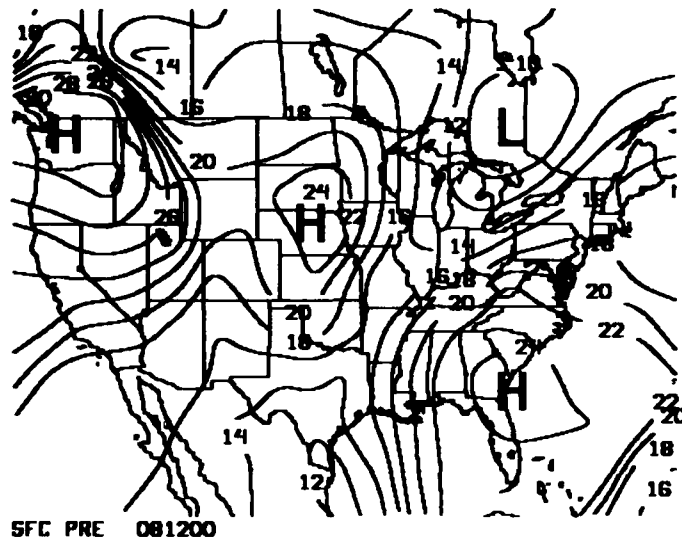
The general weather situation which existed at 1200 GMT, 8 Dec 1980, can be examined with a four-panel national analysis of: (1) surface pressure; (2) surface temperature; (3) 500-mb heights; and (4) 500-mb vorticity. The surface pressure analysis (Figure A2a) shows a low pressure system north of Lake Huron with its associated surface trough stretching southwestward across the Midwest. The rest of the country is dominated by high pressure systems (centered off the northeastern Florida coast, over Nebraska and over Washington State). The surface temperature analysis (Figure A2b) shows a band of strong temperature gradient (approximately $16^{\circ}\text{C}/450\text{ km}$) marking the position of the cold front associated with the Lake Huron low, extending from the western Great Lakes region southwestward into central Texas. Very cold air is moving out of Canada into the upper Midwest with afternoon temperatures as low as -25°C in south central Canada. The 500-mb height analysis (Figure A2c) shows a broad ridge on the east coast and a weak trough associated with the Lake Huron low moving into the upper Midwest. The 500-mb vorticity analysis with overlaid 500-mb wind flags (Figure A2d) indicates very weak vorticity advection into the Midwest system.

Another four-panel analysis at 1700 GMT, just prior to forecast time, zooms in on the regional analysis centered on Toledo. This analysis displays: (1) surface pressure with overlaid wind flags and weather symbols; (2) surface temperature; (3) 3-h surface isallobars; and (4) surface streamlines (Figures A3a-A3d).

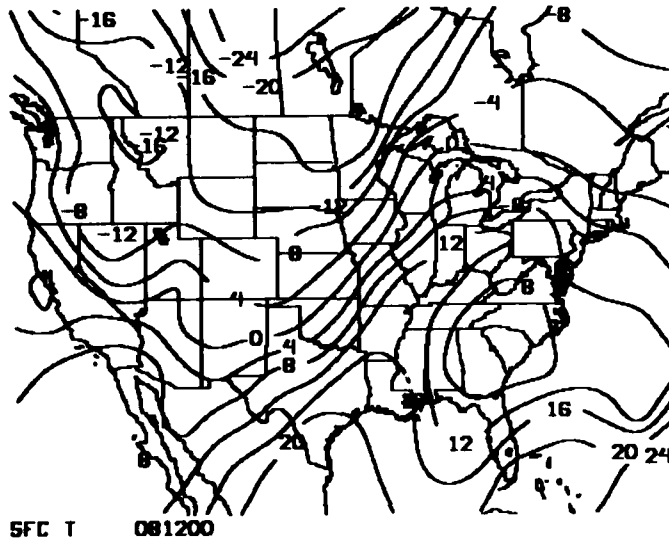
The regional surface pressure analysis with overlaid weather symbols and wind flags (Figure A3a) indicates a sharp surface trough with light precipitation ahead of and behind the cold front associated with the Lake Huron low. The regional temperature analysis (Figure A3b) shows the strong temperature gradient lying just to the west of Toledo. The isalobaric analysis (Figure A3c) shows only minor pressure falls of less than 2 mb in 3 h ahead of the front. The streamline analysis (Figure A3d) and pressure analysis with overlaid wind flags (Figure A3a) indicates a well defined wind shift from SSW to NW as the trough line passes. An analysis of wind gusts (not shown) shows no strong or gusty winds behind the front.

Based on the assessment of the general weather situation it appears that a cold front will certainly affect the Toledo area within the next 12 h. The four-panel regional analysis demonstrates that the timing of the front is critical because a rapid wind shift, rapid temperature drop and light rain are all occurring in a narrow band along the front.

During the morning, thunderstorms were not observed along the cold front. Satellite and radar data indicated only low stratus with light rain. The weak 500-mb vorticity advection and sounding data imply that conditions are not favorable for thunderstorm development in the next 12 h.

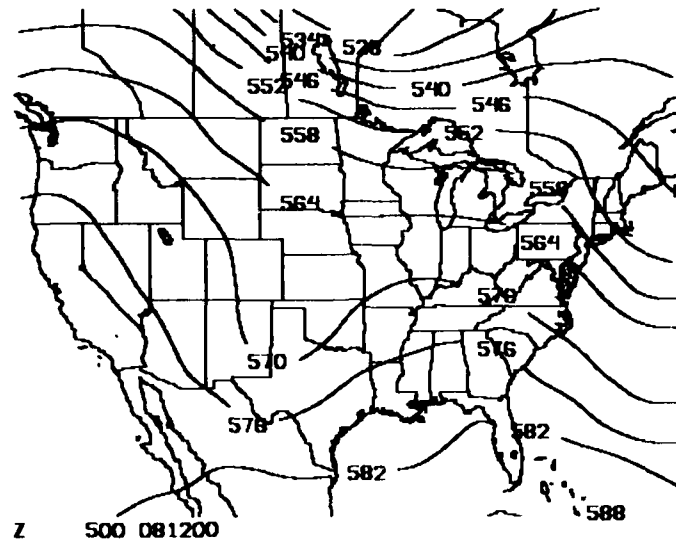


(a) Pressure (mb Deviation from 1000 mb)

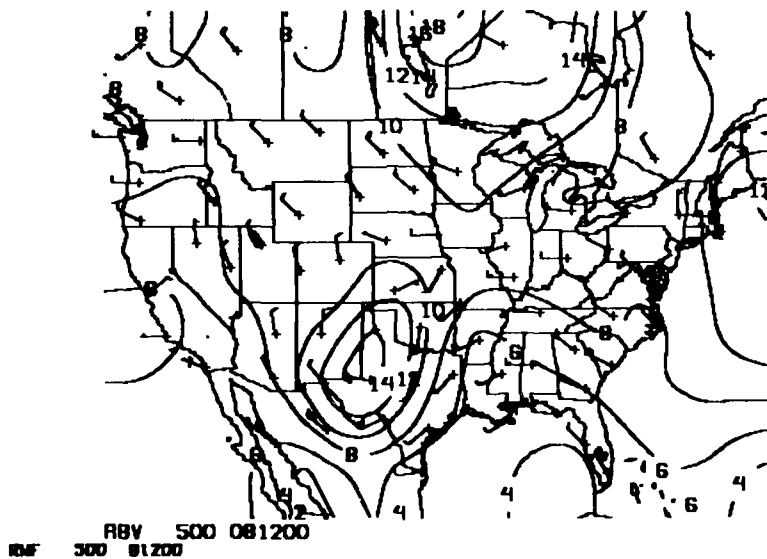


(b) Temperature (°C)

Figure A2. Four Panel Analysis of General Weather Situation (National): (a) Pressure (mb Deviation from 1000 mb) (b) Temperature (°C), (c) 500-mb Heights (decameters), and (d) 500-mb Absolute Vorticity ($\times 10^{-5} \text{ sec}^{-1}$) and 500-mb Wind Flags (m/sec)

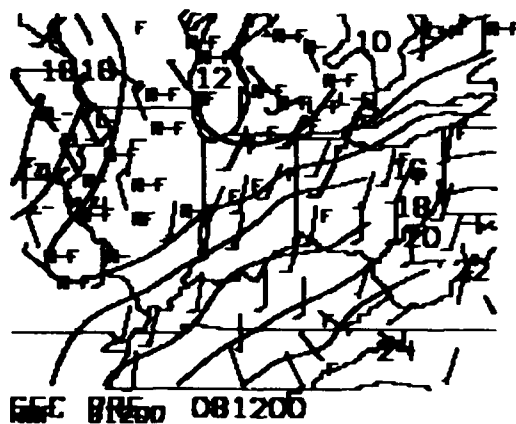


(c) 500-mb Heights (decameters)

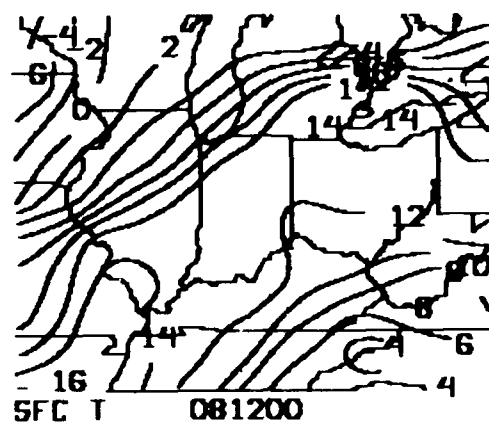


(d) 500-mb Absolute Vorticity ($\times 10^{-5} \text{ sec}^{-1}$) and
500-mb Wind Flags (m/sec)

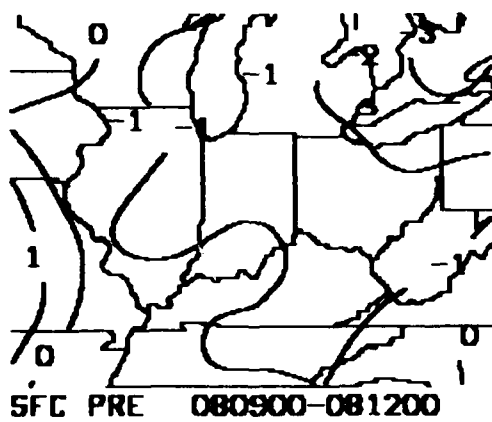
Figure A2. Four Panel Analysis of General Weather Situation (National): (a) Pressure (mb Deviation from 1000 mb), (b) Temperature ('C), (c) 500-mb Heights (decameters), and (d) 500-mb Absolute Vorticity ($\times 10^{-5} \text{ sec}^{-1}$) and 500-mb Wind Flags (m/sec). (Contd)



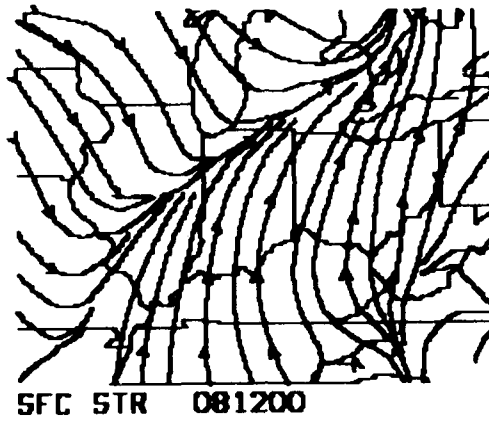
(a) Pressure (mb Deviation from 1000 mb) and Surface Wind Flags (knots)



(b) Temperature (°C)



(c) 3-h Pressure Change (mb)



(d) Surface Streamlines

Figure A3. Four Panel Analysis of General Weather Situation (Regional);
 (a) Pressure (mb Deviation from 1000 mb) and Surface Wind Flags (knots),
 (b) Temperature (°C), (c) 3-h Pressure Change (mb), and (d) Surface Streamlines

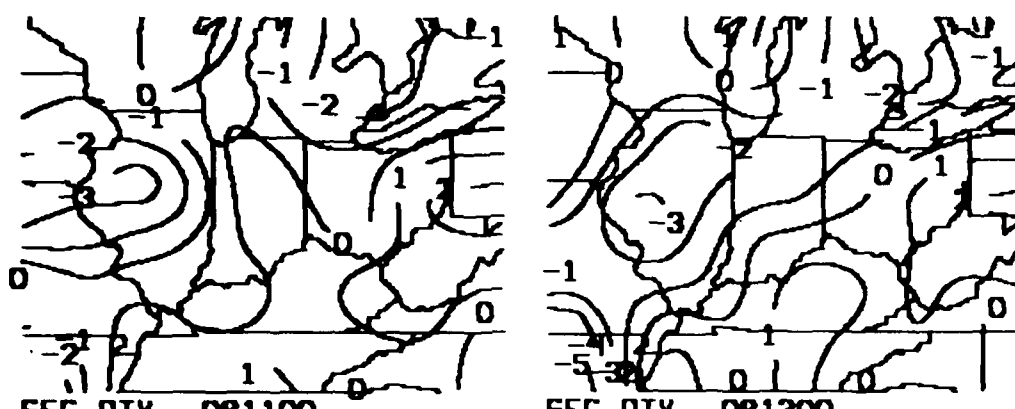
The minor 3-h pressure fall area ahead of the front (Figure A3c) and weak upper level support indicate that frontal cyclogenesis is unlikely during the next 12 h. The wind divergence analyses from 11 GMT to 17 GMT (Figure A4) show a moderate band of convergence steadily progressing southeastward across the Midwest. This band marks the convergence zone associated with the cold front. The divergence analyses show no intensifying areas of convergence along the front during the last 6 h which is in agreement with the isallobaric analysis and upper air data in predicting that cyclogenesis is unlikely. The surface streamline analyses from 11 to 17 GMT (Figure A5) also show no sign of a developing cyclonic circulation.

In this particular situation with a strong cold front, the past and present frontal positions can be accurately determined with a series of 3-hourly temperature analyses with overlaid wind flags. These analyses can be displayed on a four-panel analysis (Figure A6) so that four frontal positions can be viewed simultaneously. By drawing the past frontal positions on a regional map, it is determined that the cold front is moving steadily southeastward at 33 km/h.

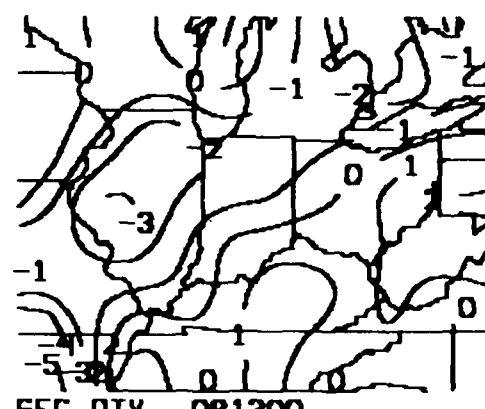
Streamline analyses from 11 GMT to 17 GMT (Figure A5) also show the steady southeastward movement of the cold front. The cold front can be located on the 17 GMT streamline analysis (Figure A5d) along the "trough" of rapid wind direction change. Because there was no frontal cyclogenesis or digging upper level trough to impede frontal movement, the front was forecast to continue moving southeastward at about 30 km/h. Therefore FROPA was predicted to occur in Toledo at 20 GMT.

Surface observations and satellite data indicate that clouds and precipitation are found in a narrow band ahead of and behind the front in the forecast region. Over the past several hours the cloud band and associated precipitation area has been steadily moving southeastward along with the front. Surface observations recorded on a trend chart for upstream stations show that the occurrence of overcast skies is followed within the hour by light rain or showers and lower visibilities of around 2 to 3 km.

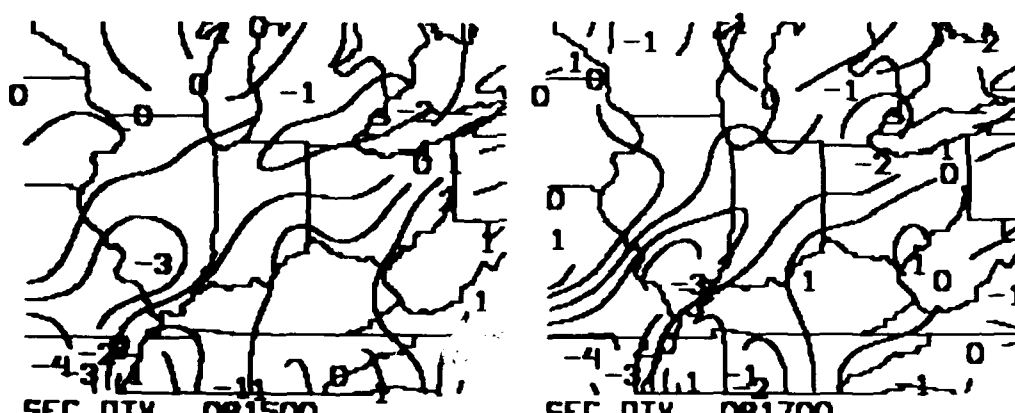
Since there is only weak vorticity advection and virtually no chance of thunderstorms or cyclogenesis one should expect precipitation amounts to remain light. Also, it is predicted that the cloud and precipitation area will continue its steady southeastward motion. Light rain is forecast to continue in Toledo for several hours after FROPA with broken clouds and improved visibilities thereafter.



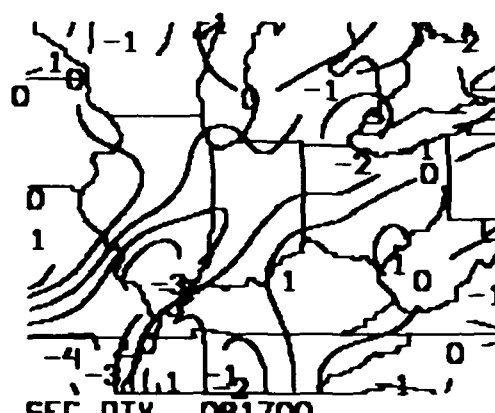
(a)



(b)



(c)



(d)

Figure A4. Surface Divergence ($\times 10^{-5}$ sec $^{-1}$)

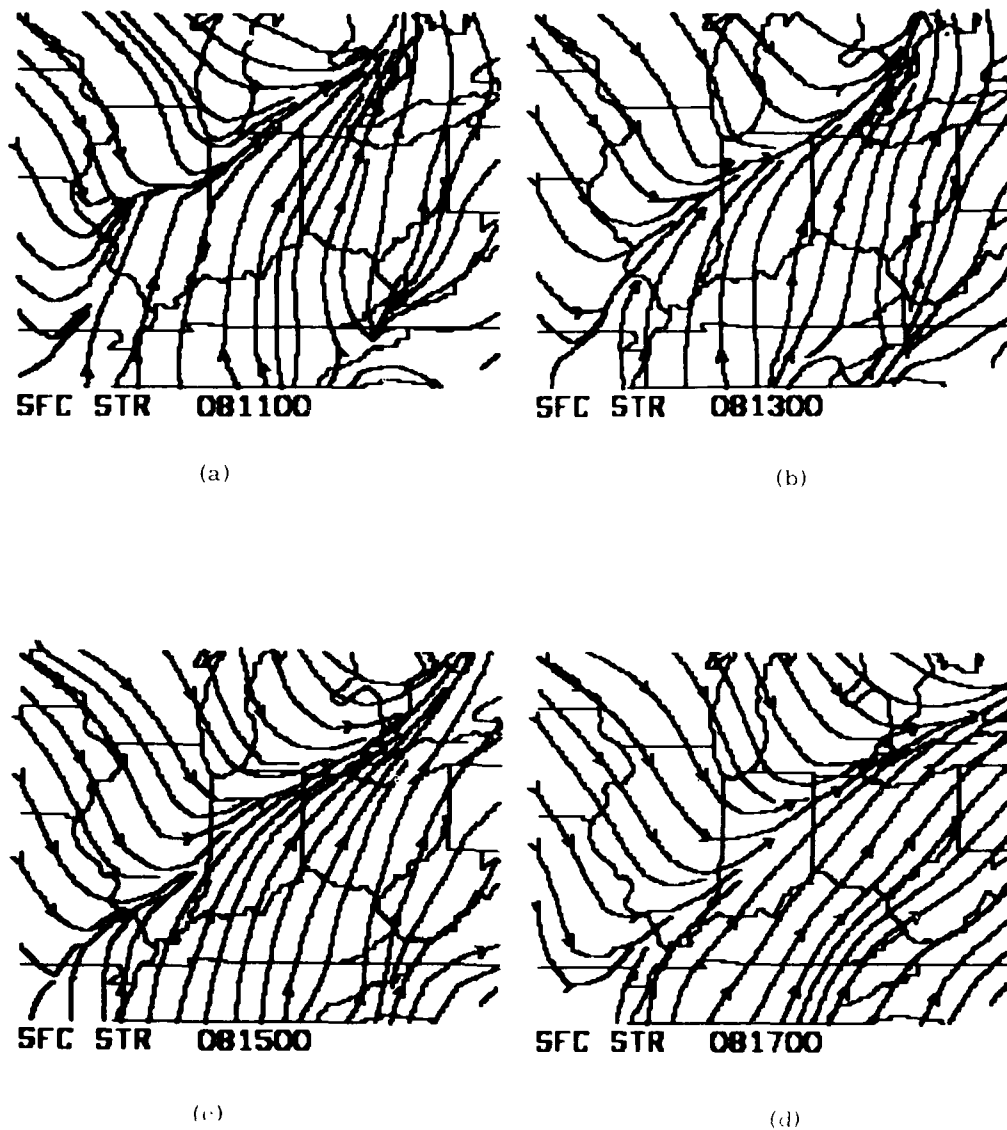


Figure A5. Surface Streamlines

AD-A137 165

THE USE OF INTERACTIVE GRAPHICS PROCESSING IN
SHORT-RANGE TERMINAL WEATHER. (U) AIR FORCE GEOPHYSICS
LAB HANSCOM AFB MA D A CHISHOLM ET AL. 31 MAR 83

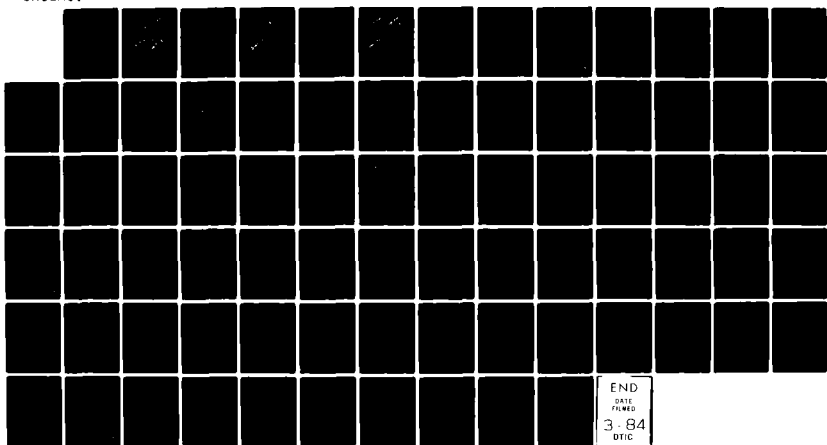
UNCLASSIFIED

AFGL-TR-83-0093

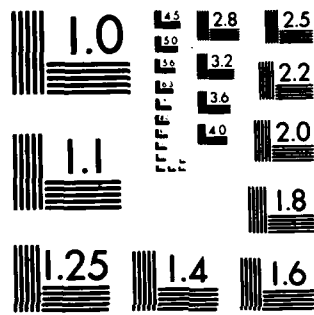
F/G 4/2

NL

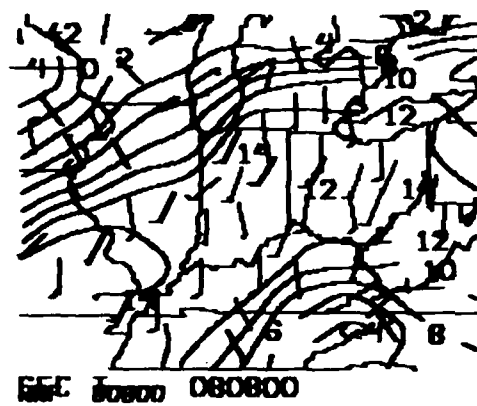
2/2



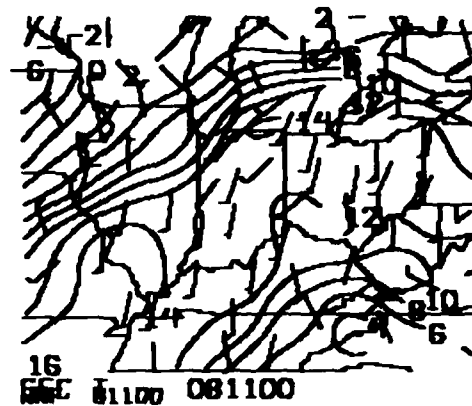
END
DATE FILMED
3-84
DTIC



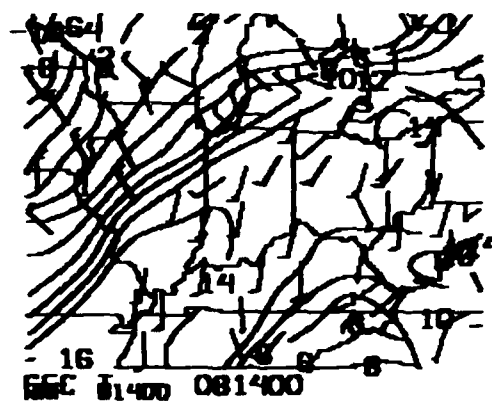
MICROCOPY RESOLUTION TEST CHART
NATIONAL BUREAU OF STANDARDS-1963-A



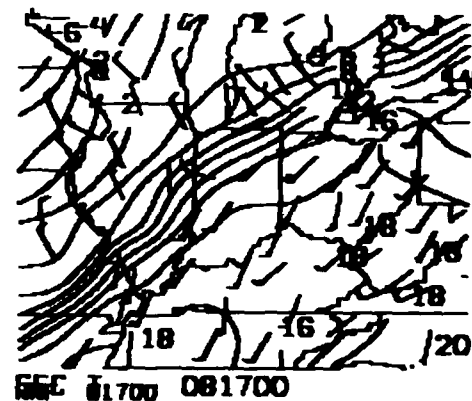
(a)



(b)



(c)



(d)

Figure A6. Surface Temperature ($^{\circ}\text{C}$) With Overlaid Surface Wind Flags (knots)

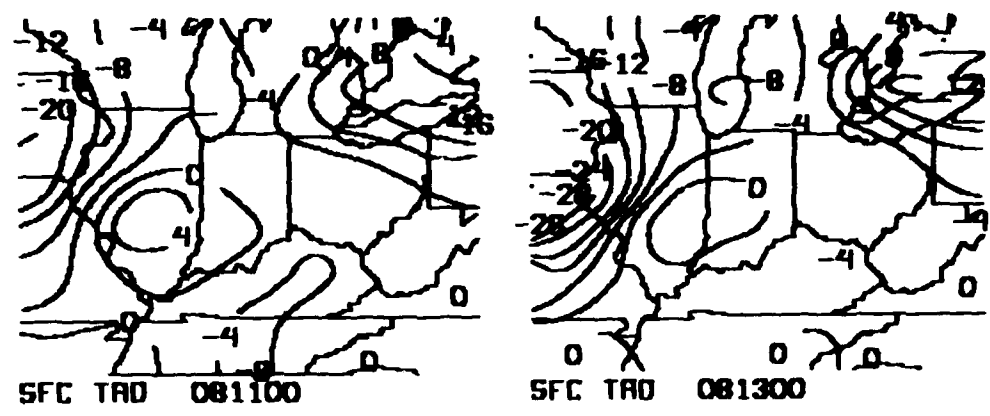
In making a temperature forecast for this situation, a series of temperature advection analyses (Figure A7) at 2-h intervals shows the progression of the temperature advection bands and changes in intensity. At 11 GMT (Figure A7a), an area of warm advection associated with the warm front is centered over Lake Erie. The area of weak cold advection over Tennessee and Kentucky is the result of intense radiational cooling beneath a ridge of high pressure east of the cold front. The radiational cooling produced a pocket of significantly colder temperatures thus creating a temperature gradient with colder temperatures to the south. This resulted in the area of weak cold advection with southerly winds. The band of cold advection associated with the cold front is readily apparent as it approaches western Illinois.

At 13 GMT (Figure A7b), the area of warm advection associated with the warm front has moved north of Lake Erie. The area of cold advection associated with the radiational cooling in Tennessee has weakened as the temperatures rose rapidly in daylight. The band of cold advection associated with the cold front has advanced through central Illinois, the northwestern corner of Indiana and central Michigan. The strongest area of cold advection is just beginning to spread into western Illinois.

At 15 GMT (Figure A7c), the band of cold advection associated with the cold front has continued its steady southeast movement. A second area of cold advection well behind the front is associated with an area of strong temperature gradient that is beginning to appear in western Wisconsin.

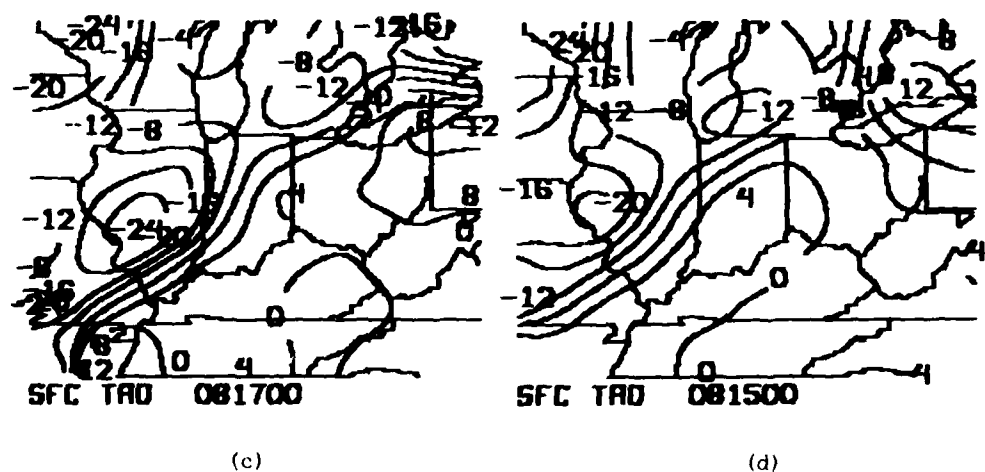
By 17 GMT (Figure A7d), the band of cold advection associated with the cold front is well defined. Notice on the 17 GMT wind and temperature analysis (Figure A6d) and the 17 GMT temperature advection analysis (Figure A7d) how the 0°C/day isoline nearly marks the frontal boundary.

The four temperature advection analyses (Figure A7) give an indication of frontal movement and intensity over the 6-h period from 11 GMT to 17 GMT. The nearly neutral temperature advection ahead of the cold front in the vicinity of Toledo during this period indicates that little temperature change can be expected until FROPA. The steady southeastward movement of the large band of cold temperature advection is in agreement with the prognosis that the front will continue to move steadily southeastward passing Toledo in about 3 h, resulting in a rapid temperature drop. The second area of cold advection moving into central Wisconsin at 17 GMT indicates that temperatures will continue to fall steadily, though not as dramatically as after FROPA.



(a)

(b)



(c)

(d)

Figure A7. Surface Temperature Advection ($^{\circ}\text{C}/\text{day}$)

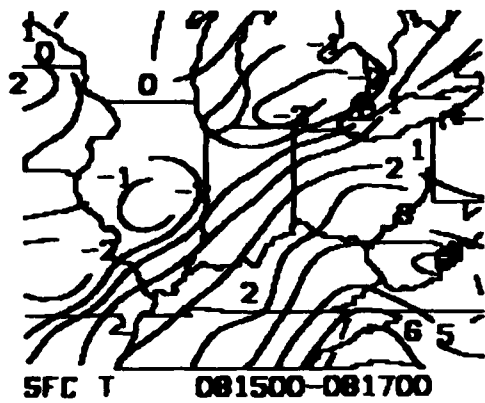
Another analysis that has proven to be useful in many cold front situations is the temperature change analysis (shown in Figure A8). The 6-h temperature change analysis from 11 GMT to 17 GMT (Figure A8c) shows a band of 8° C temperature drop immediately behind the front. On the plot of 6-h temperature change (Figure A8d), for the same 6-h period, some stations show temperature drops as large as 12° C. The 3-h temperature change analysis from 14 GMT to 17 GMT (Figure A8b) shows a band of 4° C temperature drop while some individual stations have temperature drops of 6° C. The 2-h temperature change analysis (Figure A8a) shows an area of 3° C temperature drops. Therefore temperature change analyses indicate a rapid fall in temperature of 5 or 6° C in the first 3 h after FROPA with a slower decrease in temperature thereafter. The forecaster should remember that the temperature change analyses often underestimate areas of rapid temperature change due to smoothing in the objective analysis routine.

Streamlines (Figure A5) and wind flags (Figure A6) show the wind direction became more parallel to the front as the front approached Toledo, with an abrupt change to WNW at FROPA and finally to NNW as the front moved farther east. Wind speeds remain constant at 6 to 8 m/sec on both sides of the front with little gustiness.

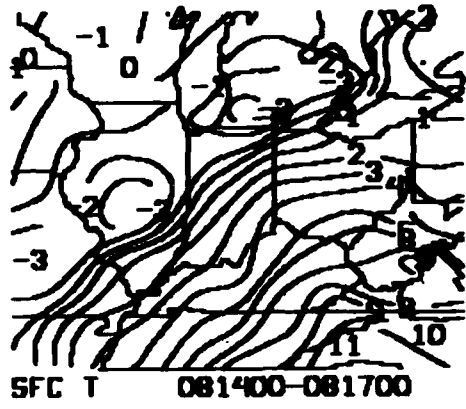
A5. RECOMMENDATIONS AND CONCLUSIONS

McIDAS's ability to display conventional and computed meteorological data in real time makes it an ideal tool for forecasting the rapidly changing weather associated with cold fronts. Displays of temperature advection, streamlines, divergence, isallobars and temperature change (which are not readily available at conventional weather stations) have been shown to be good forecaster aids in cold front situations. These analyses, along with conventional meteorological data, are especially helpful in determining frontal speed and location, and in forecasting the rapidly changing weather associated with an approaching cold front.

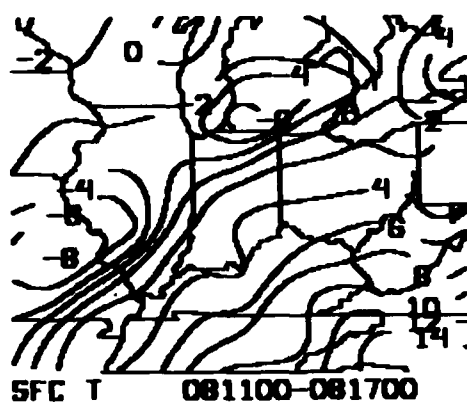
The cold front situation on 8 Dec 1980 was a relatively simple one to forecast because it was fast moving and well defined. It was a good episode to demonstrate the ability of a McIDAS-type system to aid a forecaster in a short range cold frontal forecast. Surface observations along with real-time satellite data showed that thunderstorms were not occurring and were not expected to occur during the next 12 h. The surface isallobaric, divergence, and streamline analyses in conjunction with weak upper level support indicated that the development of a frontal cyclone was unlikely. Following the movement of the front with various wind and temperature fields, the front was forecast to continue its steady southeastward movement at 30 km/h passing Toledo around 20 GMT. Since cyclogenesis was unlikely and



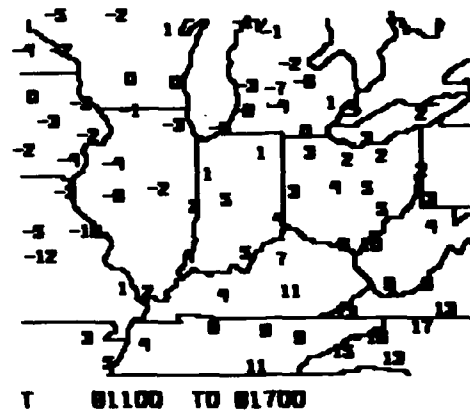
(a) 2-h Change ($^{\circ}\text{C}$)



(b) 3-h Change ($^{\circ}\text{C}$)



(c) 6-h Change ($^{\circ}\text{C}$)



(d) Plot of 6-h Change ($^{\circ}\text{C}$)

Figure A8. Surface Temperature Change Analysis: (a) 2-h Change ($^{\circ}\text{C}$),
(b) 3-h Change ($^{\circ}\text{C}$), (c) 6-h Change ($^{\circ}\text{C}$), and (d) Plot of 6-h Change ($^{\circ}\text{C}$)

upper level support was weak, the cloud mass associated with the front was forecast to continue moving steadily southeastward with the continuation of light rain in a narrow band ahead of and behind the front. Temperature advection and temperature change analyses aided in forecasting the timing and magnitude of the temperature drop occurring behind the front. Temperatures were forecast to stay within 1° C of the 17 GMT temperature until FROPA, then drop by 5 or 6° C within 3 h following FROPA, with slowly falling temperatures thereafter. Using streamline analyses and wind flag plots, winds were forecast to become more southwesterly as the front approached with a rapid windshift to northwest after FROPA.

FROPA actually occurred in Toledo about 19:15 GMT, about 45 min earlier than forecast and 2 h earlier than forecast operationally. The temperature remained between 13° C and 14° C until FROPA, then dropped 6° C in the 3 h after FROPA and another 2° C by 6 h after FROPA, a 6-h temperature change of -8° C. These temperature changes fall nicely in the range expected from the 3-h and 6-h temperature change analyses of 5-6° C/3 h and 6-9° C/6 h respectively. At FROPA, wind speeds remained constant while the direction shifted from southwest to northwest. Precipitation remained light and ended by 23 GMT, an hour earlier than forecast.

Many cold fronts are more difficult to forecast due to inconsistent forward speed, developing cyclones or thunderstorms, and changes in cloud coverage and precipitation rates. However, McIDAS's real-time capability and the use of forecaster aids like the Cold Front Decision Assistance Procedure should help to increase the short-range forecast accuracy of such changeable weather events.

References

- A1. Gulezian, D. P. (1980) Severe weather checklist used at national weather service forecast office, Portland, Maine. Bull. Am. Meteorol. Soc., 61(12):1592-1599.
- A2. Petterson, S. (1956) Weather Analysis and Forecasting, Second Edition, Volume I., McGraw-Hill Book Company, Inc., New York.
- A3. Air Weather Service (1970) Some Techniques for Short-Range Terminal Forecasting. AWSTR 233.
- A4. Moncrieff, M. W., and Green, J. S. A. (1972) The propagation and transfer properties of steady convective overturning in shear, Quart. J. Roy. Meteor. Soc., 98:336-352.
- A5. Bellon, A., Lovejoy, S., and Austin, G. L. (1980) Combining satellite and radar data for the short-range forecasting of precipitation. Mon. Wea. Rev. 108:1554-1566.

Appendix B

Coastal Cyclogenesis Decision Assistance Procedure

B1. THE COASTAL CYCLOGENESIS PROBLEM

Coastal cyclogenesis is a relatively common occurrence along the east coast of the United States.^{B1} Cyclone frequency analyses show maximum cyclone occurrences to be during the winter months from the North Carolina coast to Cape Cod and along the northern edge of the Gulf Stream.^{B2} The flow of cold continental air over the relatively warm ocean, which is a heat and moisture source, as well as the orographic effect of the Appalachian Mountains are factors believed to significantly contribute to the development of these cyclones. Flow from a high friction land surface to a low friction ocean surface has also been suggested as an enhancement mechanism for coastal cyclogenesis.^{B3}

Accurate short-range forecasting of the development and movement of these cyclones is of particular interest to air and sea traffic as well as the general public along the eastern seaboard. Increasing and/or lowering clouds, precipitation, deteriorating visibilities, and stronger winds often accompany these coastal cyclones.

-
- B1. Reitan, C. H. (1974) Frequencies of cyclones and cyclogenesis for North America, 1951-1970, Mon. Wea. Rev., 102:861-868.
 - B2. Collucci, S. J. (1976) Winter cyclone frequencies over the eastern United States and adjacent western Atlantic, 1964-1973, Bull. Am. Meteor. Soc., 57:548-553.
 - B3. Danard, M. B., and Ellenton, G. E. (1980) Physical influences on east coast cyclogenesis, Atmosphere-Ocean, 18:65-82.

The effects of coastal cyclogenesis on a coastal station can vary from merely an increase in cirrus clouds as a weak cyclone moves northeastward several hundred kilometers out to sea to heavy rain or snow and hurricane force winds as a cyclone explodes while moving north-northeastward just offshore.

A factor in establishing the critical need for accurate forecasts of the development and movement of these cyclones is their potential for explosive development. In the western Atlantic these rapidly developing cyclones occur rather frequently during winter months with central pressure falls of 20 mb/24 h to occasionally greater than 60 mb/24 h.^{B4} Few of these affect land, but those that do cause hundreds of millions of dollars in damage each year from the heavy rain or snow, extremely high tides and sometimes hurricane force winds. Those that don't affect land bring rough seas and high winds to fishing grounds and shipping lanes, sometimes interrupting marine traffic for several days.

It is the purpose of the Coastal Cyclogenesis Decision Assistance Procedure to aid the forecaster in determining:

- (1) whether or not coastal cyclogenesis will occur,
- (2) where coastal cyclogenesis will occur,
- (3) the developing cyclone's potential for intensification,
- (4) the speed and path of the developing cyclone,
- (5) the effect the cyclone will have on the weather (clouds, precipitation, visibility, wind, temperature) in the forecast area.

The use of McIDAS and its ability to display real-time half-hourly visible and IR satellite imagery along with displays of near-real time surface data and the latest upper air data offer the potential for improved short-range forecasting of the development, location, movement and weather associated with developing coastal cyclones. Half hourly satellite imagery and loops of that imagery can be especially useful in studying and forecasting coastal cyclogenesis due to the lack of data over the coastal waters.

B2. COASTAL CYCLOGENESIS DIAGNOSTIC AIDS

A weather forecaster using an interactive graphics minicomputer system like the McIDAS system has a potentially valuable tool not available to most forecasters today. Analyses of conventional surface data can be displayed within 5 to 10 min of observation time. The McIDAS forecaster has many computer analyses to aid him that are not available to forecasters relying on conventional teletype and

B4. Sanders, F., and Gyakum, J. R. (1980) Synoptic-dynamic climatology of the "bomb". Mon. Wea. Rev., 108:1589-1606.

facsimile products. These capabilities have been found to be valuable in developing forecaster aids for use in short-range prediction problems. Several forecast aids that may be particularly useful in forecasting cyclogenesis situations will be discussed below.

B2.1 Satellite Data

Satellite imagery has become a valuable data source that can be used extensively in short-range forecasting. Visible and infrared (IR) images received half hourly provide valuable information on the development, growth, and movement of cloud and precipitation areas. Satellite data can be useful in situations where cyclogenesis is possible by pointing out areas of horizontal and vertical cloud growth associated with a developing cyclone as early as 12 to 18 h in advance of significant surface development. This information can be especially useful in coastal situations where cyclones frequently develop along the coast, or just offshore where real-time surface data is extremely sparse.

The first visible sign of cyclogenesis often appears as a pronounced widening of the frontal cloud band in the vicinity of the newly developing cyclone.^{B5} Coincident with this event is the growth of higher clouds to the northeast of the new cyclone's center, which is observed as a decrease in the equivalent black body temperature depicted in the IR satellite image. Shenk^{B6} has indicated that the probability of cyclogenesis is increased when IR temperatures decrease along an expanding frontal cloud band.

The decreased IR temperatures and widening cloud band indicate a trend toward increased upward vertical motions. Generally, the more rapid the expansion of the frontal cloud band and the greater the decrease in IR temperature, the more rapid and intense the development of the surface cyclone. Also, as the cloud top temperature decreases in a developing cyclone, precipitation rates tend to increase.^{B7}

In secondary cyclone development, the area of vertical cloud growth evident in the IR satellite imagery is usually detached from the higher clouds associated with the primary cyclone.^{B6}

-
- B5. Heckman, B. E., and Thompson, A. H. (1978) Extratropical cyclogenesis over the Gulf of Mexico, Conference on Weather Forecasting and Analysis and Aviation Meteorology, pp 118-124.
 - B6. Shenk, W. E. (1970) Meteorological satellite infrared views of cloud growth associated with the development of secondary cyclones, Mon. Wea. Rev. 98:861-868.
 - B7. Scofield, R. A., and Oliver, V. J. (1981) Preliminary efforts in developing a technique that uses satellite data for analyzing precipitation from extratropical cyclones, Ninth Conference on Weather Forecasting and Analysis, pp 235-244.

In situations where significant cyclogenesis did not occur, Shenk^{B6} found that cloud top temperatures typically increased by 4° K/day. In situations where significant cyclogenesis did occur, cloud top temperatures were found to decrease by 6° K to 23° K per day in the area to the northeast of the developing cyclone.

For cyclones developing offshore where surface data are not available, valuable information concerning the intensity of the developing cyclone can be extracted from the satellite images. The rapid growth of well defined spiral bands suggests rapid development of moderate to strong intensity. The development of a clear dry tongue at the rear edge of the bright clouds behind the surface cyclone suggests substantial cold advection and subsidence at low levels. When rapid deepening is occurring, subsidence beyond the cyclone is great, thus there is little or no cumulus development in the dry tongue. When a cyclone is slowly deepening, subsidence is less and cumulus readily develops in the dry tongue.^{B8}

A loop of several consecutive half-hourly satellite images shown in chronological order on a TV screen is one of the most valuable tools available to a forecaster in following the growth and movement of cloud and precipitation areas associated with developing cyclones. The ability to correlate the patterns of cloud growth and decay to developing surface weather conditions can be a tremendous aid to a short-range forecaster, especially in areas where surface data is scarce or nonexistent.

B2.2 Color Enhancement of Satellite Data

The ability to color enhance IR satellite imagery enables the forecaster to better define the cloud top temperature distribution of a particular image and to study the vertical and horizontal growth of a cloud area more closely.

Color enhancement consists of defining a specific temperature interval to be represented on the satellite image by a particular color. This allows for the choice between narrow categories or wide categories depending on forecaster needs. It also gives the forecaster the option of defining many temperature intervals so that the entire IR image is enhanced, or defining only one carefully chosen temperature interval that may enhance only a small fraction of the IR image of particular interest.

Color enhancement can be useful to quantify cloud top temperature changes for areas of horizontal and vertical cloud growth where the potential for cyclogenesis exists. For example, if an area of clouds along a front is rapidly expanding with a significant decrease in cloud top temperature, the initial stages of cyclogenesis may be occurring at the surface.

B8. Burtt, T.G., and Junker, N.L. (1976) A typical rapidly developing extra-tropical cyclone as viewed in SMSII imagery, Mon. Wea. Rev., 104:489-490.

B2.3 Absolute Vorticity Analysis

Vorticity measures the degree of rotation in the atmosphere. Most vorticity analyses and prognoses available to the forecaster display absolute vorticity while the advection of vorticity is of most importance in forecasting sea-level cyclogenesis. Cyclogenesis most frequently occurs when an upper-level trough and its associated area of positive vorticity advection (PVA) approaches and becomes superimposed upon a slow moving, quasi-stationary or developing surface front. In general, when all the ingredients necessary for cyclogenesis are available, the rapidity of cyclone development is correlated with the intensity of the vorticity advection,^{B8} that is, the more intense the PVA, the more rapid and more intense the surface cyclone development.

Since vorticity advection is proportional to the square of the windspeed, cyclogenesis tends to occur in association with the jet stream. Vorticity advection is positive (negative) where the wind blows from high to low (low to high) values of vorticity. For a given upper-air height (streamline) analysis with overlaid absolute vorticity analysis, the more perpendicular the height contours (streamlines) are to the contours of a vorticity maximum, and the smaller the quadrilaterals they form, the more intense the vorticity advection.

It is important to note that since the jet stream is typically located between the 200 and 300 mb levels, the data at these levels are most useful in forecasting cyclone development although during the winter season the 500-mb level data often provides equal results. Also, the absolute vorticity analysis is most useful when overlaid upon the upper air height contours at the given level so that the regions of most intense PVA can be determined.

B2.4 Divergence

Horizontal divergence is defined as the net flow of air through a boundary. Divergence occurs when the net flow through a boundary is outward, while convergence results when the net flow through the boundary is inward. For cyclogenesis to occur at sea-level there must be a region of upper-air divergence superimposed upon a region of appreciable low-level convergence.

Upper-air divergence that is a product of positive vorticity advection attains the greatest magnitude in the vicinity of the jet stream.^{B9} The stronger the wind speeds in the jet stream the greater the upper-air divergence. In general, as a trough deepens, the upper-air divergence associated with it increases. Since developing surface cyclones require appreciable low-level convergence to produce upward

B9. Palmen, E., and Newton, C. W. (1969) Atmospheric Circulation Systems, Academic Press.

vertical motion and upper-level divergence to produce surface pressure falls, they are found in close association with upper-air jet streams and troughs that provide upper-air divergence, and surface fronts that provide low-level convergence.

The existence of an area of divergence at 200 or 300 mb superimposed upon a sea-level frontal zone can be indicative of potential cyclogenesis if other necessary ingredients are available. Also, a surface analysis showing strong convergence (negative divergence) in an area of rapid surface pressure falls along a front can suggest the development of a frontal cyclone.

B2.5 Isallobaric Analysis

A pressure change (isallobaric) analysis is probably the most useful analysis available to forecasters during a cyclogenesis forecast situation since cyclones tend to develop in the area of greatest sea-level pressure falls. Integrating the isallobaric analysis with information from the wind and pressure fields can aid the forecaster in accurately predicting where a new cyclone will develop and can sometimes provide insight into the potential intensity of the new cyclone as early as 6 to 12 h before the initial development.

In a situation where cyclogenesis is possible the forecaster should follow the motion and development of 3-h pressure changes over at least the past 6 h. When a system is developing very slowly, the 6-h pressure change analysis may be more useful. Generally, an organized area with 3-h pressure falls of at least 2 to 3 mb is necessary for cyclogenesis. Rapid pressure falls of 5 to 6 mb/sec or greater usually indicate the development of a moderate to intense cyclone. When analyzing pressure changes, the forecaster should consider the effect of the diurnal pressure cycle.

The isallobaric analysis can also be useful in forecasting cyclone movement since cyclones tend to move toward the region of most rapid pressure falls.

B2.6 Cross Section Analysis

The vertical cross-section analysis has several potential uses capable of providing valuable information in a cyclogenesis situation. The McIDAS system at AFGL has the ability to display the cross-section analyses of potential temperature, mixing ratio, wind speed and wind direction.

The cross-section analysis of potential temperature is useful in locating surface and upper air fronts, determining stability, recognizing relative warm and cold pockets and locating jet streams. The crowding of isentropes (line of constant potential temperature) in the horizontal indicates a front. Vertical crowding of isentropes indicates an inversion, thus a stable region. Wide vertical spacing of isentropes indicates a relatively unstable region. Relative warm regions are found

where isentropes sag toward the surface while relative cold regions are found where isentropes bulge upward. The greatest vertical wind shear and thus the jet stream is usually found in the vicinity of the greatest concentration of isentropes.

The cross-sectional analysis of mixing ratio suggests the location of dry and moist regions while the wind analyses point out low-level and upper-level jets.

B3. INGREDIENTS NECESSARY FOR CYCLOGENESIS

The ingredients most necessary for cyclogenesis are: (1) a baroclinic zone, (2) low level moisture, (3) an unstable atmosphere, and (4) a source of energy in the upper atmosphere.

Cyclogenesis almost always occurs in the vicinity of the baroclinic zone surrounding a front. Generally, the greater the temperature contrast across a front, the greater the intensity of development. During the cold season, the land-sea temperature difference creates a natural baroclinic zone, often intensifying the temperature contrast of approaching fronts. Cyclogenesis frequency analyses suggest that the enhanced baroclinic zone along the east coast of the United States apparently leads to increased cyclogenesis frequencies. Coastal fronts which develop along the east coast due to the land-sea temperature difference under certain synoptic conditions can produce significant temperature contrasts along with enhanced precipitation rates. The presence of the warm Gulf Stream along the east coast also increases the baroclinicity of the area and supplies the atmosphere with tremendous amounts of sensible and latent heat energy.

Low static stability (steep lapse rate) and high moisture content (particularly in warm air) are favorable for development.^{A2} The major moisture supplies for developing cyclones affecting the eastern half of North America are the Gulf of Mexico and the Atlantic Ocean. If low level and middle level flow does not advect moisture from one of these sources into an approaching system, development will tend to be weak or non-existent. It is not unusual under a dry synoptic pattern for a cold front to march from the Midwest to the east coast with little or no precipitation and occasionally only a narrow band of broken clouds. In these situations cyclogenesis should not be forecast due to a lack of moisture. However, when moisture from one or both of these sources is advected into an approaching system, development can take place quite rapidly. A front that stalls off the east coast after having been deprived of moisture while moving across the continent can develop an impressive cloud and precipitation shield within one or two days as the front awaits the approach of the next upper level trough that may initiate cyclogenesis. In these situations, especially during the winter months, the flow of cold continental air over the warmer ocean often results in further instability, cloud growth and the increased potential of cyclogenesis.

The upper-level support necessary to initiate and intensify a developing cyclone is usually provided by an upper-level trough or a short-wave vorticity maximum moving through an upper-level trough and its associated PVA. The presence of PVA in the upper atmosphere implies that upper-level divergence is occurring, a necessary condition for surface cyclogenesis. Cyclogenesis occurs most frequently and most intensely during the coldest months when upper level winds and baroclinicity are strongest.

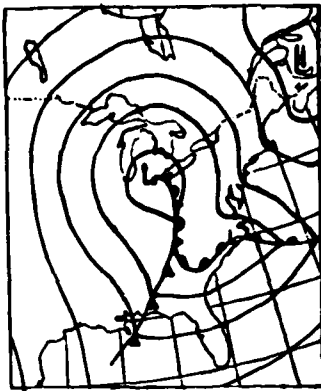
B4. TYPICAL CYCLOGENESIS SITUATIONS

East coast cyclogenesis tends to occur with several recognizable upper air and surface synoptic situations. Figure B1 illustrates the general synoptic scale surface patterns that most frequently lead to east coast cyclogenesis and which will be described below.

The situations shown in Figures B1a, B1b, and B1c are very similar to each other. Typically, a moderately intense primary low center moves from the Midwest to around the eastern Great Lakes region with a trailing cold front slowly marching toward the east coast. A strong, cold anticyclone is usually present in north-eastern New England or eastern Canada with a wedge of cold air and associated inverted pressure ridge-trough system between the mountains and the ocean. In most situations, for cyclogenesis to occur along the front south of the primary low, the primary must occlude and weaken. While the primary is weakening, the forecaster should watch for signs of secondary development between Cape Hatteras and Long Island. Cyclogenesis can occur very rapidly and intensely in situations like types a, b and c.

Type d illustrates a front which has marched through the eastern United States, then settles southward and stalls across the Gulf of Mexico, extending eastward to northeastward across Florida into the Atlantic. This front may remain quasi-stationary for several days, remaining distinguishable as a band of clouds with the more active areas exhibiting embedded thunderstorms. Cyclogenesis may occur between the northern Florida coast and Cape Hatteras right along the coast or as far as 300 to 500 km offshore.

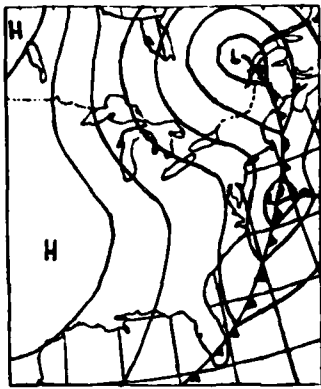
Type e describes the situation where a strong, cold anticyclone is situated just north to northeast of New England. With the land-sea temperature difference, northerly flow in the cold air trapped between the mountains and the coast and moist easterly flow along the coast from the eastern side of the anticyclone, an inverted surface pressure trough may develop along the east coast, or just offshore. Cyclogenesis will occur along the front or coastal front that develops within the inverted surface pressure trough.



(a) Secondary Cyclogenesis
Along Bulge in Warm Front

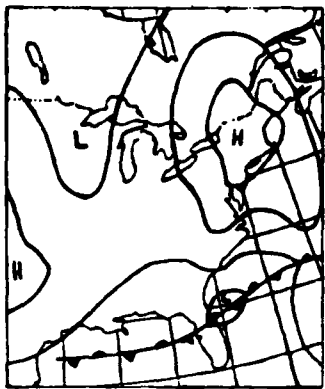


(b) Secondary Cyclogenesis
Near Triple Point Along
Coast

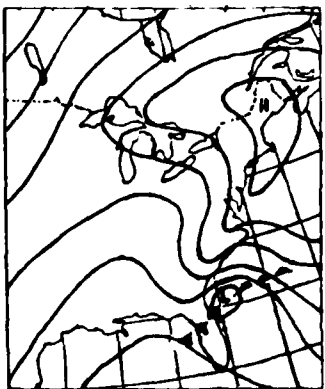


(c) Secondary Cyclogenesis
Near Triple Point Well Offshore

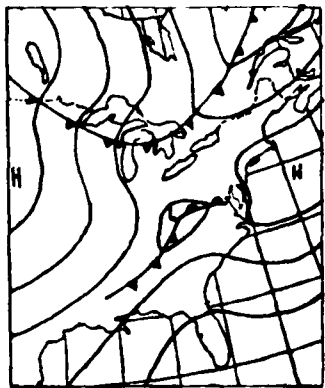
Figure B1. Typical East Coast Cyclogenesis Situations: (a) Secondary Cyclogenesis Along Bulge in Warm Front, (b) Secondary Cyclogenesis Near Triple Point Along Coast, (c) Secondary Cyclogenesis Near Triple Point Well Offshore, (d) Cyclogenesis Near Southeast Coast on a Stationary Front, (e) Cyclogenesis Along a Developing Front Within an Inverted Surface Pressure Trough Along Southeast Coast, and (f) Inland Cyclone Moves Toward Coast, Redvelops or Intensifies Along the Coast



(d) Cyclogenesis Near Southeast Coast on a Stationary Front



(e) Cyclogenesis Along a Developing Front Within an Inverted Surface Pressure Trough Along Southeast Coast



(f) Inland Cyclone Moves Toward Coast, Redevelops or Intensifies Along the Coast

Figure B1. Typical East Coast Cyclogenesis Situations: (a) Secondary Cyclogenesis Along Bulge in Warm Front, (b) Secondary Cyclogenesis Near Triple Point Along Coast, (c) Secondary Cyclogenesis Near Triple Point Well Offshore, (d) Cyclogenesis Near Southeast Coast on a Stationary Front, (e) Cyclogenesis Along a Developing Front Within an Inverted Surface Pressure Trough Along Southeast Coast, and (f) Inland Cyclone Moves Toward Coast, Redevelops or Intensifies Along the Coast
(Contd)

The initial stages of cyclogenesis in situations similar to type d and e tend to occur slowly. However, once they receive upper level support, rapid intensification can occur.

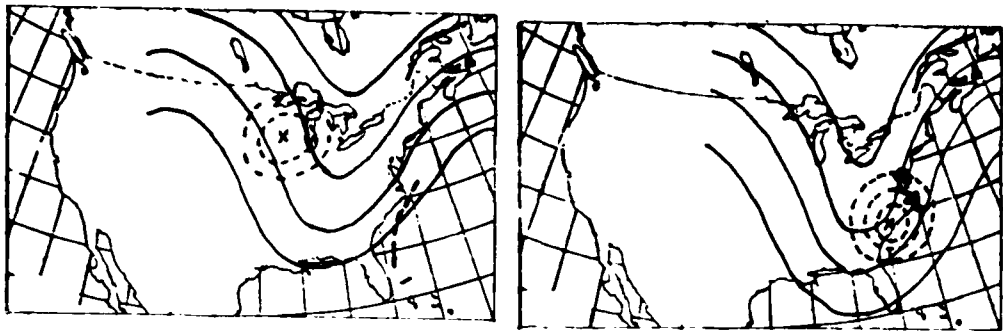
Type f shows a situation in which a weak cyclone from the midwest or southeast moves toward the coast with redevelopment (that is, a new cyclone) or intensification along the coast. This type of cyclogenesis occurs most frequently during the colder months when the ocean is warm relative to the land. These cyclones are difficult to forecast because they can be weak and dry over land, especially those which move toward the southeast from Canada, then suddenly intensify upon reaching the warm coastal waters, often resulting in "surprise snowstorms" for the northeastern and mid-Atlantic states. The heat release from the relatively warm ocean, and especially the Gulf Stream, may be responsible for the increased and often unexpected development.

There are three types of upper air patterns associated with the majority of east coast cyclogenesis situations. They are illustrated in Figures B2-B4.

Figure B2 is an example of meridional trough cyclogenesis. This type occurs most frequently in the eastern third of the U.S. and in the western Atlantic when a slow moving or quasi-stationary long wave trough is present over the eastern U.S. A more rapidly moving short wave vorticity maximum progresses southeastward then northeastward within the long wave trough and triggers cyclogenesis when the short wave overspreads the surface frontal zone to the east of the trough line.

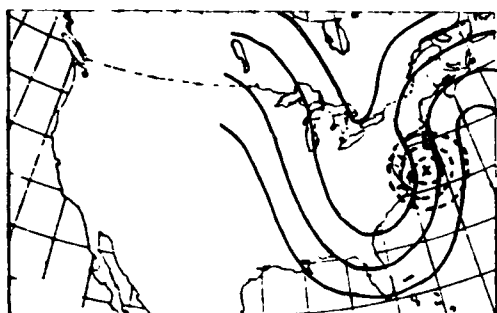
Figure B3 illustrates what can be called "phased short-wave cyclogenesis". In this situation a faster moving northern short wave trough approaches and "phases in" with a southern long wave trough to form a deeper, more intense long wave trough with surface development east of the trough line. If conditions are not favorable for immediate surface development after this interaction, the resultant long wave trough may become a quasi-stationary meridional trough similar to the illustration in Figure B2, awaiting yet another short-wave vorticity maximum to move through the trough to initiate cyclogenesis.

Figure B4 is an example of short-wave trough cyclogenesis. This type of cyclogenesis occurs most frequently in the northern and eastern regions of the U.S. Typically, a strong short-wave trough moves eastward or southeastward out of Canada, showing signs of intensification as it progresses. The amplitude of the trough may increase considerably, and the vorticity advection may become very strong, spawning weak to moderate cyclogenesis. Due to the lack of sufficient moisture, development rarely is intense while over land. However, once these short-wave trough cyclones move over the heat and moisture source of the Atlantic and Gulf Stream, rapid cyclogenesis may ensue.



(a)

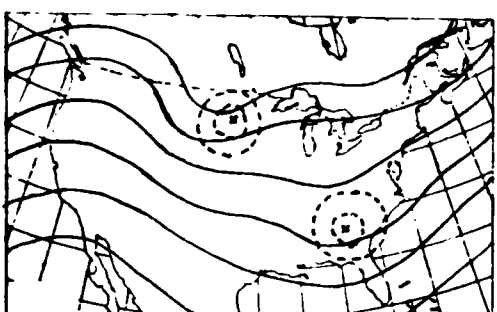
(b)



(c)

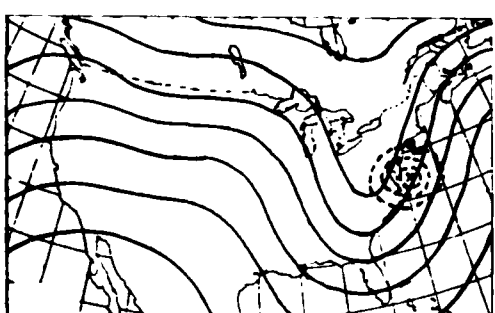
—— 500 millibar height contours
 - - - 500 millibar vorticity contours
 - - - surface trough
 L surface cyclone

Figure B2. Meridional Trough Cyclogenesis



(a)

(b)



(c)

—— 500 millibar height contours
 - - - 500 millibar vorticity contours
 - - - surface trough
 L surface cyclone

Figure B3. Phased Short-Wave Cyclogenesis

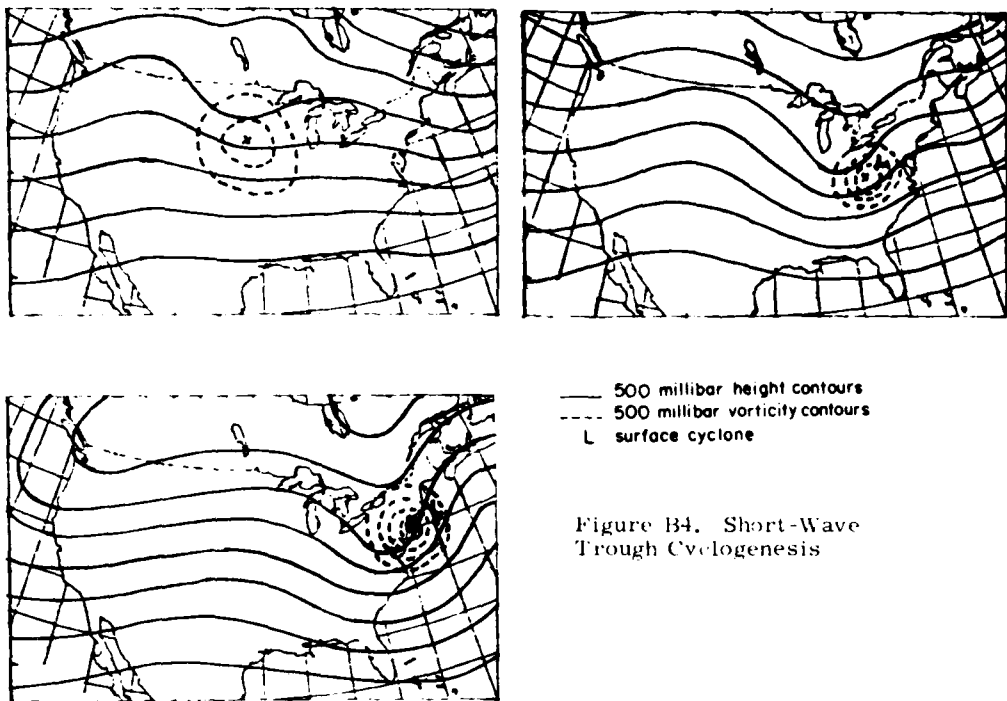


Figure B4. Short-Wave Trough Cyclogenesis

B5. A COASTAL CYCLOGENESIS FORECAST ASSISTANCE PROCEDURE

Employing the diagnostic aids described in Section B2 and the general information concerning east coast cyclogenesis discussed in Sections B3 and B4, an interactive forecast assistance procedure was developed to deal with short-range coastal cyclogenesis situations. It is broadly structured as shown in Figure B5 and the details of it are described below.

B5.1 Assess General Weather Situation

Before proceeding into any forecast situation, the forecaster should first be familiarized with the overall weather situation on both a national and a regional scale. A general understanding of the present national weather situation can be attained by studying several analyses using McIDAS' four-panel display option to evaluate surface pressure, surface temperature, 500-mb height, and absolute vorticity with overlaid 500-mb wind flags, and surface streamlines. An understanding of the regional weather situation can be achieved with a four-panel analysis

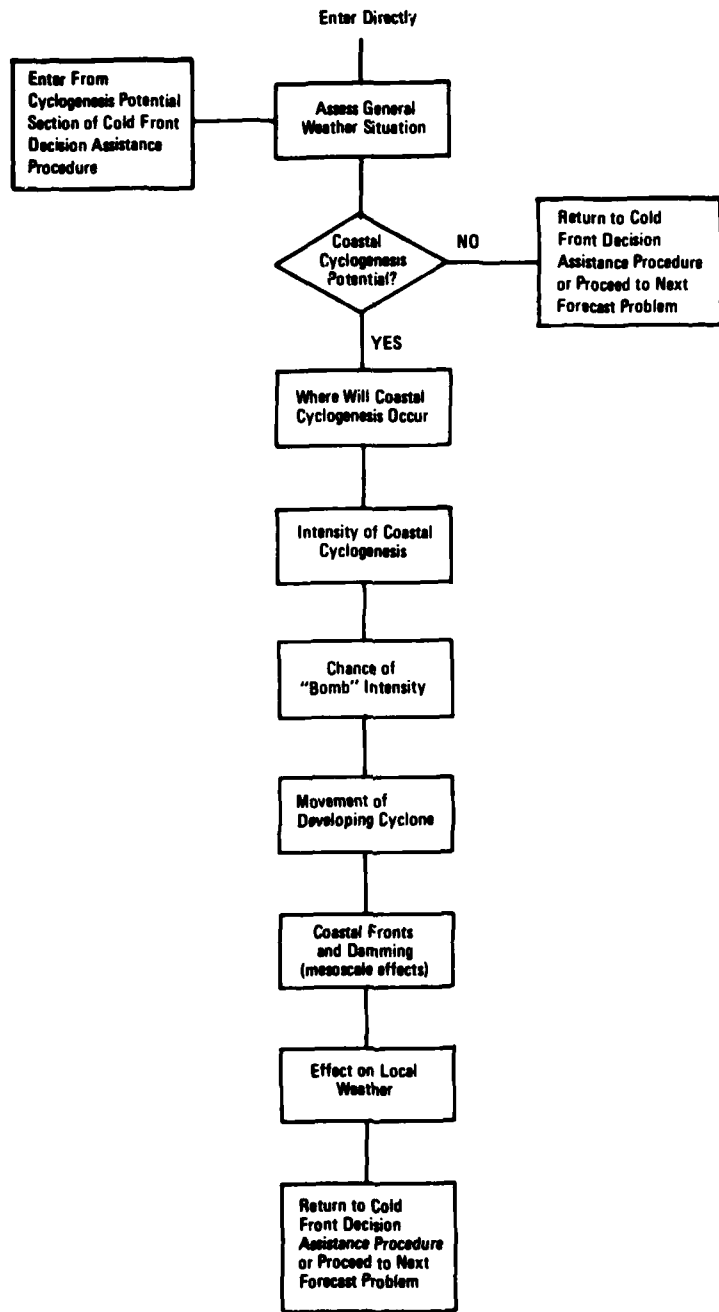


Figure B5. Diagram of Coastal Cyclogenesis Decision Assistance Procedure

of surface pressure with overlaid wind flags and weather symbols, 3-h pressure change, streamlines, and temperature along with a cross-section analysis of potential temperature, winds, and mixing ratio. Areas of "baggy" isobars, surface troughs and coastal inverted surface troughs and ridges appear in much greater detail on a regional or a mesoscale surface pressure analysis. The 3-h regional pressure change analysis shows areas of falling pressure and is probably the most useful tool available to the forecaster in forecasting coastal cyclogenesis occurring along the coast or just offshore. Streamlines can point out the convergence zone of a coastal front or a circulation associated with a developing cyclone. The regional temperature analysis amplifies mesoscale features such as coastal fronts and baroclinic zones, and provides more accurate frontal positions. The cross-section analysis can locate surface and upper-air fronts, determine stability, locate warm, cold and moist pockets, and determine the strength and location of jet streams, all in one display.

The analyses suggested above can provide a reasonable assessment of the general weather situation. Four-panel displays using overlays on an interactive graphics systems provides the forecaster with a large volume of information that can be viewed and digested easily. The forecaster should consult:

National Analyses: surface pressure, surface temperature, 500 mb, and vorticity analysis (with overlaid 500-mb wind flags), and surface streamlines.

Regional Analyses: surface pressure with overlaid wind flags and weather symbols, 3-h pressure change, surface temperature, surface streamlines, and cross-section analysis (potential temperature, winds, and mixing ratio).

B5.2 Coastal Cyclogenesis Potential

This section will be concerned with determining if cyclogenesis will occur for a short-range mesoscale forecast. Referring back to Figure B1, if the situation under consideration is similar to type a, b or c, the most important factor determining the potential for secondary development is the strength of the primary. If the primary is still deepening significantly or if the pressure gradient from the primary is strong along the coast, secondary coastal cyclogenesis is unlikely in the next 0 to 6 h. Conversely, the chance of secondary cyclogenesis is increased dramatically if:

- (1) the primary cyclone is occluding and/or deepening, has slowed considerably, or if the primary is forecast to weaken,
- (2) the primary is becoming vertical with upper air systems,
- (3) PVA into the primary is weakened,

- (4) the primary cyclone is being blocked and weakened by a strong cold anticyclone centered just north of the Great Lakes.

The initial signs of cyclogenesis in these situations are usually the rapid development of a cloud and precipitation area along the coast, an area of falling pressure, and the development of an inverted trough or baggy isobars. The farther offshore a cyclone develops, the more dependent the forecaster is on available satellite and/or radar data.

In situations similar to types d and e the initial developmental stages occur more slowly than in types a, b and c. The gradual spreading of low and middle clouds, a slowly developing area of light to moderate precipitation, a decrease in cloud top temperature, or the development of thunderstorms can signal development. If cyclogenesis is occurring near the coast, the surface pressure analysis will show an intensifying inverted trough initiated by the southeasterly flow of warm air over the ocean in the vicinity of a quasi-stationary or a developing front. Systems like this may sit along or just off the coast between North Carolina and Florida as long as 2 or 3 days, slowly developing and expanding until an upper level trough and its associated vorticity maximum increases the rate of intensification and forces the developing system northeastward.

Type f describes the situation in which a weak cyclone moves toward the coast and redevelops or intensifies along the coast. The first sign of cyclogenesis can be an area of pressure falls, an inverted pressure trough or baggy isobars and precipitation along the coast. Redevelopment may be spawned by the Appalachian Mountains acting as a barrier to the original low pressure system to the west and the lee-side cyclogenesis effect common to regions east of mountain range. Type f situations can produce heavy snowfalls on the east coast from the Carolinas to New England each year; most, however, move out to sea before rapid development occurs.

In situations analogous to Figure B1, coastal cyclogenesis will occur if several of the following conditions exist:

- (1) the cloud mass associated with a quasi-stationary or developing frontal zone exhibits steady or rapid growth in the horizontal (widening frontal band) and vertical (decreasing cloud top temperatures),
- (2) a kink develops in the slow-moving or quasi-stationary front,
- (3) an area of thunderstorms develops in an area of rapid horizontal cloud growth,
- (4) an area of steady precipitation develops and/or expands along the coast in the vicinity of a developing cloud mass, especially if moderate precipitation develops,

(5) wind reports suggest the development of a circulation or become stronger from an easterly direction in the vicinity of a developing frontal zone exhibiting steady cloud growth,

(6) an area of pressure falls (2-4 mb/3 h or greater) develops along the coast in the vicinity of a developing cloud mass.

(7) an area of "baggy" or closed isobars develops along the coast in the vicinity of a developing cloud mass, or

(8) a surface pressure trough (inverted or upright) develops along the coast in the vicinity of a developing cloud mass.

The likelihood of cyclogenesis is greater if several or many of the above conditions exist in the vicinity of the triple point (of an occlusion), a kink in a cold front, a bulge in a warm front or along a developing front.

Consult: satellite data, satellite data color enhancement, MDR data, pressure analysis, 3-h pressure change analysis, wind flag plot, weather plot, and precipitation amount plot.

B5.3 Where Will Cyclogenesis Occur?

Given that cyclogenesis is likely, the next most difficult task is to determine where it will occur. A 150 to 300 km error in that determination can have a major impact on the accuracy of the weather forecast. The cyclogenesis types in Figure B1 each have preferred locations for development. The first step then is to look in that general area for clues in the surface data (pressure analyses, precipitation, and so on) or satellite imagery to pinpoint where development will take place. In a situation like type a, cyclogenesis occurs near the bulge in the warm front where the northward progress of the warm air is retarded by the wedge of cold air trapped between the coastline and the Appalachian Mountains. The cyclone will develop between the mountains and just offshore within the area of most rapid pressure falls and/or the inverted surface pressure trough or baggy isobars that have developed. In these cases, very weak waves may form on the warm front, with significant development not occurring until the upper air PVA overspreads the suspect area. Types b and c spawn cyclogenesis within an area of pressure falls and/or baggy isobars near the triple point of the occlusion. In Types d and e cyclogenesis tends to occur just offshore (100 to 300 km from the coast) more frequently than along the coast, near or to the east of the greatest surface pressure falls within the inverted surface pressure trough. Whether development is occurring along the coast or well offshore, a very weak cyclone may develop on the front as early as 12 to 36 h before the onset of rapid development. This weak cyclone may remain stationary or slowly drift with the low level winds (850 mb) until intensification occurs upon the approach of the upper level support. In Type f situations a weak

cyclone moving eastward ahead of an upper-air trough is slowed down by the Appalachians. This results in secondary development ahead or slightly to the south of the path of the primary within the area of greatest pressure falls, usually marked by an area of baggy isobars and a newly developing precipitation shield.

In summary, cyclogenesis occurs with one or more of the following:

- (1) an area of organized pressure falls,
- (2) an area of baggy isobars,
- (3) a surface trough (inverted or upright),
- (4) a developing area of steady precipitation,
- (5) beneath a cloud mass exhibiting steady or rapid horizontal growth,
- (6) southwest of an area of steadily decreasing cloud top temperatures,
- (7) just west or beneath an area of developing thunderstorms,
- (8) near a developing circulation that has become evident in wind flags or satellite imagery,
- (9) near a kink or bulge in a front,
- (10) in the area where the maximum PVA and surface front becomes superimposed.

Consult: pressure analysis, 3-h pressure change analysis, satellite imagery, imagery color enhancement, wind flag plot, weather plot, and precipitation amount plot.

B5.4 Intensity of Coastal Cyclogenesis

Petterssen^{A2} outlined some basic rules for cyclone intensity that suggest that the greater the baroclinicity, the stronger the PVA, the lower the static stability, and the greater the available moisture, the greater the chance of cyclogenesis and the more intense the developing cyclone. The proximity to the moisture and heat source of the Atlantic provides moisture, instability and enhanced baroclinicity to approaching frontal systems, thereby providing the necessary ingredients for the cyclogenesis that occurs so frequently along the east coast during the colder seasons.

The key to the intensity of coastal cyclogenesis is the strength of the upper-air trough and its associated PVA. Using MCDAS, the forecaster can focus on 300- and 500-mb analyses and 12-h forecast fields to resolve the timing and intensity of cyclogenesis. Specifically, one should focus on:

- (1) the intensity of the 300-mb (500-mb) trough:
 - (a) a digging or intensifying trough is most favorable for development, especially for moderate to strong developments,
 - (b) a negatively tilted trough is especially favorable for rapid, moderate to strong development,
 - (c) a diffluent trough is favorable for rapid, moderate to strong development,

- (2) the strength of the approaching 300-mb (500-mb) vorticity maximum;
- (3) the strength of the jet stream at 300 mb (or an expected intrusion of a jet at 300 mb);
- (4) the magnitude of divergence at 300 mb;
- (5) the magnitude of height falls (500 mb, 300 mb) in advance of the trough.

The upper-level factors (especially at 300 mb), coupled with lower tropospheric factors such as the strength of the baroclinic zone, the availability of moisture, and the degree of instability, will largely determine the strength of a developing cyclone. Lower-atmospheric conditions that should be analyzed using MELDAs are:

- (1) pressure falls: >6 mb 3 h = intense cyclogenesis,
 3-5 mb 3 h = moderate cyclogenesis,
 1-2 mb 3 h = weak (or no) cyclogenesis,
- (2) the strength of the baroclinic zone;
- (3) the strength of surface and low level (850 mb) warm advection;
- (4) the availability of moisture;
- (5) the degree of instability;
- (6) the rate of growth (horizontal and vertical) of the developing cloud mass and precipitation areas, especially with convection;
- (7) the effects of the land-sea temperature and moisture contrasts.

In general, the greater the strength of each of the parameters listed above, the greater the developing cyclone's potential for intensification.

In a situation where weak pressure falls are occurring in a suspect area, but the bulk of the upper-level support is still well to the west, greater pressure falls can be expected, thus the intensity should be forecast according to the strength of the PVA and the degree of baroclinicity.

During the colder months, weak or developing cyclones often develop considerably more than might be expected due to the available upper-air PVA, especially when development occurs in the vicinity of the greatest sea-surface temperature gradient found near the Gulf Stream.

The presence and intensity of these upper and lower atmospheric conditions determines the degree to which cyclogenesis will occur. If one or more of the ingredients are missing, cyclogenesis that occurs will be very weak. When all the ingredients are present in moderate to strong amounts, cyclogenesis will almost certainly occur to a moderate to strong degree. When all the ingredients are present, but one or more is weak (particularly if the upper-air PVA or baroclinicity is weak) cyclogenesis will probably occur, but the intensity will be weak to perhaps moderate.

Cases of explosive cyclogenesis in the winter are not uncommon along the east coast (especially offshore). They present a serious forecast problem because of the strong winds, rough seas, heavy precipitation and low visibilities they produce. Recent studies of these storms^{B4} suggest that the ingredients necessary for this explosive cyclogenesis are:

- (1) a strong, cold anticyclone centered over the northeastern states or southeastern Canada,
- (2) a strong baroclinic zone evident at the surface and the 850-mb level enhanced by cold air trapped east of the Appalachians with warm moist easterly flow along the coast,
- (3) strong warm advection at the surface and 850-mb level,
- (4) a strong sea surface temperature gradient, usually in the vicinity of the Gulf Stream,
- (5) abundant low-level moisture,
- (6) low static stability,
- (7) a vigorous, intensifying, diffluent short-wave trough with strong PVA,
- (8) a strong upper-air jet stream.

B5.5 Movement of a Developing Cyclone

Developing cyclones generally move slightly to the right of the instantaneous 500-mb flow with 50-70 percent of the 500-mb wind speed. Thus, to forecast cyclone movement the forecaster should focus on interactive graphics displays that examine the following:

- (1) Change in 500-mb flow patterns:
 - (a) deepening of trough can increase northward movement,
 - (b) building of downstream ridge can increase northward movement,
 - (c) eastward translation of trough.
- (2) If the surface low and 500-mb low are forecast to become vertical, forecast very slow movement (usually toward the northeast) of the surface low.
- (3) Extreme building of the upstream ridge westward or a negatively tilted trough can cause a surface low to slow down and curve strongly northward or even northwestward.
- (4) A very strong, cold surface high north of the developing cyclone can decrease the cyclone's forward speed.
- (5) A weak, shallow cyclone in its early stages may move according to the lower-level 850-mb flow.
^{B10}

B10. Bosart, L.F. (1981) The President's Day snowstorm of 18-19 February 1979: a subsynoptic scale event, Mon. Wea. Rev., 109:1542-1566.

- (6) East coast cyclones tend to move slowly during the first few hours of their development.
- (7) Surface cyclone centers move toward the area of maximum surface pressure falls.
- (8) Surface cyclone centers move from the area of maximum cold advection toward the area of maximum warm advection.

B5.6 Coastal Fronts and Damming

Coastal fronts are mesoscale phenomena that occur during certain synoptic situations resulting from the effects of orography, coastal configuration, land-sea temperature contrast, sensible and latent heat transfer, and differential friction.^{B11} Temperature gradients of 5-10° C over 5-10 km separating light north or northwest winds from stronger easterly flow are common. Coastal fronts generally extend vertically to about 300 to 500 m above sea level and exist on a time scale of 6 to 12 h. The coastal front is a relatively common occurrence on the east coast during the winter months with a maximum frequency in December. They generally form in advance of developing cyclones and often produce significant local weather effects. Coastal fronts often develop 12 to 18 h before the arrival of a cyclone developing to the south, and will weaken when the cyclone approaches and its circulation becomes too strong. The strength of the coastal front depends on the strength of the anticyclone to the north and the cyclone to the south, that is a strong anticyclone and a strongly developing cyclone yield a well-developed coastal front. The preferred location for coastal frontogenesis is in southern New England and in the Cape Hatteras area extending southward to South Carolina and northward to the Chesapeake Bay area.

Coastal front development most commonly occurs when a strong, cold anticyclone becomes situated north to northeast of New England (as in Figure B1e) in conjunction with a cyclone developing to the south and a 700-mb wave disturbance approaching from the west.^{B12} As the cold anticyclone moves eastward, approaching its preferred location for coastal frontogenesis, polar continental air is pushed southward east of the Appalachians and over the Atlantic on north to northeasterly winds. As the anticyclone moves farther east and the 700-mb trough approaches from the west, the low level flow over the ocean becomes more easterly, increasing the trajectory over the ocean. This air is rapidly modified by sensible and latent heat transfer from the warm Atlantic. Meanwhile the low level flow over the land backs to more northerly due to surface friction and the effects of heat fluxes from

B11. Bosart, L. F. (1975) New England coastal frontogenesis, Quart. J. Roy. Meteor. Soc., 101:957-978.

B12. Ballantine, R. J. (1980) A numerical investigation of New England coastal frontogenesis, Mon. Wea. Rev., 108:1479-1497.

the ocean. Thus, low-level cold air is "dammed" against the mountains, while warmer, moister air is advecting onshore over it. The immediate effect of these processes is the development of an inverted surface pressure ridge in the cold air just east of the mountains, which is usually accompanied by an inverted trough near the coast line. If this situation, with light northerly winds in the cold air inland and stronger easterly winds in the warm air offshore, continues for 12 to 24 h, surface isotherms become packed along the coast and a narrow convergence zone with its associated mesoscale baroclinic zone develops along the coast or several kilometers inland.

It is important to note that the inverted trough that develops during these situations is sometimes the preferred location for a developing cyclone. In most coastal front situations a cyclone is developing several hundred kilometers south of the developing coastal front, although occasionally cyclogenesis as described by Bosart^{B10} will occur along the coastal front itself.

A developing coastal front often affects the precipitation amounts and intensity, temperature, wind, and ceiling and often marks the boundary between frozen and liquid precipitation. Due to enhanced moisture advection and convergence into the mesoscale frontal zone, precipitation amounts are typically enhanced 20 to 50 percent along the cold boundary of the coastal front.^{B11} Temperature and winds can vary sharply along the front, depending on its movement and location. Winds are typically light from the north on the cold air side of the front and considerably stronger from the east on the warm air side. The wind in the shallow layer of cold air at the surface can blow at 90 to 180° across the isobars and with considerably less speed than suggested by the sea-level isobars. The temperatures are often influenced on the synoptic scale also because the cold air trapped against the mountains often retards the northward progress of the warm front associated with the developing cyclone to the south. Cloud ceilings are generally lower on the cold side of the coastal front due to fog and/or low stratus that is formed as warm, moist air is lifted over the pool of cold air at the coastal front boundary.^{B12}

Recognition of damming or a developing coastal front can result in a more accurate short-range forecast of winds, precipitation type and amounts, temperature, cloud conditions, and visibility during coastal cyclogenesis situations, especially within 100 km of the coast.

Consult: wind flag plot, temperature plot, mesoscale pressure analysis, MDR analysis.

B13. Marks, F. D., and Austin, P. M. (1979) Effects of New England coastal front on the distribution of precipitation, Mon. Wea. Rev., 107, 53-61.

B5.7 Effect on Local Weather

The effect a particular developing coastal cyclone will have on the mesoscale weather forecast at a given location depends on several factors:

- (1) the track of the cyclone will affect the type and intensity of precipitation;
- (2) the intensity of the cyclone determines potential wind and precipitation intensity;
- (3) the horizontal extent and movement of precipitation, cloud cover, low ceilings, and strong winds;
- (4) local weather enhancements that must be considered:
 - (a) orographic effects on wind, precipitation, and visibility,
 - (b) coastal front effects,
 - (c) special synoptic scale effects.

Although general rules can be made for cyclones developing under certain synoptic conditions, each cyclone and its associated weather must be forecast individually due to the wide variety of tracks, intensities, areal coverage and enhancement effects that can result. It is in this regard that the power and flexibility of interactive graphics systems become important.

The path of a particular cyclone and its closeness to the forecast area generally determine the precipitation intensity, wind conditions, visibility, and ceiling height. Typically, the closer the cyclone center tracks to the forecast area, the greater the precipitation intensity, the stronger the winds, and the lower the visibilities and cloud ceilings. Cyclone centers that track more than 500 km offshore (except for the most intense cyclones) usually affect coastal stations with no more than very light precipitation or as little as scattered clouds and an increased northerly wind. The success of the short-range forecast is dependent on a complete description (nowcast) of the weather-cyclone model that exists and to update it hour-by-hour. Interactive systems with real-time conventional and satellite data bases are ideal for this process. The complexity and dynamicism of the developing system precludes the use of sophisticated models or approaches. Heavy reliance should be placed on conventional graphical plots and analyses and special purpose plots such as trend charts of key variables at upstream stations and station-time series plots. When available, ship and buoy data can aid substantially in locating and tracking offshore systems. In conjunction with plots and analyses of current observational data, the broader potential of the developing cyclone can be assessed from interactive graphing of numerically-based guidance (such as ceiling, cloud cover, precipitation, visibility, and wind vector from Model Output Statistics). Subjective integration of current short-term trends based on observations (surface, satellite and radar) with MOS and LFM 6-to-12-h prediction guidance is the only practical procedure to effective met-watching and forecast updating.

B6. CASE STUDY: EAST COAST CYCLOGENESIS ON 15 DECEMBER 1981

This section shows the application of the Coastal Cyclogenesis Decision Assistance Procedure in the preparation of short-range (0-12 h) terminal forecasts for Boston, Massachusetts, in a coastal cyclogenesis forecast situation. The cyclone developed over the southeastern states along a strong, but slow moving, cold front that nearly paralleled the east coast. The cyclone-suspect area moved east-northeastward, developing slowly over the southeastern states, then turned to a more northerly track as it moved offshore in the vicinity of Cape Hatteras, developing rapidly into a moderate to strong cyclone as it moved toward Cape Cod.

The general weather situation at 1500 GMT, 15 Dec 1981, can be examined with a four-panel analysis which includes (1) surface pressure, (2) surface temperature, (3) 500-mb heights (with overlaid 500-mb absolute vorticity and 500-mb wind flags), and (4) surface streamlines. The 1500 GMT surface pressure analysis (Figure B6a) shows two weak frontal waves along the east coast. One is located just east of Cape Cod and the other on the South Carolina-Georgia border. A ridge of high pressure centered in central Canada is pushing southward into the upper Midwest. The 1500 GMT surface temperature analysis (Figure B6b) shows a strong baroclinic zone across the southeastern states separating temperatures in the 20-23° C range from colder 0-5° C temperatures. A reinforcement of the cold air (-5° to -30° C) is filtering into the upper and western Midwest, associated with the high pressure ridge moving southward out of central Canada. The 1200 GMT 500-mb height-500-mb vorticity analysis (Figure B6c) shows a moderately deep long-wave trough centered through Wisconsin and Illinois, extending southward into the Gulf of Mexico, with strong southwesterly flow aloft along the entire east coast. A potent vorticity maximum with moderate to strong vorticity advection is beginning to overspread the surface baroclinic zone in the southeastern states. The 1500 GMT national streamline analysis (Figure B6d) shows a strong convergence zone over the southeastern states, marking the position of the surface front and the developing frontal wave.

A four-panel regional analysis at 1500 GMT over the southeastern states, zooms in on the region of suspected cyclogenesis. This analysis displays (1) surface pressure with overlaid wind flags and weather symbols, (2) 3-h surface isallobars, (3) surface temperature and (4) surface streamlines. The surface pressure analysis with overlaid wind flags and weather symbols (Figure B7a) shows a weak 1005-mb frontal wave over the South Carolina-Georgia border. The wind flags show north to northwesterly winds inland with south to southeasterly winds along the coast, clearly marking the position of the front, which is located only several kilometers inland from just west of Cape Hatteras southward through South Carolina and Georgia. The weather symbol plot shows an area of light to moderate rainfall north and

northeast of the wave throughout the Carolinas and Virginia and just beginning to spread into Maryland. Pressure falls (Figure B7b) of 3 mb/3h are occurring along the Georgia coast, however it must be remembered that the maximum upper-air PVA is still well to the west. The regional temperature analysis (Figure B7c) shows the strong baroclinic zone present over the southeastern states, probably enhanced by the warm, moist easterly flow off the Atlantic. Surface streamlines (Figure B7d) show the convergence zone associated with the surface front along with the first signs of a developing circulation around the weak frontal wave.

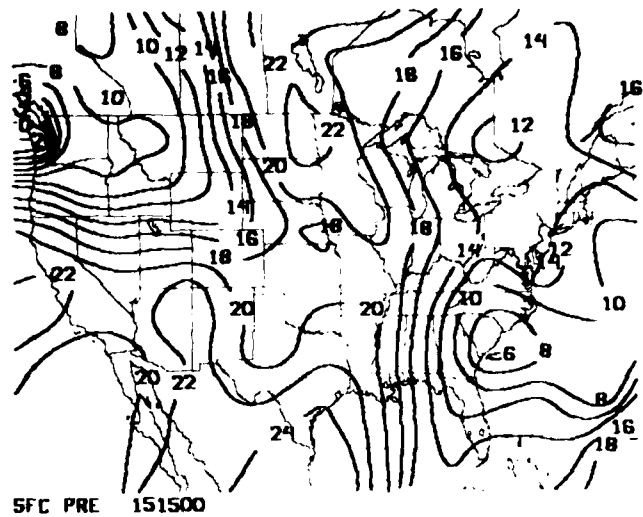
The cross-section analysis (Figure B8) on a line from Cape Hatteras to New Orleans shows a jet stream between the 200- and 250-mb levels over the South Carolina-Georgia area oriented toward the northeast, nearly paralleling the coast. An area of packed isentropes shows the position of the front just inland from the Carolina coast. The mixing ratio analysis (not shown) shows moist air to the east of the front and much drier air to the west.

Based on the assessment of the general weather situation, cyclogenesis is a distinct possibility along the front in the vicinity of the eastern Carolinas. With a large precipitation shield already present over the southeastern states along with high dewpoints and southwesterly upper-level flow, a significant precipitation event may develop for the mid-Atlantic and New England states.

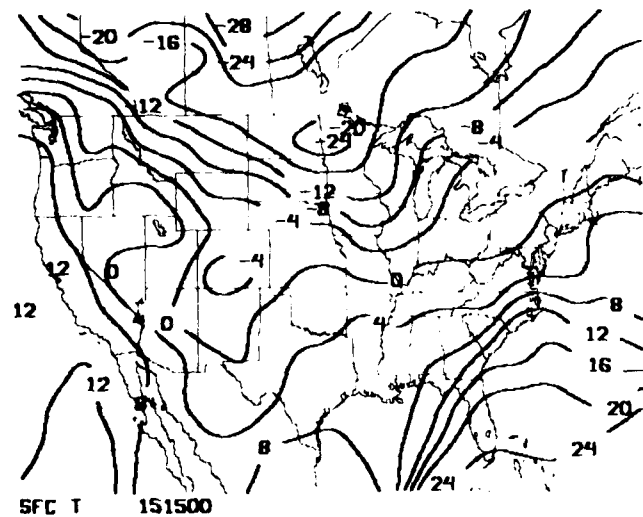
The present situation is similar to types b and c described in Figure B1, Section B4. The northern part of the cold front has passed just offshore while the southern part is still trudging eastward toward the coast. The remnants of an old, very weak occluded low that has become disassociated from the front lies north of the eastern Great Lakes. Intensification in these situations is often very rapid, especially when the developing cyclone moves over the warmer ocean.

With a moderately deep trough at 300 mb and moderate to strong vorticity advection beginning to overspread the moist, unstable baroclinic zone (Figure B9), all the ingredients necessary for cyclogenesis are present. Satellite imagery and surface data will aid in determining whether or not cyclogenesis will occur.

By 1300 GMT a broken line of convection was beginning to develop on a line from near Cape Hatteras southwestward to 100 to 150 km off the Georgia coast. Recall that an outbreak of convection in a suspect area is often one of the first signs that cyclogenesis will occur. In this particular situation it is difficult to determine whether there is steady horizontal cloud growth since the frontal cloud band covers the entire east coast from northern Maine to southern Florida, extending westward well into Kentucky and Tennessee. However, an area of expanding high clouds is beginning to develop just off the South Carolina coast.

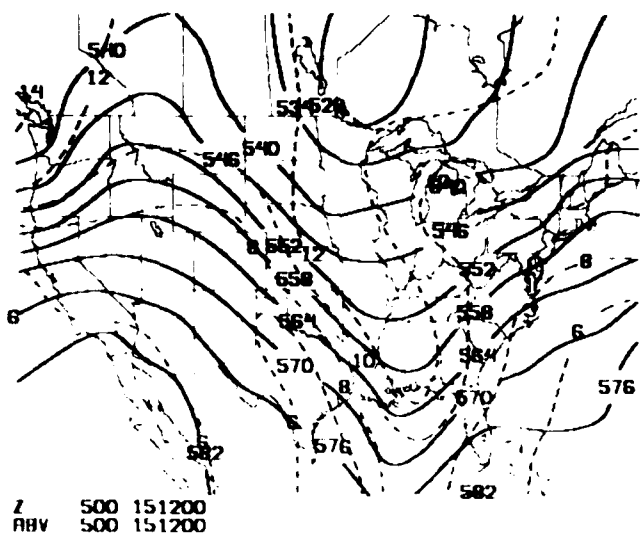


(a) Pressure (mb) Deviation from 1000 mb

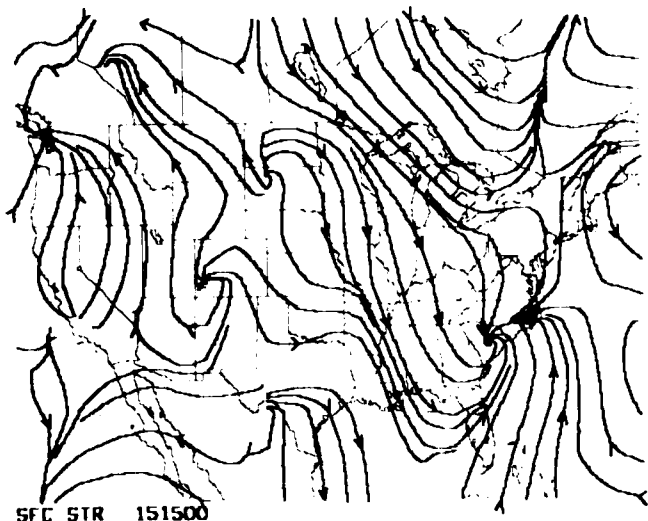


(b) Temperature (°C)

Figure B6. Four-Panel Analysis of General Weather Situation (National): (a) Pressure (mb) Deviation from 1000 mb, (b) Temperature (°C), (c) 500-mb Heights and 500-mb Absolute Vorticity, and (d) Surface Streamlines

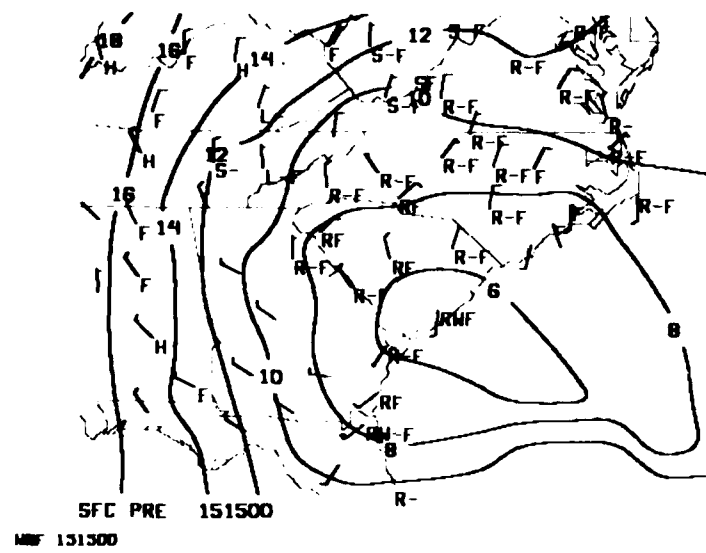


500 mb Heights and 500 mb Absolute Vorticity

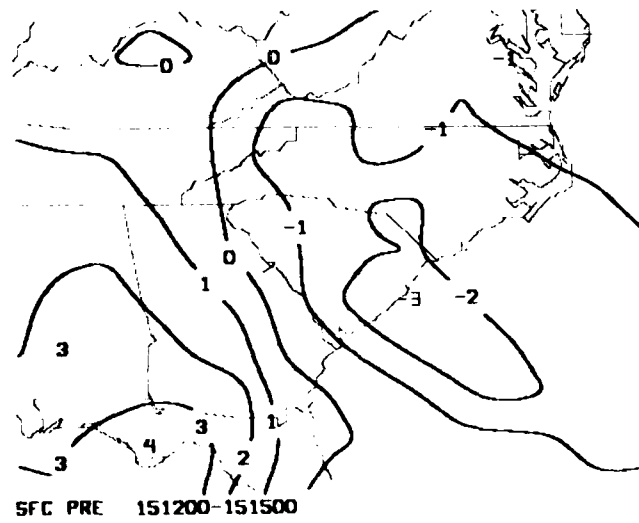


(d) Surface Streamlines

Figure B6. Four-Panel Analysis of General Weather Situation (National): (a) Pressure (mb) Deviation from 1000 mb, (b) Temperature ($^{\circ}$ C), (c) 500-mb Heights and 500-mb Absolute Vorticity, and (d) Surface Streamlines (Cont'd)

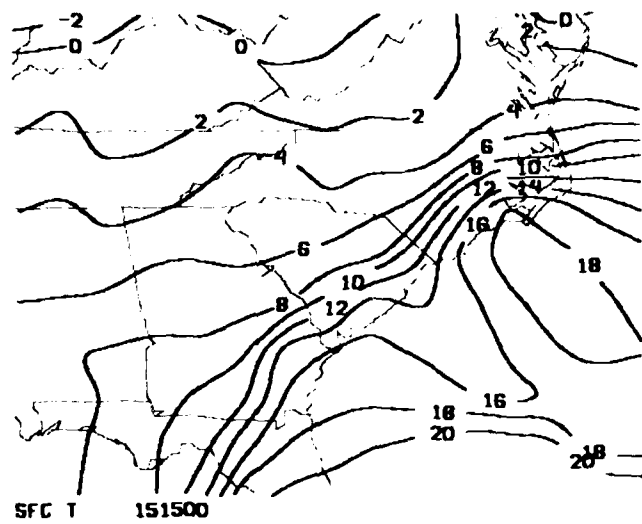


(a) Pressure (mb Deviation from 1000 mb), Surface Wind Flags (knots), Weather Symbols,

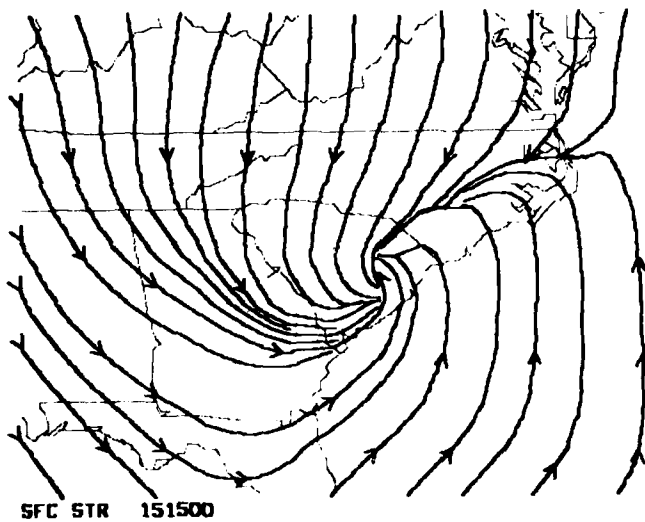


(b) Three-Hour Pressure Change (mb)

Figure B7. Four-Panel Analysis of General Weather Situation (Regional); (a) Pressure (mb Deviation from 1000 mb), Surface Wind Flags (knots), Weather Symbols, (b) Three Hour Pressure Change (mb), (c) Temperature ($^{\circ}\text{C}$), and (d) Streamlines



(c) Three-Hour Pressure Change (mb)



(d) Surface Streamlines

Figure B7. Four-Panel Analysis of General Weather Situation (Regional): (a) Pressure (mb), Deviation from 1000 mb, Surface Wind Flags (knots), Weather Symbols, (b) Temperature (°C), (c) Three-Hour Pressure Change (mb), and (d) Surface Streamlines (Contd)

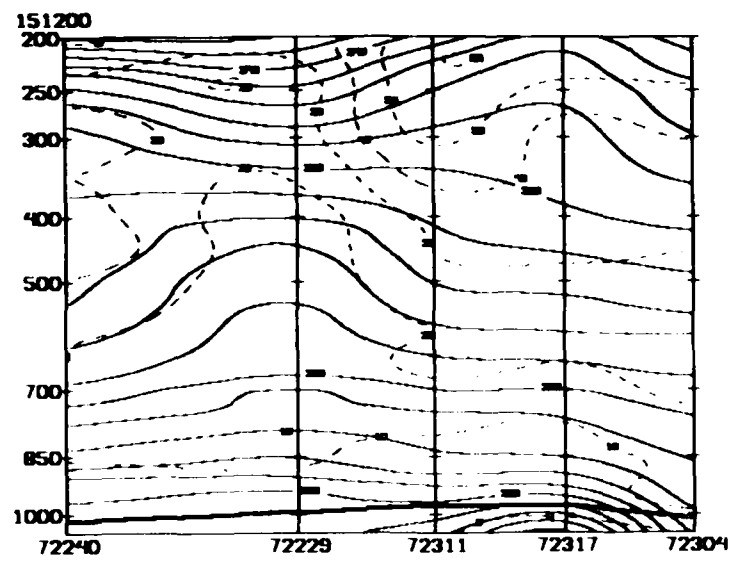


Figure B8. Cross-Section Analysis. (Solid lines - potential temperature, °K; dashed lines - wind speed, m sec; heavy solid line near bottom of figure indicates surface topography)

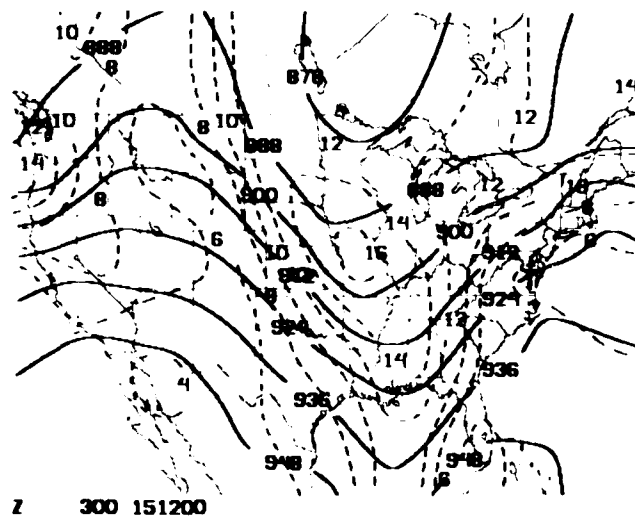


Figure B9. 300-mb Heights (solid, decameters) and 300-mb Absolute Vorticity (dashed, $\cdot 10^{-5} \text{ sec}^{-1}$)

By 1500 GMT other signs of cyclogenesis have appeared on the surface. A substantial kink has become evident in the surface cold front, while an area of 3 mb/3 h pressure falls (Figure B7b) and a closed isobar have developed. Also, 6-h precipitation amounts (not shown) in the southeast have increased dramatically from ≤ 0.1 in. (00 GMT - 06 GMT) to between 0.25 and 0.75 in. (06 GMT - 12 GMT) while moderate rain has become more widespread in the vicinity of the wave. The streamlines (Figure B7d) have begun to show a circulation near the South Carolina-Georgia border whereas earlier only frontal convergence was evident. These developments suggest that cyclogenesis will almost certainly occur, and since the bulk of the PVA has not yet overspread the frontal zone, further strengthening of each cyclogenesis-indicator is expected during the next 6 to 12 h.

In this situation, forecasting the location and timing of significant cyclogenesis is fairly straightforward. The area of minimum pressure and the area of maximum pressure falls have been moving steadily east-northeastward at around 75 km/h with a tendency toward more northerly movement and decreased forward speed. Advecting the developing surface system according to this trend would place it in the vicinity of Cape Hatteras at around 00 GMT. Advecting the vorticity maximum eastward suggests the area of maximum PVA will overspread the developing frontal wave in the vicinity of Cape Hatteras between 2100 GMT and 0000 GMT. Thus between 2100 GMT and 0000 GMT, rapid cyclogenesis can be expected in the Cape Hatteras area.

In determining the intensity to which the incipient cyclone may develop, the strength of the upper air trough and associated vorticity maximum, and the strength of the baroclinic zone are of most importance. The 300- and 500-mb height analyses (Figure B9 and Figure B6c, respectively) show a trough that has been steadily deepening as it slowly progressed eastward during the past 24 h. The 300-mb vorticity analysis overlaid on 300-mb height contours (Figure 9) shows the short-wave vorticity maximum has steadily progressed southeastward on the back side of the trough and by 12 GMT on 15 December has begun to move toward the northeast in the southwesterly flow east of the trough line with an area of moderate PVA over Alabama and Tennessee. With moderate cold advection into the 500-mb trough and weak to moderate cold advection into the 300-mb trough, further deepening of the trough and intensification of the PVA can be expected. Only weak warm advection is present at the 500- and 300-mb levels ahead of the respective troughs. Pressure falls of 3 mb/3h are already occurring in advance of the area of maximum PVA. The moderate to strong baroclinic zone, high dewpoints, strong surface warm advection over the southeastern coast, an area of convection just east of the developing frontal wave, and the rapidly intensifying precipitation area are all signs of an impending significant cyclogenesis event. Thus, with favorable surface developments,

moderate to strong PVA and the presence of a jet stream (220 km/h) in the vicinity of a developing frontal wave, moderate to strong cyclogenesis can be expected. Also, the cyclone will be developing in a geographically preferred region (Cape Hatteras) where oceanic heat and moisture effects often enhance similar developments. Intense cyclogenesis is unlikely due to the absence of strong warm advection at 850 mb, a cold quasi-stationary anticyclone centered over the northeastern states and a polar outbreak.

To forecast the movement of this cyclone, the changes in the upper level flow must be considered. With moderate cold advection into the 500-mb trough, weak warm advection ahead of the trough and the increasing strength of the vorticity maximum, the flow is forecast to force the developing cyclone on a more north-easterly track. With 500-mb winds of 100 to 110 km/h in the cyclone was forecast to move northeastward at 65 to 75 km/h (~70 percent of the 500 mb flow). This would place the cyclone just north of Cape Hatteras at 00 GMT (6 h after forecast time), about 100 km southeast of Salisbury, Maryland at 05 GMT (12 h after forecast time) and at the eastern tip of Cape Cod by 12 GMT on 16 Dec (21 h after forecast time).

Since the developing cyclone is forecast to deepen rapidly as it moves toward Cape Cod during the next 21 h, terminal weather at Boston will change substantially. The 1500 GMT satellite image shows overcast conditions over the entire east coast, implying that overcast conditions will prevail during the entire 12-h forecast period and probably extending well into the following 12-h period until the cyclone moves to the northeast of southern New England. The area of light to moderate precipitation has steadily moved northward at about 75 km/h. With the present steady movement, precipitation can be expected in Boston by 2200 GMT.

Visibility is expected to remain the same or improve slightly during the next few hours as the weak wave off Cape Cod moves away. A trend chart of stations along the mid-Atlantic coast where precipitation has already begun by 1500 GMT shows visibilities dropping to 5 to 7 km when precipitation begins. Thus the visibility was forecast to remain between 12 and 16 km until 2200 GMT, lowering to around 5 to 7 km in precipitation through the rest of the forecast period. Ceiling heights should also improve somewhat, to 300-600 m during the next few hours, then decrease to 150-250 m with the onset of precipitation after 2200 GMT.

While precipitation in the Boston area may begin as snow, it is forecast to change rapidly to rain with easterly flow off the relatively warm ocean that will keep temperatures above freezing in southern New England. In central and northern New England however, temperatures could remain cold enough for a substantial early-winter snowfall. Precipitation will be light to moderate in the Boston area and mostly moderate toward eastern Cape Cod, closer to the cyclone's center. Based on the 6-h precipitation amounts (from 0600 GMT to 1200 GMT), the intensity

and the forecast path of the developing cyclone, precipitation amounts were forecast to be between 3/4 to 1 in. in the Boston area with increasing amounts toward Cape Cod.

Winds will remain from the NNW for several hours as the weak wave off Cape Cod moves away, then turn northeasterly as the cyclone to the south moves northward. Winds will turn to the northeast by 00 GMT (when the cyclone moves off the mid-Atlantic coast and begins to deepen rapidly) at around 10 kt and begin to increase from 10 kt to 15 kt by 0300 GMT (12-h forecast) with gusts of 20 to 25 kt. Later, during the second 12-h period, winds will increase to 20 to 30 kt with gusts of 30 to 40 kt, since a moderate to strong cyclone will pass within 100 km of Boston. Winds will remain from the northeast from 0300 GMT until the cyclone passes off to the northeast.

Since the developing cyclone is expected to pass 100 km east of Boston, winds will remain from the northeast, and no warm frontal passage will occur, temperatures were forecast to rise only slightly through the entire cyclogenesis event, remaining between 2 to 4° C throughout the 12-h forecast period.

Rapid cyclogenesis actually took place in the vicinity of Cape Hatteras between 2100 GMT and 0000 GMT. Pressure falls of 5 to 6 mb/3 h were occurring along the North Carolina-Virginia border by 2200 GMT. The developing cyclone moved northeastward at around 75 km/h and was located about 100 km northeast of Boston by 1200 GMT, 16 December. Precipitation began in Boston at 2100 GMT with visibilities and ceiling heights decreasing to 4-6 km and 150-200 m, respectively. The total precipitation during storm was 0.72 in. in Boston. Winds became north-northeasterly and increased to 15 to 20 kt with gusts of 30 to 35 kt as the cyclone moved off to the northeast of Boston. Temperatures remained between 1 and 3° C during the entire event.

References

- B1. Reitan, C.H. (1974) Frequencies of cyclones and cyclogenesis for North America, 1951-1970, Mon. Wea. Rev., 102:861-868.
- B2. Collucci, S.J. (1976) Winter cyclone frequencies over the eastern United States and adjacent western Atlantic, 1964-1973, Bull. Am. Meteor. Soc., 57:543-553.
- B3. Denard, M.B., and Ellenton, G.E. (1980) Physical influences on east coast cyclogenesis, Atmosphere-Ocean, 18:65-82.
- B4. Sanders, F., and Gyakum, J.R. (1980) Synoptic-dynamic climatology of the "bomb", Mon. Wea. Rev., 108:1589-1606.
- B5. Heckman, B.E., and Thompson, A.H. (1978) Extratropical cyclogenesis over the Gulf of Mexico, Conference on Weather Forecasting and Analysis and Aviation Meteorology, pp 119-124.
- B6. Shenk, W.E. (1970) Meteorological satellite infrared views of cloud growth associated with the development of secondary cyclones, Mon. Wea. Rev., 98:361-368.
- B7. Scofield, R.A., and Oliver, A.J. (1971) Preliminary efforts in developing a technique that uses satellite data for analyzing precipitation from extratropical cyclones, Ninth Conference on Weather Forecasting and Analysis, pp 235-244.
- B8. Burt, T.G., and Jenker, N.L. (1976) A typical rapidly developing extratropical cyclone as viewed in SSM/I imagery, Mon. Wea. Rev., 104:489-490.
- B9. Palmen, E., and Newton, C.W. (1969) Atmospheric Circulation Systems, Academic Press.

References

- B10. Bosart, L. F. (1981) The President's Day snowstorm of 18-19 February 1979: a subsynoptic scale event, Mon. Wea. Rev., 109:1542-1566.
- B11. Bosart, L. F. (1975) New England coastal frontogenesis, Quart. J. Roy. Meteor. Soc., 101:957-978.
- B12. Ballantine, R. J. (1980) A numerical investigation of New England coastal frontogenesis, Mon. Wea. Rev., 108:1479-1497.
- B13. Marks, F. D., and Austin, P. M. (1979) Effects of New England coastal front on the distribution of precipitation, Mon. Wea. Rev., 107:53-67.

Appendix C

Inland Cyclogenesis Decision Assistance Procedure

C1. THE INLAND CYCLOGENESIS PROBLEM

Cyclogenesis within the continental U.S. is a common occurrence. Frequency distributions of cyclonic events indicate a maximum occurrence during the winter months in the lee of the Rocky Mountains and the Great Lakes region with a swath of significant occurrences stretching across much of the United States, excluding the extreme southwestern corner of the U.S., southern parts of Texas, and Florida.^{B1} The largest winter maximum is located off the northeast coast. By the summer months the swath of maximum cyclonic events has shifted northward well into Canada with hints of a relative maximum still evident in the lee of the northern Rockies.^{B1} The maximum frequency of cyclonic events and cyclogenesis on the lee slopes of the Rockies is probably due to an induced upper-level trough caused by persistent westerly flow across the mountain barrier.

Accurate short-range forecasting of the development and movement of these cyclones is of particular interest to air traffic and agricultural interests as well as the general public. Increasing and/or lowering clouds, precipitation, deteriorating visibilities, and stronger winds often accompany these cyclones. The effects of cyclogenesis on a region can vary from merely an increase in cirrus clouds as a weak cyclone passes within several hundred kilometers of a region to heavy rain or snow and strong winds as a rapidly intensifying cyclone passes nearby.

Inland cyclogenesis events tend to be more predictable than the coastal cyclones whose development may be unexpectedly enhanced by the oceanic influences found

along the coast. These inland cyclones seldom reach the destructive intensities often observed during coastal cyclogenesis events; however, several destructive land-locked cyclones (usually blizzards) do occur each year. Unlike coastal cyclones, which sometimes intensify to stronger than expected intensities, inland cyclones tend to be more consistently predictable. The extensive data coverage inland may be an important factor in producing more accurate forecasts.

The Inland Cyclogenesis Decision Assistance Procedure aids the forecaster in determining:

- (1) whether or not cyclogenesis will occur,
- (2) where cyclogenesis will occur,
- (3) the developing cyclone's potential for intensification,
- (4) the speed and path of the developing cyclone,
- (5) the effect the cyclone will have on the weather (clouds, visibility, winds, temperature) in the forecast area.

MeIDAS, with its ability to display real-time half-hourly visible and IR satellite images along with displays of near real-time surface data and the latest upper air data, offers the potential for improved short-range forecasting of the potential development, location, movement, and weather associated with developing cyclones.

C2. INLAND CYCLOGENESIS DIAGNOSTIC AIDS

C2.1 Satellite Data

Satellite imagery has become a valuable data source that can be used extensively in short-range forecasting. Visible and infrared (IR) images received half hourly provide valuable information on the development, growth, and movement of cloud and precipitation areas. Satellite data can be useful in situations where cyclogenesis is possible by pointing out areas of horizontal and vertical cloud growth associated with a developing cyclone as early as 12 to 18 h before significant surface development. This information can be especially useful in coastal situations where cyclones frequently develop along the coast, or just offshore where real-time surface data is extremely sparse.

The first visible sign of cyclogenesis often appears as a pronounced widening of the frontal cloud band in the vicinity of the newly developing cyclone.^{B5} Coincident with this event is the growth of higher clouds to the northeast of the new cyclone's center, which is observed as a decrease in the equivalent black body temperature depicted in the IR satellite image. Shenk^{B6} has indicated that the probability of cyclogenesis is increased when IR temperatures decrease along an expanding frontal cloud band.

The decreased IR temperatures and widening cloud band indicate a trend toward increased upward vertical motions. Generally, the more rapid the expansion of the frontal cloud band and the greater the decrease in IR temperature, the more rapid and intense the development of the surface cyclone. Also, as the cloud top temperature decreases in a developing cyclone, precipitation rates tend to increase. ^{B7}

When a secondary cyclone develops, the area of vertical cloud growth evident in the IR satellite imagery is usually detached from the higher clouds associated with the primary cyclone. ^{B6}

In situations where significant cyclogenesis did not occur, Shenk^{B6} found that cloud top temperatures typically increased by 4° K/day. In situations where significant cyclogenesis did occur cloud top temperatures were found to decrease by 6 to 23° K per day in the area to the northeast of the developing cyclone.

For cyclones developing offshore where surface data are not available, valuable information concerning the intensity of the developing cyclone can be extracted from the satellite images. The rapid growth of well defined spiral bands suggests rapid development of moderate to strong intensity. The development of a clear dry tongue at the rear edge of the bright clouds behind the surface cyclone suggests substantial cold advection and subsidence at low levels. When rapid deepening is occurring, subsidence behind the cyclone is great, thus there is little or no cumulus development in the dry tongue. When a cyclone is slowly deepening, subsidence is weak and cumulus readily develops in the dry tongue. ^{B8}

A loop of several consecutive half-hourly satellite images shown in chronological order on a TV screen is one of the most valuable tools available to a forecaster in following the growth and movement of cloud and precipitation areas associated with developing cyclones. The ability to correlate the patterns of cloud growth and decay to developing surface weather conditions can be a tremendous aid to a short-range forecaster, especially in areas where surface data are scarce or nonexistent.

C2.2 Color Enhancement of Satellite Data

The ability to color enhance IR satellite imagery enables the forecaster to define the cloud top temperature distribution of a particular image better and to study the vertical and horizontal growth of a cloud area more closely.

Color enhancement consists of defining a specific temperature interval to be represented on the satellite image by a particular color. This allows for the choice between narrow categories or wide categories depending on forecaster needs. It also gives the forecaster the option of defining many temperature intervals so that the entire IR image is enhanced or defining only one carefully chosen temperature interval to enhance only a small fraction of the IR image which is of particular interest.

Color enhancement can be useful to quantify cloud top temperature changes for areas of horizontal and vertical cloud growth where the potential for cyclogenesis exists. For example, if an area of clouds along a front is rapidly expanding with a significant decrease in cloud top temperature, the initial stages of cyclogenesis may be occurring at the surface.

C2.3 Absolute Vorticity Analysis

Vorticity measures the degree of rotation in the atmosphere. Most vorticity analyses and prognoses available to the forecaster display absolute vorticity while the advection of vorticity is of most importance in forecasting sea-level cyclogenesis. Cyclogenesis most frequently occurs when an upper-level trough and its associated area of positive vorticity advection (PVA) approaches and becomes superimposed upon a slow moving, quasi-stationary or developing surface front. In general, when all the ingredients necessary for cyclogenesis are available, the rapidity of cyclone development is correlated with the intensity of the vorticity advection,^{B9} that is, the more intense the PVA, the more rapid and more intense the surface cyclone development.

Since vorticity advection is proportional to the square of the windspeed, cyclogenesis tends to occur in association with the jet stream. Vorticity advection is positive (negative) where the wind blows from high to low (low to high) values of vorticity. For a given upper-air height (streamline) analysis with overlaid absolute vorticity analysis, the more perpendicular the height contours (streamlines) are to the contours of a vorticity maximum, and the smaller the quadrilaterals they form, the more intense the vorticity advection.

It is important to note that since the jet stream is typically located between the 200- and 300-mb levels, the data at these levels are most useful in forecasting cyclone development although during the winter season the 500 mb level data often provides equal results. Also, the absolute vorticity analysis is most useful when overlaid upon the upper air height contours at the given level so that the regions of most intense PVA can be determined.

C2.4 Divergence

Horizontal divergence is defined as the net flow of air through a boundary. Divergence occurs when the net flow through a boundary is outward, while convergence results when the net flow through the boundary is inward. In order for cyclogenesis to occur at sea-level there must be a region of upper-air divergence superimposed upon a region of appreciable low-level convergence.

Upper-air divergence that is a product of positive vorticity advection attains the greatest magnitude in the vicinity of the jet stream.^{B9} The stronger the wind speeds

in the jet stream the greater the upper-air divergence. In general, as a trough deepens, the upper-air divergence associated with it increases. Since developing surface cyclones require appreciable low-level convergence to produce upward vertical motion and upper-level divergence to produce surface pressure falls, they are found in close association with upper-air jet streams and troughs that provide upper-air divergence, and surface fronts that provide low-level convergence.

The existence of an area of divergence at 200 or 300 mb superimposed upon a sea-level frontal zone can be indicative of potential cyclogenesis if other necessary ingredients are available. Also, a surface analysis showing strong convergence (negative divergence) in an area of rapid surface pressure falls along a front can suggest the development of a frontal cyclone.

C2.5 Isallobaric Analysis

A pressure change (isallobaric) analysis is probably the most useful analysis available to forecasters during a cyclogenesis forecast situation since cyclones tend to develop in the area of greatest sea-level pressure falls. Integrating the isallobaric analysis with information from the wind and pressure fields can aid the forecaster in accurately predicting where a new cyclone will develop and can sometimes provide insight into the potential intensity of the new cyclone as early as 6 to 12 h before the initial development.

In a situation where cyclogenesis is possible the forecaster should follow the motion and development of 3-h pressure changes over at least the past 6 h. When a system is developing very slowly, the 6-h pressure change analysis may be more useful. Generally, an organized area with 3-h pressure falls of at least 2 to 3 mb is necessary for cyclogenesis. Rapid pressure falls of 5 to 6 mb/3 h or greater usually indicate the development of a moderate to intense cyclone. When analyzing pressure changes, the forecaster should consider the effect of the diurnal pressure cycle.

The isallobaric analysis can also be useful in forecasting cyclone movement since cyclones tend to move toward the region of most rapid pressure falls.

C2.6 Cross Section Analysis

The vertical cross-section analysis has several potential uses capable of providing valuable information in a cyclogenesis situation. The McIDAS system at AFGL has the ability to display the cross-section analysis of potential temperature, mixing ratio, wind speed, and wind direction.

The cross-section analysis of potential temperature is useful in locating surface and upper air fronts, determining stability, recognizing relative warm and cold pockets, and locating jet streams. The crowding of isentropes (lines of constant

potential temperature) in the horizontal indicates a front. Vertical crowding of isentropes indicates an inversion, thus a stable region. Wide vertical spacing of isentropes indicates a relatively unstable region. Relative warm regions are found where isentropes sag toward the surface while relative cold regions are found where isentropes bulge upward. The greatest vertical wind shear and thus the jet stream is usually found in the vicinity of the greatest concentration of isentropes. The cross-sectional analysis of mixing ratio suggests the location of dry and moist regions while the wind analyses point out low-level and upper-level jets.

C3. INGREDIENTS NECESSARY FOR CYCLOGENESIS

The ingredients most necessary for cyclogenesis are (1) a baroclinic zone, (2) low level moisture, (3) an unstable atmosphere, and (4) a source of energy in the upper atmosphere.

Cyclogenesis almost always occurs in the vicinity of the baroclinic zone surrounding a front. Generally, the greater the temperature contrast across a front, the greater the intensity of development. Since cold fronts are more intense and exhibit greater temperature contrasts during the colder months, cyclogenesis tends to occur more frequently and with greater intensity during the cold season. Warm, moist southerly flow from the Gulf of Mexico ahead of an advancing front or into a quasi-stationary frontal zone can significantly enhance the baroclinicity of the frontal zone, increasing the chances of cyclogenesis.

Low static stability (steep lapse rate) and high moisture content (particularly in warm air) are favorable for development.^{A2} The major moisture supplies for developing cyclones affecting the eastern two-thirds of the United States are the Gulf of Mexico and the Atlantic Ocean. The Pacific Ocean may supply some of the moisture to cyclones developing in the lee of the Rockies. Vigorous fronts and cyclones that move onto the west coast and across the mountains may supply moisture to a developing lee-side cyclone, however significant development probably will not occur without substantial moisture advection from the Gulf of Mexico. If low level and middle level flow does not advect moisture from one of these sources into an approaching system, development will tend to be weak or non-existent. It is not unusual under a dry synoptic pattern for a cold front to march across the country with little or no precipitation and occasionally only a narrow band of broken clouds. In these situations cyclogenesis should not be forecast due to a lack of moisture. However, when moisture from one of these sources is advected into an approaching system, development can take place quite rapidly.

The upper-level support necessary to initiate and intensify a developing cyclone is usually provided by an upper-level trough or a short-wave vorticity maximum moving through an upper-level trough and its associated PVA. The presence of PVA in the upper atmosphere implies that upper-level divergence is occurring, a necessary condition for surface cyclogenesis.

Since cyclogenesis is more likely to occur the greater the PVA and the greater the temperature gradient, and since upper-level winds and temperature gradients are strongest in the cold seasons, cyclogenesis occurs most frequently and with more intensity during the coldest months.

C4. AN INLAND CYCLOGENESIS FORECAST ASSISTANCE PROCEDURE

Employing the diagnostic aids described in Section C2, and the general information concerning cyclogenesis discussed in Section C3, an interactive forecast assistance procedure was developed to deal with short-range inland cyclogenesis situations. It is broadly structured as shown in Figure C1 and the details of it are described below.

C4.1 Assess General Weather Situation

Before proceeding into any forecast situation, the forecaster should first be familiarized with the overall weather situation on both a national and a regional scale. A general understanding of the present national weather situation can be attained by studying several analyses using McIDAS' four-panel display option to evaluate surface pressure, surface temperature, 500-mb height and absolute vorticity with overlaid 500-mb wind flags, and surface streamlines. An understanding of the regional weather situation can be achieved with a four-panel analysis of surface pressure with overlaid wind flags and weather symbols, 3-h pressure change, streamlines, and temperature, along with a cross-section analysis of potential temperature, winds, and mixing ratio. Areas of "baggy" isobars or surface troughs appear in much greater detail on a regional or a mesoscale surface pressure analysis. The 3-h regional pressure change analysis shows areas of falling pressure and is often the most useful tool available to the forecaster in forecasting cyclogenesis. Streamlines can point out the convergence zone associated with the front (or developing front) or the circulation associated with a developing cyclone. The regional temperature analysis amplifies mesoscale features of the baroclinic zone and provides more accurate frontal positions. The cross-section analysis can locate surface and upper-air fronts, determine stability, locate warm, cold and moist pockets, and determine the strength and location of jet streams, all in one display.

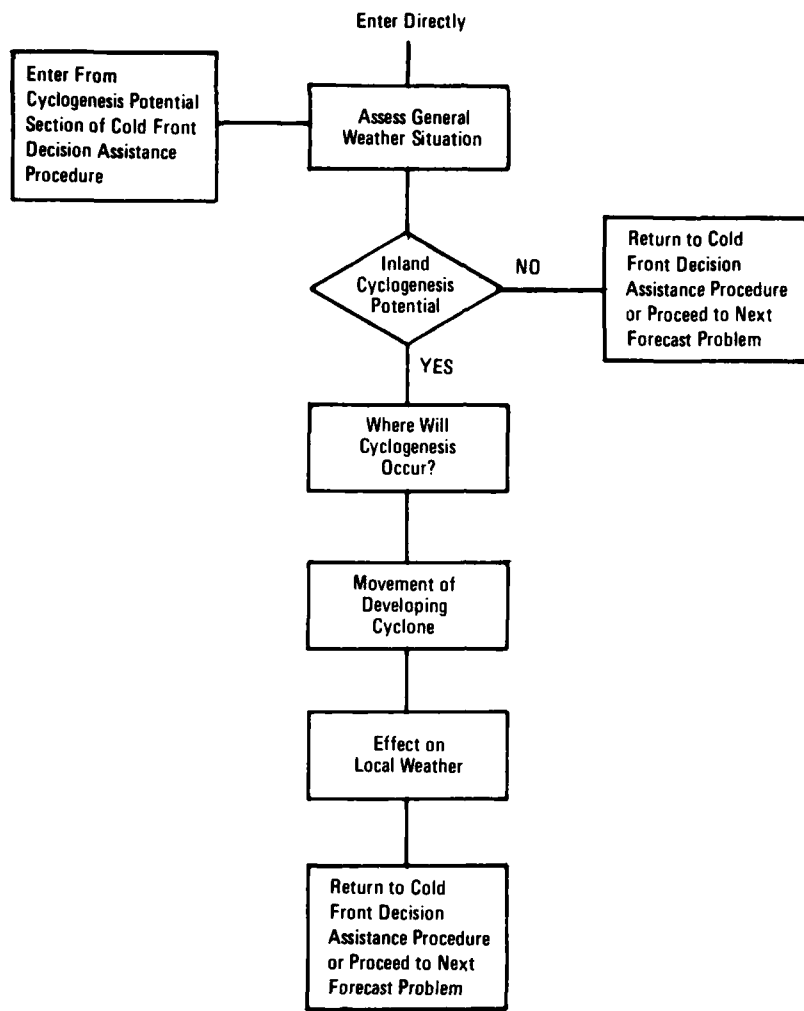


Figure C1. Diagram of Inland Cyclogenesis Decision Assistance Procedure

The analyses suggested above can provide a reasonable assessment of the general weather situation. Four-panel displays using overlays on an interactive graphics system provide a large volume of information that the forecaster can view and digest easily. The forecaster should consult:

National Analyses: surface pressure, surface temperature, 500-mb height, and vorticity analysis (with overlaid 500-mb wind flags), and surface streamlines.

Regional Analyses: surface pressure with overlaid wind flags and weather symbols, 3-h pressure change, surface temperature, surface streamlines, and cross-section analysis (potential temperature, winds, and mixing ratio).

C4.2 Cyclogenesis Potential

This section will be concerned with determining if cyclogenesis will occur for a short-range mesoscale forecast. To predict cyclogenesis consistently and accurately, it is necessary to recognize synoptic situations that may lead to cyclogenesis. Unlike coastal cyclogenesis situations where several typical synoptic situations account for a large portion of all coastal cyclone developments, inland cyclones demonstrate a much wider variety of synoptic situations that lead to cyclogenesis. Countless orientations of fronts, developing fronts, quasi-stationary fronts, cyclones and anticyclones can produce significant cyclogenesis almost anywhere in the continent. Several of the most common upper-level flow patterns that initiate surface cyclogenesis are shown in Figures C2-C5 and briefly described below.

Figure C2 is an example of meridional trough cyclogenesis. This type occurs most frequently in the eastern third of the U.S. when a slow moving or quasi-stationary long wave trough is present over the eastern U.S. A more rapidly moving short wave vorticity maximum progresses southeastward, then northeastward within the long wave trough, triggering cyclogenesis when the short wave overspreads the surface frontal zone to the east of the trough line.

Figure C3 illustrates Split-Flow Cyclogenesis. The split-flow pattern is often induced by a major mountain chain, thus it is most common over the west central U.S., east of the Rockies. In this situation, the upper level flow splits into two branches. For cyclogenesis to occur, a jet or vorticity maximum must move into the southern branch with surface cyclogenesis occurring ahead of the trough line in association with the southern branch. Split flow occurs much more frequently than split flow cyclogenesis.

Figure C4 illustrates what can be called "phased short wave cyclogenesis." In this situation a faster moving northern short wave trough approaches and "phases in" with a southern long wave trough to form a deeper, more intense long wave trough with development east of the trough line. If conditions are not favorable for immediate surface development after this interaction, the long wave trough may become a quasi-stationary meridional trough similar to the illustration in Figure C2, awaiting yet another short wave vorticity maximum to move through the trough to initiate cyclogenesis.

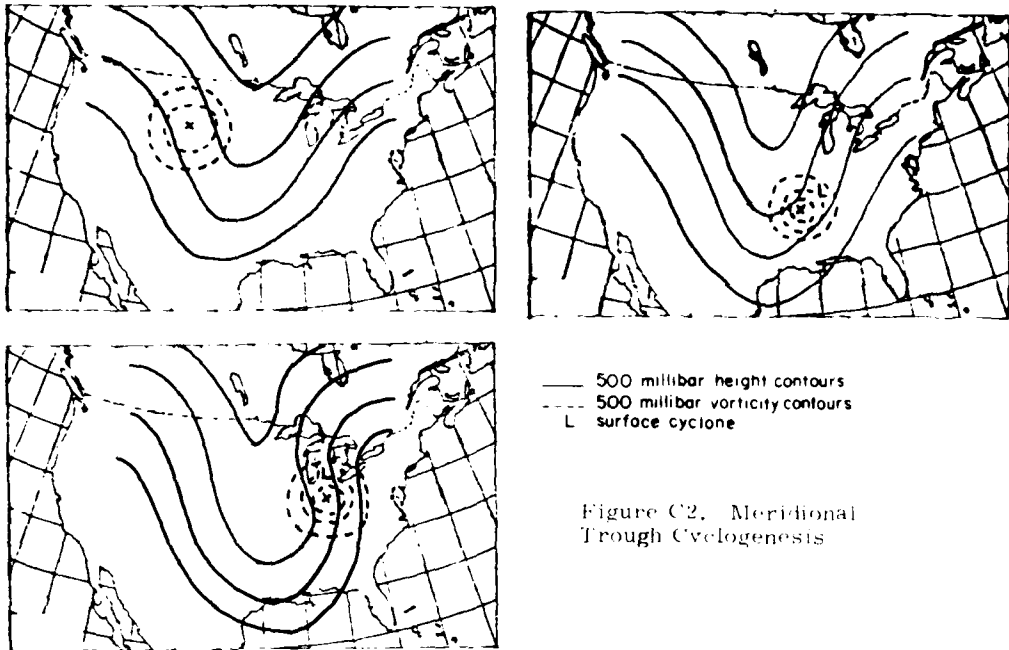


Figure C2. Meridional Trough Cyclogenesis

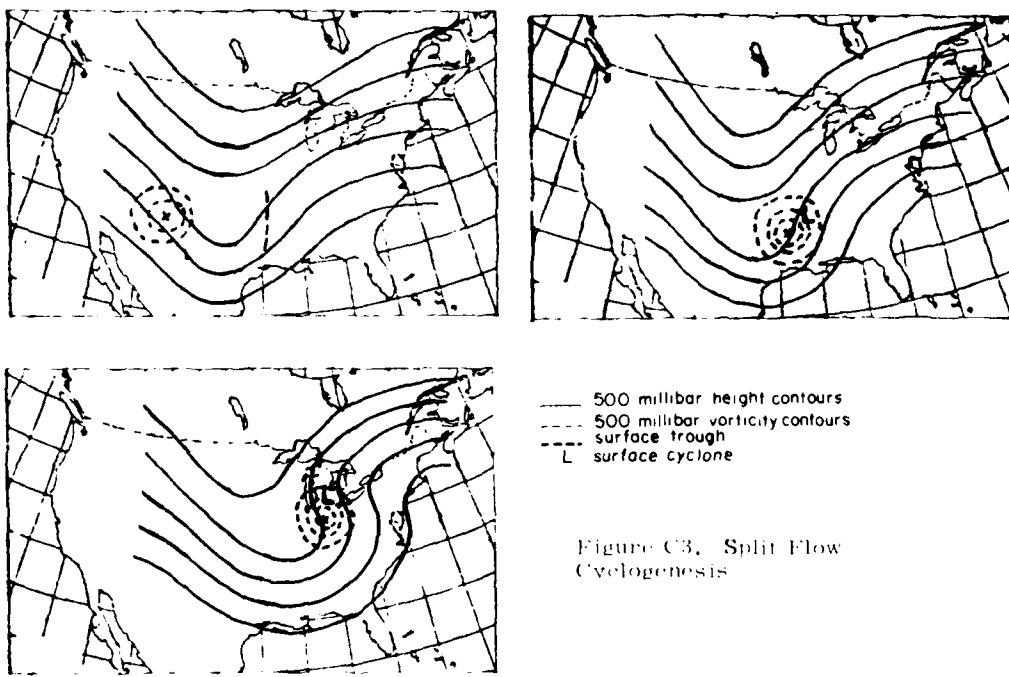


Figure C3. Split Flow Cyclogenesis

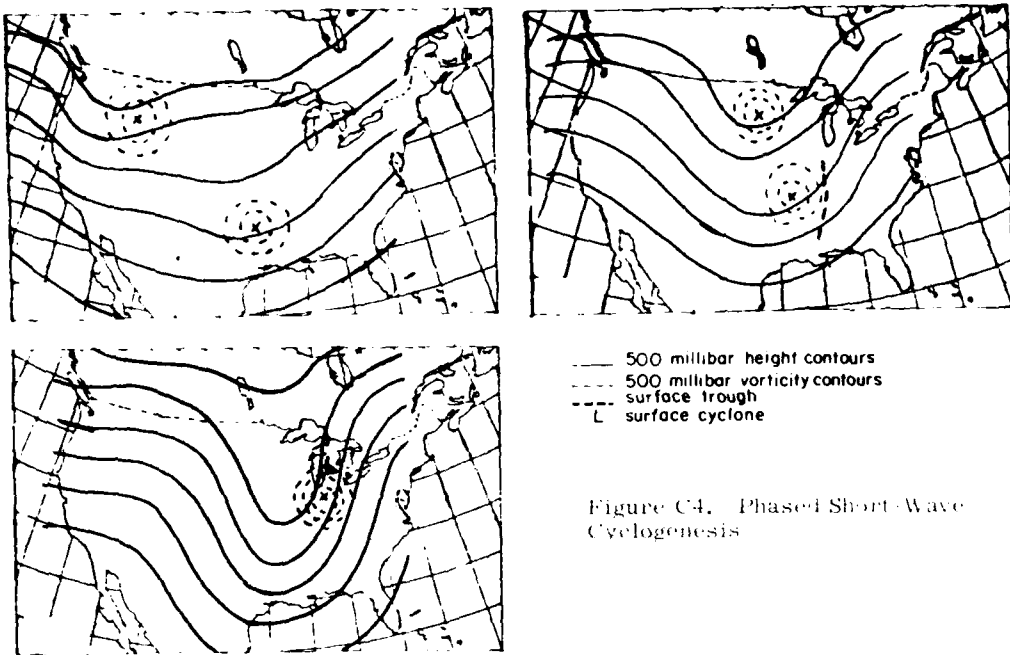


Figure C4. Phased Short-Wave Cyclogenesis

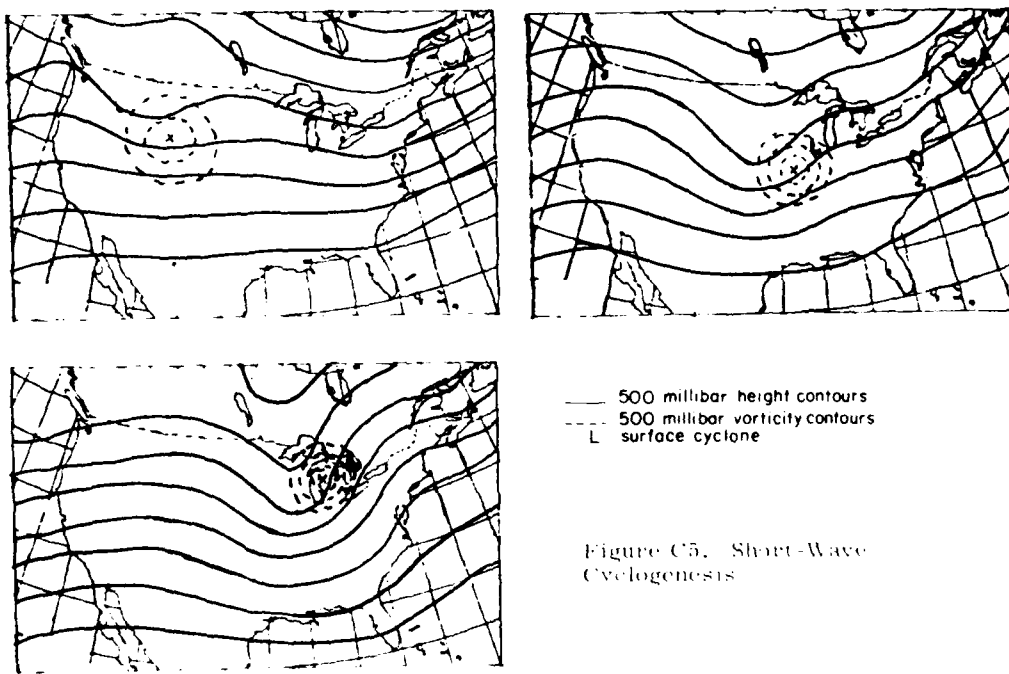


Figure C5. Short-Wave Cyclogenesis

Figure C5 is an example of short wave trough cyclogenesis. This type occurs most frequently in the northern and eastern U.S. Typically a strong short wave trough moves eastward or southeastward out of Canada, showing signs of intensification as it progresses. The amplitude of the trough may increase considerably, and the vorticity advection may become very strong, spawning weak to moderate cyclogenesis. Due to the typically dry conditions found in the northern U.S., development is rarely intense while over land. However, once these short wave trough cyclones move over the heat and moisture source of the ocean, rapid cyclogenesis may ensue.

When all of the conditions necessary for cyclogenesis are present, the forecaster should begin to look for signs of cyclogenesis in the surface data and satellite imagery. The first indication of cyclogenesis is often the gradual widening of the frontal band and a decrease in cloud top temperature or the development of a wiggle or bend in the front in the area where the suspected cyclogenesis potential exists. These signs may exist as early as 12 to 24 h before a new cyclone develops. If the cloud area associated with the front is steadily diminishing in size and cloud top temperatures are slowly increasing, cyclogenesis should not be forecast. The development of a new area of precipitation or the intensification of an existing precipitation area, especially if it is beneath an area of decreasing cloud top temperatures, is a good sign that cyclogenesis may occur during the next 12 to 24 h.

The appearance of a weakness in the pressure pattern in association with the above mentioned developments is often a positive sign that cyclogenesis will occur. If an organized area of 2-4 mb/3 h (or greater) pressure falls, an area of "baggy" isobars, or a surface pressure trough (inverted or upright) develops in the vicinity of an expanding cloud and precipitation area along a front, cyclogenesis is a near certainty, with the intensity of cyclogenesis dependent on the degree of baroclinicity and the strength of the approaching upper air trough and/or vorticity maximum.

Frequently a disturbance in the form of a weak frontal wave or closed isobar may develop well in advance of the upper level support; however, rapid development generally will not occur until the bulk of the PVA overspreads the frontal zone.

In a region dominated by a synoptic pattern (at both the surface and upper levels) which appears to have the potential for surface cyclone development, cyclogenesis will probably occur if several of the following conditions exist:

- (1) the cloud mass associated with a quasi-stationary, slow moving or developing frontal zone exhibits steady or rapid growth in the horizontal (widening frontal band) and vertical (decreasing cloud top temperatures),
- (2) a bend or wiggle develops in the slow-moving or quasi-stationary front,
- (3) an area of thunderstorms develops in an area of rapid horizontal cloud growth,

(4) an area of steady precipitation develops and/or intensifies and expands in the vicinity of a developing cloud mass, especially if moderate precipitation develops.

(5) winds reported in the suspect area suggest the development of a circulation or become stronger in the vicinity of a developing frontal zone exhibiting steady cloud growth.

(6) an area of pressure falls (2-4 mb/3 h or greater) develops along the front in the vicinity of a developing cloud mass,

(7) an area of "baggy" or closed isobars develops along the front in the vicinity of a developing cloud mass,

(8) a surface pressure trough (inverted or upright) develops in the vicinity of the front and the developing cloud mass.

The likelihood of cyclogenesis is greater if several or many of the above conditions exist in the vicinity of the triple point (of an occlusion), a wiggle or bend in the front, a weakness in the surface pressure pattern (trough or baggy isobars), or along a developing front.

Consult: satellite data, satellite data color enhancement, MDR data, pressure analysis, 3-h pressure change analysis, wind flag plot, weather plot, and precipitation amount plot.

G4.3 Where Will Cyclogenesis Occur?

Given that cyclogenesis is likely, the next most difficult task is to determine where it will occur. A 150 to 300 km error in determining where a new cyclone will form can have a major impact on the accuracy of the weather forecast. Usually within at least 6 to 12 h of the initial development of a new cyclone, clues as to the probable location of the suspected development are present in the surface analysis and/or satellite and radar data. The first step is to look in these suspect areas for clues to pinpoint where development will take place.

Generally, the first hint of cyclogenesis will be the gradual widening of the frontal cloud band and a decrease in cloud top temperature, and/or the development of a wiggle or bend in the front in the area where the new cyclone will form. An area of "baggy" isobars or a surface trough (inverted or upright) will often develop at least 6 to 12 h and sometimes as early as 12 to 24 h before significant cyclogenesis. Cyclogenesis will usually occur within one of these surface features in the vicinity of the greatest surface pressure falls and/or an area of newly developing or intensifying precipitation. An area exhibiting 3-h pressure falls of at least 2 to 3 mb is the most likely area for cyclogenesis, especially if the magnitude of the pressure falls is increasing. In some cases, such an area of organized pressure falls may exist for 12 to 24 h prior to cyclogenesis, allowing great

accuracy in determining where the new cyclone will develop. However, in other cases, several areas of weak pressure falls may develop well ahead of the upper-level support with one becoming dominant and intensifying only several hours before significant development occurs. In these situations the forecaster should look for clues in the satellite imagery, precipitation data and wind fields, as well as determine which area will be most favorably located when the bulk of the vorticity advection overspreads the frontal zone.

When the frontal zone of interest is quasi-stationary, the surface pressure pattern may be stationary or slowly moving, that is, the surface trough, baggy isobars, and pressure fall areas may remain nearly stationary or move slowly along the front as they intensify. In these situations the location of cyclone development can be accurately determined at least 6 to 12 h before development, thus the forecaster need only advect the upper air PVA toward the developing frontal zone to determine when cyclogenesis will occur. When the frontal system and its surface trough, baggy isobars, and/or pressure fall area are steadily moving the situation is much more difficult. The movement of both the front and the upper-air PVA must be accurately forecast in order to determine when and where the PVA will overspread the surface front to initiate cyclogenesis. Fortunately, cyclogenesis typically occurs on slow moving or stationary fronts.

In summary, cyclogenesis occurs with one or more of the following:

- (1) an area of organized pressure falls,
 - (2) an area of baggy isobars,
 - (3) a surface trough (inverted or upright),
 - (4) a developing area of steady precipitation,
 - (5) a cloud mass exhibiting steady or rapid horizontal growth,
 - (6) southwest of an area of steadily decreasing cloud top temperatures,
 - (7) just west or beneath an area of developing thunderstorms,
 - (8) near a developing circulation that has become evident in wind flags or satellite imagery,
 - (9) near a bend or wiggle in the front (noticeable in surface data or satellite imagery),
 - (10) in the area where the maximum PVA and surface front become superimposed.
- In situations where the surface front and surface pressure features are not stationary, both the front and the upper-air PVA must be accurately advected to determine when and where the PVA will overspread the surface front to initiate cyclogenesis.
- Consult: pressure analysis, 3-h pressure change analysis, satellite imagery, imagery color enhancement, wind flag plot, weather plot, and precipitation amount plot.

C4.4 Intensity of Inland Cyclogenesis

Patterssen^{A2} outlined some basic rules for cyclone intensity that suggest that the greater the baroclinicity, the stronger the PVA, the lower the static stability, and the greater the available moisture, the greater the chance of cyclogenesis and the more intense the developing cyclone.

The ingredient most influential on the intensity of inland cyclogenesis is the strength of the upper-air PVA. Using McIDAS, the forecaster can focus on 300- and 500-mb analyses and 12-h forecast fields to resolve the timing and intensity of cyclogenesis. Specifically, one should focus on:

- (1) the intensity of the 300-mb (500-mb) trough:
 - (a) a digging or intensifying trough is most favorable for development, especially for moderate to strong developments,
 - (b) a negatively tilted trough is especially favorable for rapid, moderate to strong development,
 - (c) a diffluent trough is favorable for rapid development,
- (2) the strength of the approaching 300-mb (500-mb) vorticity maximum;
- (3) the strength of the jet stream at 300 mb (or an expected intrusion of a jet at 300 mb);
- (4) the magnitude of divergence at 300 mb;
- (5) the magnitude of height falls (500 mb, 300 mb) in advance of the trough.

The strength of the upper level factors (especially at 300 mb), coupled with lower tropospheric factors such as the strength of the baroclinic zone, the availability of moisture, and the degree of instability, will largely determine the strength of a developing cyclone. Lower atmospheric conditions that should be analyzed using McIDAS are:

- (1) pressure falls: $\geq 6 \text{ mb/3 h}$ - intense cyclogenesis,
 $3-5 \text{ mb/3 h}$ - moderate cyclogenesis,
 $1-2 \text{ mb/3 h}$ - weak (or no) cyclogenesis,
- (2) the strength of the baroclinic zone;
- (3) the strength of surface and low level (850 mb) warm advection;
- (4) the availability of moisture;
- (5) the degree of instability;
- (6) the rate of growth (horizontal and vertical) of the developing cloud mass and precipitation areas, especially with convection.

In general, the greater the strength of each of the parameters listed above, the greater the developing cyclone's potential for intensification.

In a situation where 1-2 mb/3 h pressure falls are occurring in a suspect area, but the bulk of the upper-level support is still well to the west, greater pressure falls can be expected, thus the intensity of cyclogenesis should be forecast according to the strength of the PVA and the degree of baroclinicity.

The presence and intensity of these upper and lower atmospheric conditions determines the degree to which cyclogenesis will occur. If one or more of the ingredients are missing, cyclogenesis probably will not occur during the next 12 h, and if it does, it will probably be very weak. When all the ingredients are present, but one or more is weak (particularly if the upper-air PVA or baroclinicity is weak) cyclogenesis will probably occur, but the intensity will be weak to perhaps moderate. Those more typical cases where all ingredients are present in weak to moderate degrees will normally result in weak to moderate cyclogenesis. When all the ingredients are present in moderate to strong amounts, cyclogenesis will almost certainly occur to a moderate to strong degree.

C4.5 Movement of a Developing Cyclone

Developing cyclones generally move slightly to the right of the instantaneous 500-mb flow with 50-70 percent of the 500-mb wind speed. Thus to forecast cyclone movement the forecasters should focus on interactive graphics displays that examine the following:

- (1) Change in 500-mb flow pattern;
 - (a) deepening of trough can increase northward movement,
 - (b) building of downstream ridge can increase northward movement,
 - (c) eastward translation of trough.
- (2) If the surface low and 500-mb low are forecast to become vertical; forecast very slow movement (usually toward the *northeast*) of the surface low.
- (3) Extreme building of the upstream ridge westward or a negatively tilted trough can cause a surface low to slow down and curve strongly northward or even northwestward.
- (4) A very strong, cold surface high north of the developing cyclone can decrease the cyclone's forward speed.
- (5) A weak, shallow cyclone in its early stages may move according to the lower-level 850-mb flow.
B10
- (6) The majority of cyclones developing on quasi-stationary or very slow moving fronts usually move slowly during the first few hours of their development.
- (7) Surface cyclone centers move toward the area of maximum surface pressure falls.
- (8) Surface cyclone centers move from the area of maximum cold advection toward the area of maximum warm advection.

C4.6 Effect on Local Weather

The effect a particular developing cyclone will have on the mesoscale weather forecast at a given location depends on several factors:

- (1) the track of the cyclone will affect the type and intensity of precipitation;
- (2) the intensity of the cyclone determines potential wind and precipitation intensity;
- (3) the horizontal extent and movement of precipitation, cloud cover, low ceilings, and strong winds;
- (4) local weather enhancements which must be considered;
 - (a) orographic effects on wind, precipitation, and visibility,
 - (b) special synoptic scale effects.

Although general rules can be made for cyclones developing under certain synoptic conditions, each cyclone and its associated weather must be forecast individually due to the wide variety of tracks, intensities, areal coverage, and enhancement effects that can result. It is in this regard that the power and flexibility of interactive graphics systems become important.

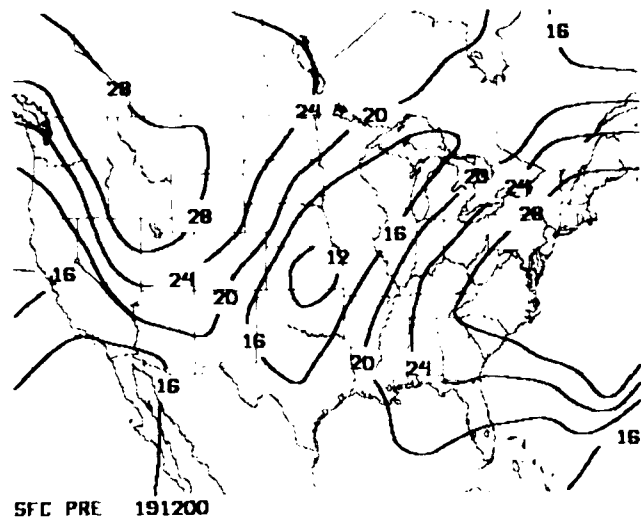
The paths of a particular cyclone and its closeness to the forecast area generally determine the precipitation intensity, wind conditions, visibility, and ceiling height. Typically, the closer the cyclone center tracks to the forecast area, the greater the precipitation intensity, the stronger the winds, and the lower the visibilities and cloud ceilings. Cyclone centers that track more than about 600 km from a particular forecast region (except for the most intense cyclones) usually affect the region with no more than showery precipitation or as little as scattered clouds and increased winds. However, if the warm or cold frontal precipitation band associated with a cyclone is particularly active, considerable steady precipitation may occur much farther from the cyclone center in regions under the influence of such fronts.

The success of the short range forecast is dependent on a complete description (nowcast) of the weather-cyclone model that exists and an hour-by-hour update. Interactive systems with real-time conventional and satellite data bases are ideal for this process. The complexity and dynamicism of the developing system precludes the use of sophisticated models or approaches. Heavy reliance should be placed on conventional graphical plots and analyses and special purpose plots such as trend charts of key variables at upstream stations and station time series plots. In conjunction with plots and analyses of current observational data, the broader potential of the developing cyclone can be assessed from interactive graphing of numerically-based guidance (such as ceiling, cloud cover, precipitation, visibility, and wind vector from Model Output Statistics). Subjective integration of current short-term trends based on observations (surface, satellite and radar) with Model Output Statistics and I.FM 6- to 12-h precipitation guidance is the only practical procedure to effective met-watching and forecast updating.

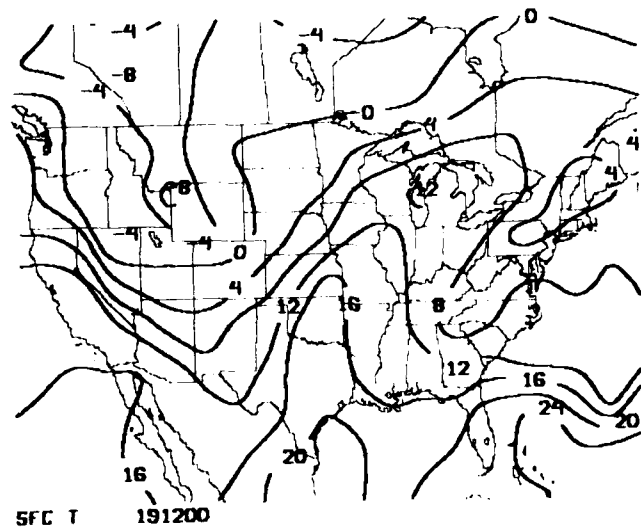
C5. CASE STUDY: MIDWEST CYCLOGENESIS ON 19-20 OCT 1982

The Inland Cyclogenesis Decision Assistance Procedure was applied in the preparation of a short-range (0-12 h) terminal forecast for Wausau, Wis., in a cyclogenesis forecast situation. The cyclone that is the subject of this case study developed along a moderately intense, slow moving cold front that stretched from Wisconsin southwestward to the northwest corner of the Texas panhandle. The cyclone-suspect area first became evident as a weak frontal wave in Kansas moving northeastward along the front. As upper-air support overspread the region, rapid deepening occurred in northern Missouri and Iowa bringing moderate to heavy precipitation amounts, strong winds and colder temperatures to much of the upper Midwest and Great Lakes region.

The general weather situation present at 1200 GMT, 19 Oct 1982, can be examined with a four-panel national analysis which includes (1) surface pressure, (2) surface temperature, (3) 500-mb heights (with overlaid 500-mb absolute vorticity and 500-mb wind flags), and (4) surface streamlines. The 1200 GMT surface pressure analysis (Figure C6a) shows a weak trough of low pressure from Wisconsin southwestward to Texas with a weak frontal wave (1008 mb) centered over eastern Kansas. Strong anticyclones centered off the mid-Atlantic coast and over Idaho dominate the weather in the eastern and western regions of the nation. The 1200 GMT surface temperature analysis (Figure C6b) shows a moderately strong baroclinic zone stretching from Wisconsin southwestward to western Texas, separating 20° C temperatures in eastern Kansas from temperatures around 4° C in western Kansas. The 1200 GMT 500-mb vorticity analysis (Figure C6c) shows a deepening short wave trough with moderate vorticity advection moving through the Dakotas and Nebraska, approaching the Midwest frontal system. The 1200 GMT surface streamline analysis (Figure C6d) clearly marks the position of the frontal convergence zone that separates easterly winds ahead of the front from north and northwest winds behind the front.

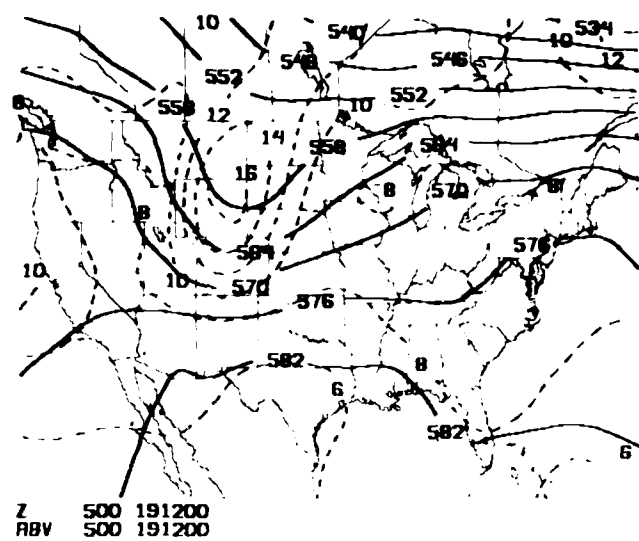


(a) Pressure (mb Deviation from 1000 mb)



(b) Temperature ($^{\circ}\text{C}$)

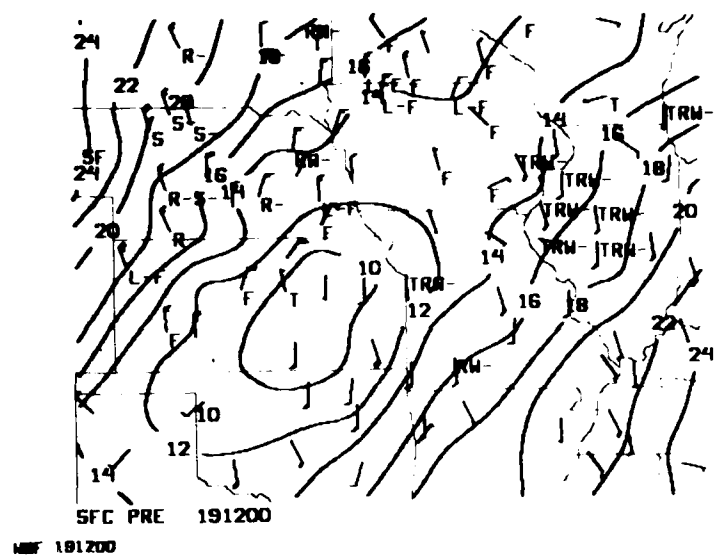
Figure C6. Four-Panel Analysis of General Weather Situation (National); (a) Pressure (mb Deviation from 1000 mb), (b) Temperature ($^{\circ}\text{C}$), (c) 500-mb Heights and 500-mb Absolute Vorticity, and (d) Surface Streamlines



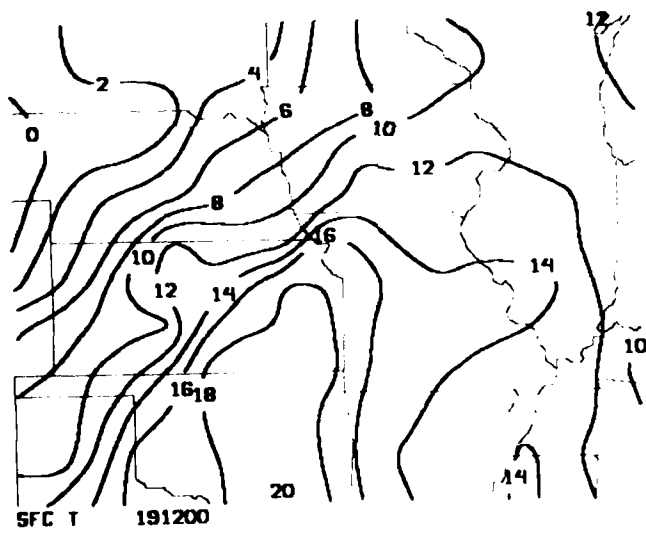
A four-panel regional analysis at 1200 GMT, centered on the Missouri-Iowa area, zooms in on the region of suspected cyclogenesis. This analysis displays (1) surface pressure with overlaid wind flags and weather symbols, (2) 3-h surface isallobars, (3) surface temperature and (4) surface streamlines. The surface pressure analysis (Figure C7a) shows a weak 1007 mb frontal wave centered over eastern Kansas. Wind flags indicate strong convergence at the frontal zone, however there is little evidence of a circulation associated with the frontal wave. Strong northerly winds are present to the north of the frontal wave (in Nebraska, eastern Colorado and western Kansas) with gusts of 12 to 18 m/sec. The weather plot shows a large area of showers and thunderstorms ahead of the front in Missouri and Illinois. The surface temperature analysis (Figure C7b) clearly shows the location of the surface front through central Iowa, extreme southeastern Nebraska and Kansas with the strongest temperature gradient ($16^{\circ}\text{C}/500\text{ km}$) in Nebraska and Kansas. Figure C7c shows an unorganized area of minor pressure falls, generally less than 1 mb/3 h in the Kansas-Missouri area, however, strong pressure rises of 4-6 mb/3 h are occurring over western Kansas and eastern Colorado. The surface streamlines (Figure C7d) show the frontal convergence zone across southern Wisconsin, extreme southeastern Nebraska and across central Kansas, marking the boundary between the north winds behind the front and the east winds ahead of the front. The streamlines show little evidence of circulation in the vicinity of the frontal wave.

The present synoptic situation in the Midwest suggests that a short-wave trough cyclogenesis event is possible. During the past 24 h a potent short-wave trough has moved steadily southeastward from southwest Canada to the northern Plains states, exhibiting strengthening vorticity advection and increased amplitude. As the short-wave trough and associated vorticity advection overspread the moderately strong, slow-moving cold front and frontal wave, cyclogenesis is a distinct possibility in the Kansas-Missouri-Iowa area, thus a more comprehensive analysis of the situation is advised to more accurately determine the potential for cyclogenesis.

During the past 12 h, an area of clouds and precipitation over Nebraska, Missouri, Iowa, and Illinois has grown steadily, while an area of thunderstorms has developed in Iowa and Illinois during the past 4 h. Satellite data shows an area of high clouds associated with the PVA over the Dakotas and Nebraska moving toward Missouri and Iowa.

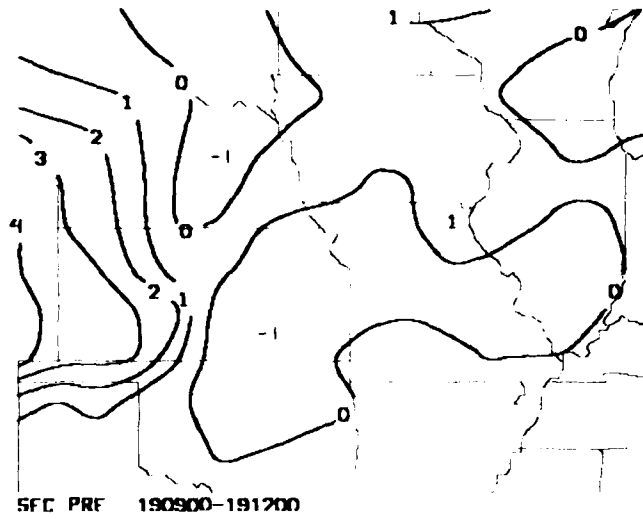


(a) Pressure (mb Deviation from 1000 mb), Surface Wind Flags (knots), Weather Symbols

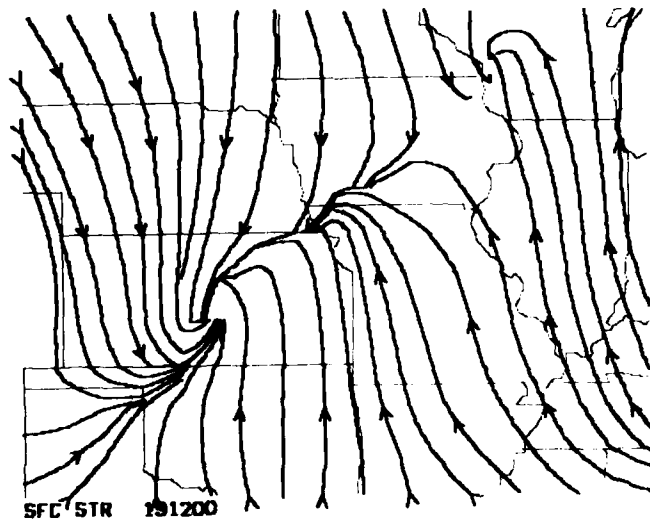


(b) Temperature (°C)

Figure C7. Four-Panel Analysis of General Weather Situation (Regional); (a) Pressure (mb Deviation from 1000 mb), Surface Wind Flags (knots), Weather Symbols, (b) Temperature (°C), (c) Three-Hour Pressure Change (mb), and (d) Surface Streamlines



(c) Three-Hour Pressure Change (mb)



(d) Surface Streamlines

Figure C7. Four-Panel Analysis of General Weather Situation (Regional): (a) Pressure (mb Deviation from 1000 mb), Surface Wind Flags (knots, Weather Symbols, (b) Temperature ($^{\circ}$ C), (c) Three-Hour Pressure Change (mb), and (d) Surface Streamlines (Contd)

At 1200 GMT, pressure falls of only 0.5 mb/3 h and 2-2.5 mb/6 h are occurring in the Missouri area. However, at this time the short-wave trough and its associated vorticity advection has not yet begun to overspread the frontal zone. This is sometimes typical of short-wave cyclogenesis situations. Since the wavelength of the trough is relatively short and the significant vorticity advection tends to be confined to a limited area, pressure falls are often minor until the compact short-wave overspreads the baroclinic zone resulting in a sudden decrease in surface pressure and rapid cyclogenesis. At 1200 GMT a surface pressure trough stretched from Wisconsin to Texas with a closed isobar centered in eastern Kansas, suggesting that a frontal cyclone may already be in its initial stages of development. Although pressure falls are very weak at 1200 GMT, with the steady growth of the cloud shield, the presence of the precipitation area in Iowa, Missouri, Nebraska, and the Dakotas, the outbreak of convection in Iowa and Illinois, and the development of a weak frontal wave within the surface trough, cyclogenesis is forecast to occur when the vorticity advection overspreads the frontal zone.

In this situation, the location of significant cyclogenesis is fairly obvious. During the past 6 h, precipitation and thunderstorms have broken out in Iowa, Missouri, and Illinois, along with weak 6-h pressure falls in Missouri. With the weak frontal wave located in Kansas at 1200 GMT expected to move northeastward at 50 km/h and the area of upper air vorticity located in Nebraska at 1200 GMT moving eastward at 80 km/h, the leading edge of the PVA should begin to overspread the frontal wave in southern Iowa between 1600 and 1800 GMT. Thus significant cyclogenesis is forecast to begin in southern Iowa by 1800 GMT.

The strength of the upper air trough and its associated vorticity advection, and the strength of the baroclinic zone are of most importance in determining the intensity to which the cyclone will develop. The 300- and 500-mb height and vorticity analysis (Figure C8 and Figure C6c, respectively) show the short-wave trough approaching the Iowa-Missouri area with moderate vorticity advection. Weak cold advection into the trough and moderate warm advection ahead of the trough suggests that the trough may deepen further, though not dramatically, during the next 12 h. At 1200 GMT, substantial divergence is occurring at the 200- and 300-mb levels above South Dakota, Nebraska, and Kansas, moving toward Missouri and Iowa, and a jet stream at the 250-mb level, with 40 m/sec winds, is approaching the Missouri-Iowa area. At the surface, the moderately intense frontal-baroclinic zone is exhibiting strong convergence, an expanding area of precipitation and an area of widespread convection just to the north of the weak frontal wave. With 16° C dewpoint and low-level (850 mb) southerly flow out of the Gulf of Mexico, plenty of moisture is available. Although pressure falls are weak at 1200 GMT, upper-air and surface analyses suggest that significant development is likely, thus moderate cyclogenesis is forecast.

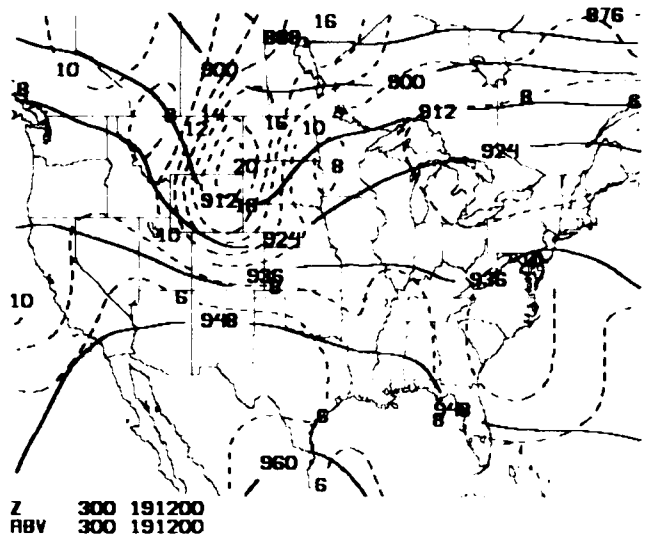


Figure C8. 300-mb Heights (solid, decameters) and 300-mb Absolute Vorticity (dashed, $\times 10^{-5} \text{ sec}^{-1}$)

At 1200 GMT, the 500-mb flow over eastern Kansas is from the southwest at 20 m/sec. With further deepening of the trough forecast, the flow is expected to become more southerly and somewhat stronger. The 500-mb winds in the vicinity of the vorticity maximum are around 20 to 25 m/sec. The cyclone is forecast to move just north of northeast at 55-65 km/h, being located in south-central Iowa by 1800 and southwest Wisconsin by 00 GMT. The cyclone is forecast to be 75 km east of Wausau at 0900 GMT and near the eastern end of Lake Superior at 1200 GMT (24 h).

The forecast path of the cyclone would move it northeastward along the nearly stationary cold front, following the "steering" trough which is clearly evident on the surface pressure analysis.

Since a moderately intense cyclone is forecast to pass within 75 km of Wausau during the next 24 h, significant weather is likely to occur. At 1200 GMT, satellite data and surface reports show that an area of low overcast covers the entire state of Wisconsin, Iowa, Missouri, northeastern Kansas, and the northern Plains states indicating that with a developing cyclone in the region, overcast conditions will be present at Wausau during the entire 12-h forecast period and beyond. An area of thunderstorms is present in western Illinois and Missouri, and an area of drizzle, light rain, and snow covers much of Iowa, Nebraska, and South Dakota. With 700-mb flow from the southwest at 10 m/sec, precipitation should move northeastward at around 25 km/h, arriving in Wausau in 8 to 10 h. Precipitation will become

more widespread and more intense near the developing cyclone when the PVA over-spreads the frontal wave. This better organized area of moderate precipitation will affect the Wausau area late in the 12-h forecast period. Thus, showers can be expected in Wausau after 2000 GMT with steady, moderate precipitation beyond 2200 GMT.

Since the cyclone center is forecast to track within 75 km of Wausau, 1 to 1-1/2 in. of melted precipitation is forecast, the majority being rainfall. With cold air lurking behind the cold front less than 150 km northwest of Wausau, precipitation could change to snow sometime after 0900 GMT (during the second 12-h period) when the cyclone moves past the forecast station and winds become northwesterly.

Visibility is expected to remain around 16 km until showers reach the Wausau area. A trend chart of stations to the south shows the visibility decreasing to 9 to 11 km in showers. Thus the visibility is forecast to remain around 16 km until 2000 GMT, lowering to 9 to 11 km in showers for several hours, then lowering to 2 to 5 km in moderate rain after 2200 GMT. Ceiling heights are forecast to decrease slowly to around 1000 m by 2000 GMT, decreasing further to 150-200 m by 2200 GMT when the precipitation intensifies.

Winds will remain light from the east to southeast at 3 to 5 m/sec until around 2200 GMT when the circulation in the developing cyclone begins to affect the forecast region. After 2200 GMT winds will increase to around 5 to 8 m/sec from the east. Around 0600 GMT winds will become more northeasterly, then northwesterly at 5 to 10 m/sec with higher gusts as the cold front trudges through and the cyclone moves by to the east of Wausau.

Since the cold front has seemingly stalled less than 125 km west of Wausau, FROPA and its associated temperature drops is not expected during the next 12 h. With southeasterly flow under low overcast skies, temperatures are forecast to rise only 2 to 3° to 12 to 14° during the daylight hours. Temperatures will begin to drop steadily around 0600 GMT when the surface cold front finally crawls past Wausau. However, the movement and timing of such a slow moving cold front is difficult, especially when significant cyclogenesis is occurring to the south along the front.

Cyclogenesis actually took place in southwestern Iowa between 1600 and 1800 GMT. By 1800 GMT pressure falls of 4 to 5 mb/3 h were occurring in southwest Iowa and a well defined, deepening low pressure system had developed on the front. The developing cyclone moved northeastward at 55 km/h and was located near the Iowa-Wisconsin border at 00 GMT. The cyclone continued moving northeastward passing 100 km east-southeast of Wausau at 0900 GMT, and was centered near Gladstone, Michigan at 1200 GMT. Thus, the forecast path of the cyclone was accurate during the first 12 h. During the second 12 h period the cyclone continued

along the forecast path, however it apparently slowed its forward speed slightly after becoming vertical with the 500-mb low, and by 24 h was located 150 km southwest of the forecast position. Precipitation arrived in Wausau as light rainshowers around 2200 GMT. By 0100 GMT the rain had become moderate. Visibility decreased to 8-13 km in the showers, then decreased further to 2-7 km during the period of steady precipitation. Ceiling heights decreased to around 600 to 800 m until the showers at 2200 GMT, then decreased further to between 100 to 250 m during much of the period of steady precipitation. Precipitation during the event totaled 2.10 in., considerably more than was forecast. Winds remained light from the east and southeast until around 0300 GMT when they began to turn northeasterly, and finally northwesterly by 0700 GMT. Temperatures varied only 3°C during the first 12-h period, with a steady decrease in temperature after 0300 GMT when winds turned northeasterly, finally dragging the cold front past Wausau.

The ability of interactive graphics systems like McIDAS to display conventional and computed meteorological data along with half-hourly satellite imagery in real-time make it a valuable tool in forecasting the development, movement and weather associated with an inland cyclone.

The Inland Cyclogenesis Decision Assistance Procedure was helpful in preparing an accurate forecast for this difficult cyclogenesis event. The forecasts for cyclone development, movement and track were particularly accurate. The forecasts for the other meteorological parameters were accurate for the first 12-h period (which is of most importance to this study) and less accurate though adequate for the second 12-h period. The combination of the step-by-step forecaster-decision process and the capability to study real-time data on the McIDAS system offer the potential for increased short-range forecast accuracy of cyclogenesis-related weather events.

Appendix D

Mesoscale Forecasting Experiment Assessment Forms

169

**PREVIOUS PAGE
IS BLANK**

Mesoscale Forecast Variable Assessment

Case No. _____ Case Date _____ Forecaster _____

Forecast Stations BOS and _____

First Forecast Time _____ Z Last Forecast Time _____ Z

Ranking of Forecast Variable, in order of difficulty using facilities available through MELDAS and MFN

A. The most difficult variable to forecast was _____; beyond _____ hours, I had little confidence in my forecasts.

Not Enough 1 2 3 4 5 Too Much

Spatial Coverage

Spatial Resolution

Time Coverage

Time Resolution

Was satellite imagery useful? If so, how?

Was MDR useful? If so, how?

Were the mesoscale plot and analysis routines useful? If so, how?

Was guidance information useful? If so, which guidance (FOR, FOUS Bulletins, Decision Assistance) and how?

Were the Wisconsin trajectory models useful? If so, how?

Did you make your forecasts based on direct advection _____ or based on advection of upstream change _____ why?

Was this forecast variable affected by local (non-translatory) factors?
If so, how did you factor that into your forecast?

Mesoscale Forecast Variable Assessment (Contd)

B. The next most difficult variable to forecast was _____; beyond ____ hours, I had little confidence in my forecasts.

Not Enough 1 2 3 4 5 Too Much

Spatial Coverage

Spatial Resolution

Time Coverage

Time Resolution

Was satellite imagery useful? If so, how?

Was MDR useful? If so, how?

Were the mesoscale plot and analysis routines useful? If so, how?

Was guidance information useful? If so, which guidance (FOR, FOUS Bulletins, Decision Assistance) and how?

Were the Wisconsin trajectory models useful? If so, how?

Did you make your forecasts based on direct advection _____ or based on advection of upstream change _____ why?

Was this forecast variable affected by local (non-translatory) factors?
If so, how did you factor that into your forecast?

Mesoscale Forecast Variable Assessment (Contd)

C. The next most difficult variable to forecast was _____; beyond _____ hours, I had little confidence in my forecasts.

Not Enough 1 2 3 4 5 Too Much

Spatial Coverage

Spatial Resolution

Time Coverage

Time Resolution

Was satellite imagery useful? If so, how?

Was MDR useful? If so, how?

Were the mesoscale plot and analysis routines useful? If so, how?

Was guidance information useful? If so, which guidance (FOR, FOUS Bulletins, Decision Assistance) and how?

Were the Wisconsin trajectory models useful? If so, how?

Did you make your forecasts based on direct advection _____ or based on advection of upstream change _____ why?

Was this forecast variable affected by local (non-translatory) factors? If so, how did you factor that into your forecast?

Mesoscale Forecast Variable Assessment (Contd)

- D. The easiest variable to forecast was _____; beyond _____ hours, I had little confidence in my forecasts.

Not Enough 1 2 3 4 5 Too Much

Spatial Coverage

Spatial Resolution

Time Coverage

Time Resolution

Was satellite imagery useful?

If so, how?

Was MDR useful?

If so, how?

Were the mesoscale plot and analysis routines useful? If so, how?

Was guidance information useful? If so, which guidance (FOR, FOUS Bulletins, Decision Assistance) and how?

Were the Wisconsin trajectory models useful? If so, how?

Did you make your forecasts based on direct advection _____ or based on advection of upstream change _____ why?

Was this forecast variable affected by local (non-translatory) factors? If so, how did you factor that into your forecast?

Product Usefulness Assessment

Case No. _____ Case Date _____ Forecaster _____

Forecast Stations BOS and _____

First Forecast Time _____ Z Last Forecast Time _____ Z

1. Most Useful

A. What new product was most useful to you?

B. Why was it so useful?

C. How did you use it?

D. In what situations was it most useful?

E. In what situations was it not useful?

F. What characteristics of the data source made it useful to you?

2. Least Useful

A. What new product was least useful?

B. What made it so useless?

C. In what situations was it most useful?

D. In what situations was it least useful?

E. How could the product be improved?

Ranking Product Characteristics: Rank in Order of Importance/Usefulness

A. Most Useful Product is _____

Not Enough 1 2 3 4 5 Too Much

Volume of Information

Newness of Information

Area Resolution

Area Coverage

Time Resolution

Time Coverage

Ease of Acquiring

Time to Acquire

B. Next Most Useful Product is _____

Not Enough 1 2 3 4 5 Too Much

Volume of Information

Newness of Information

Area Resolution

Area Coverage

Time Resolution

Time Coverage

Ease of Acquiring

Time to Acquire

C. Next Most Useful Product is _____

Not Enough 1 2 3 4 5 Too Much

Volume of Information

Newness of Information

Area Resolution

Area Coverage

Time Resolution

Time Coverage

Ease of Acquiring

Time to Acquire

Glossary of Abbreviations

AFDIGS	Air Force Digital Graphics System
AFGWC	Air Force Glocal Weather Central (Offutt AFB, Neb.)
AWDS	Automated Weather Distribution System
AWN	Automated Weather Network
BDL	Bradley International Airport (Hartford, Conn.)
BOS	Logan International Airport (Boston), Mass.
COMEDS	Continental United States Meteorological Data System
CPU	Central Processing Unit
DMSP	Defense Meteorological Satellite Program. In this program, satellites are placed into a near-polar orbit.
DVIP	Digital Video Integrator and Processor (of the National Weather Service)
FOUS	Forecast Output for United States
FROPA	Frontal Passage
GEM	Generalized Exponential Markov. This statistical operator produces probability forecasts for any time in the future, given any initial weather conditions.

GOES	Geostationary Operational Environmental Satellite. This NOAA satellite produces one visible and one infrared image each half hour.
JFK	Kennedy International Airport (New York), N.Y.
LFM	Limited Area Fine Mesh Model. This National Weather Service numerical forecasting model is revised every 12 h, and made available to forecasters. It predicts the weather for the United States and surrounding areas for the next 48 h.
MAE	Mean Absolute Error
MeIDAS	Man-computer Interactive Data Access System
MDR	Manually Digitized Radar
MFE	Mesoscale Forecast Experiment
MOS	Model Output Statistics
PVA	Positive Vorticity Advection
PVD	T. F. Green Airport (Providence), R.I.
QPF	Quantitative Precipitation Forecast
RAOB	Radiosonde Observation
rmse	Root Mean Square Error
SS	Heidke Skill Score (of a forecaster)
SGDB	Satellite Global Data Base
SVCA	Service A. A long-line teletypewriter system
UGDF	Uniformly Gridded Data Fields
WB604	The FAA medium-speed weather data link